Distribution Agreement

In presenting this thesis or dissertation as a partial fulfillment of the requirements for an advanced degree from Emory University, I hereby grant to Emory University and its agents the non-exclusive license to archive, make accessible, and display my thesis or dissertation in whole or in part in all forms of media, now or hereafter known, including display on the world wide web. I understand that I may select some access restrictions as part of the online submission of this thesis or dissertation. I retain all ownership rights to the copyright of the thesis or dissertation. I also retain the right to use in future works (such as articles or books) all or part of this thesis or dissertation.

Signature:

_____ _____

Osric Forrest Date

Pathological Conditioning of Neutrophils in Airway Inflammation

By

Osric A. Forrest
Doctor of Philosophy

Graduate Division of Biological and Biomedical Sciences
Immunology and Molecular Pathogenesis

Rabindra Tirouvanziam , Ph.D.
Advisor

Jacob Kohlmeier, Ph.D.
Committee Member

Lou Ann Brown, Ph.D.
Committee Member

Periasamy Selvaraj, Ph.D.
Committee Member

Daniel Kalman, Ph.D.
Committee Member

Accepted:

Lisa A. Tedesco, Ph.D.

Dean of the James T. Laney School of Graduate Studies

Date

Pathological Conditioning of Neutrophils in Airway Inflammation

By

Osric A. Forrest

B.S., Hampden-Sydney College, 2012

Advisor: Rabindra Tirouvanziam, Ph.D.

An abstract of
a dissertation submitted to the Faculty of the
James T. Laney School of Graduate Studies of Emory University
in partial fulfillment of the requirements for the degree of

Doctor of Philosophy
in Immunology and Molecular Pathogenesis

Abstract

Pathological Conditioning of Neutrophils in Airway Inflammation

By

Osric A. Forrest

Airway inflammation in cystic fibrosis (CF), chronic obstructive pulmonary disease (COPD), and severe asthma is marked by massive recruitment of polymorphonuclear neutrophils (PMNs) from blood into the airway lumen. Therein, PMNs may assume a pathogenic role notably via the release of toxic granule mediators such as neutrophil elastase (NE). In CF, extracellular NE activity strongly correlates (negatively) with lung function. Despite this critical pathological importance, it remains unclear how and why NE and other granule mediators from PMNs are released into the lung lumen. In studies presented here, we describe for the first time the development of an *in vitro* model system that recapitulates the functional and metabolic changes that occur upon PMN recruitment to the CF lung. Using this model, we show that airway fluid from CF patients induces rapid transepithelial migration, primary granule release, increased glycolysis, and oxidant production by recruited PMNs. We also show that CF airway PMNs *in vivo* and *in vitro* increase intracellular caspase-1 activity, and surface expression of IL-1R1, both key elements of the inflammasome pathway. Moreover, we find that extracellular vesicles (EVs) from CF airway fluid are able to induce caspase-1 activation in naïve PMNs and airway epithelial cells. Conditioned PMNs also release resistin, an immunometabolic mediator which levels correlate strongly with lung disease in both children and adults with CF. Collectively, conditioning by CF airway fluid results in the development of the pathogenic "GRIM" PMN fate, featuring heightened primary granule release, immunoregulatory functions (arginase-1 and caspase-1 activation), and metabolic licensing. We identify GRIM PMNs in COPD and severe asthma (both *in vivo* and in our *in vitro* model) suggesting that this pathogenic fate is not restricted to CF. Finally, we show that the metabolic drug metformin modulates GRIM PMNs by decreasing their metabolic activity, granule release and oxidant production. Our work open new avenues for better understanding and targeting the process of pathogenic conditioning of PMNs as it occurs in chronic inflammatory airway diseases such as CF, COPD, and severe asthma.

Pathological Conditioning of Neutrophils in Airway Inflammation

By

Osric Forrest

B.S., Hampden-Sydney College, 2012

Advisor: Rabindra Tirouvanziam, Ph.D.

A dissertation submitted to the Faculty of the
James T. Laney School of Graduate Studies of Emory University
in partial fulfillment of the requirements for the degree of

Doctor of Philosophy
in Immunology and Molecular Pathogenesis

2018

Acknowledgement

The work presented in this dissertation is the product of the collective support and mentorship of a large group of individuals, without whom none of this work would have been possible. First, I would like to thank my mentor Dr. Rabindra Tirouvanziam, who early in his time at Emory took a chance and allowed me join his new lab at the Emory Children's Center. Here he gave me the freedom to explore and drive the questions I found most interesting scientifically and supported all my endeavors, as inconvenient as they might have been, and to develop my other interests outside of the laboratory. Through our countless discussions about science, mentorship, and world politics, I learned a lot, not only about what it means to be a great scientist, but also an adult and a world citizen.

To the other members of the Tirouvanziam lab, especially the early members Dr. Julie Laval and Dr. Sarah Ingersoll, I am grateful for the strong foundation you established in the lab, and your willingness to train me. I am forever indebted to you for the feedback, peer review, and advice you have given me through the years. If my time in the lab has been such a great learning and supportive experience, it is in large part due to the guidance and cheerful disposition of Dr. Milton Brown. Thank you for your help troubleshooting last-minute experiments, and your willingness to help procure back-ordered supplies, as well as unwavering support throughout all of my experimental efforts. I am also thankful for the opportunity during my time in the lab to work and mentor several undergraduate and high school students. Most notably I am thankful for the work of Sanjana Rao and Helen Li that is showcased in this dissertation.

Finally, the work presented here is also the product of a coordinated effort of numerous clinical research coordinators, scientists, and physicians within the Center for Cystic Fibrosis and Airways Disease Research (CF-AIR), and the participation of

patients with CF and other diseases and their families, who through their effort have given me the opportunity to access clinical samples.

Lastly, I would like to acknowledge the support of my family. From an early age, my parents have fostered my unquenchable curiosity and sense of adventure. I am grateful for all the sacrifices that they made to ensure that my sister and I received the best education possible, and for their support in allowing me to pursue my dreams, even when they took me miles from home. This dissertation is a testament to your commitment to ensuring that your children had access to more opportunities than you had for yourselves, and to your dedication to prepare us to overcome the hurdles that life sometimes presents.

Thank You

Table of Contents

Chapter 5: Summary and Future Directions

Figure Index

Chapter 1: An Introduction to Neutrophil Development, Function, and Regulation, with a Focus on Their Impact on Cystic Fibrosis Airway Inflammation

Chapter 2: Pathological Conditioning of Human Neutrophils Recruited to the Airway Milieu in Cystic Fibrosis

Chapter 1

An Introduction to Neutrophil Development, Function, and Regulation, with a Focus on Their Impact on Cystic Fibrosis Airway Inflammation

Chapter 1

INTRODUCTION

Polymorphonuclear neutrophils (PMNs) have long been appreciated l their important role in innate immune responses, as they play an integral role in sensing and clearance of microorganisms. Since their identification as important phagocytes and rich sources of proteases and anti-microbial proteins, the contribution of PMNs to immunity is being re-assessed to include critical immunomodulatory functions that place them at the crossroads between innate and adaptive immune processes, and prefigure the development of novel PMN-targeted therapies for relevant pathologies. It is important not to underestimate the importance of PMNs, which represent the major leukocyte subset in human blood, accounting for 50-70% of total leukocytes (1). The abundant population of PMNs in blood is fueled by their continued production in the bone marrow at a rate of 10^9 per kg per day, which underscores the body's considerable energy commitment to PMN production (1, 2). Remarkably, this rate can increase by up to ten-fold under conditions of stress or infection, reaching 10^{10} PMNs per kg per day (2). Here, we will review conventional and novel concepts pertaining to PMN biology with a particular focus on recent studies documenting their remarkable functional, metabolic, and transcriptional plasticity in homeostasis and disease.

PMN DEVELOPMENT

Lineage origin. All immune cells in the body originate from a population of pluripotent hematopoietic stem cells (HSCs) located in the bone marrow from the third trimester of gestation and onwards (3). In the bone marrow, HSCs undergo cycles of division and differentiation to engender myeloid and lymphoid lineages of immune cells. This process,

termed hematopoiesis, allows for the production of mature red blood cells, megakaryocytes and platelets, granulocytes (including PMNs), macrophages and lymphocytes. In humans, 50-60% of the bone marrow are occupied by cells of the PMN sub-lineage (4). Although PMNs were thought to differentiate from common myeloid progenitors (CMP), recent work has linked their ontology instead to lymphoid-primed multi-potent progenitors (LMPPs), also derived from HSCs in the bone marrow, and which are now understood to differentiate into granulocyte-monocyte progenitors (GMPs) (5, 6).

PMN development from HSCs is divided into the three distinct phases, namely the stem and precursor cell stages leading to lineage commitment, mitotic proliferation of committed PMN progenitors, and post-mitotic differentiation into mature PMNs **(Table 1.1)**. During the mitotic stage, dividing PMN precursors transition from myeloblasts to myelocytes, allowing for expansion and early gradual differentiation. The post-mitotic stage encompasses three maturation steps during which cells progress from metamyelocytes, to band cells, to fully mature segmented cells (4, 7). Under homeostatic conditions, the transition time for complete PMN maturation takes between 96 and 144 hours (i.e., between 4 to 7 days), although this process can be dramatically shortened in response to acute infection, down to 48 hours (8).

Molecular control. The progressive differentiation and development of PMNs in the bone marrow is controlled by distinct cues from the bone marrow stroma, which is composed of a mix of osteoclasts, osteoblasts, fibroblasts, endothelial cells, and macrophages. As PMNs differentiate in the bone marrow, they receive distinct signals such as CXCL12 (CXC chemokine ligand 12, also known as stromal derived factor-1, or SDF-1) and VLA-4 (very-late antigen-4) that together orchestrate their retention in the bone marrow. As PMNs

mature, the expression of both CXCR4 (CXC chemokine receptor 4, which binds CXCL12) and VCAM-1 (vascular cell adhesion molecule 1, which binds VLA-4) decreases, allowing them to exit the bone marrow following cues from the periphery (9). Granulocyte colony stimulating factor (G-CSF) is another important regulator of PMN development that stimulates increased proliferation and differentiation of PMN progenitors, and release of mature PMNs into the periphery through the regulation of the CXCR4/CXCL12 axis.

Development of PMNs from HSCs in the bone marrow depends on the integration of signals that modulate transcription factors, which in turn genetically control the commitment of the chain of precursors along the myeloid lineage to granulocytic and PMN sub-lineages. In particular, the commitment of myeloid precursors toward granulocyte or monocyte sub-lineages is dictated by the balance between expression of the transcription factors C/EBP alpha and PU.1 (10-13), while the transcription factor GFI-1 is required for downstream PMN differentiation. In addition, to transcription factors, the induction of autophagy has been shown recently to be a negative regulator of PMN development (14).

The pace of PMN production in the bone marrow and overall number of PMNs released in to the bloodstream are modulated by signals from the periphery (15). For example, during the resolution of an acute inflammatory episode, PMNs die by apoptosis and are cleared by scavenging macrophages and dendritic cells in peripheral organs, which leads to a reduction in the levels of interleukin (IL)-23. This, in turn, down-regulates the amount of IL-17A produced by regulatory T cells, which leads to decreased granulocyte/monocyte-colony stimulating factor (GM-CSF) signaling, and a lower pace of PMN production in the bone marrow (8)

Granule biogenesis. A hallmark of PMNs and other granulocytes is the presence of a dense population of cytosolic granules containing membrane receptors, enzymes and antimicrobial effector molecules (16, 17. During PMN development, the various granule components emerge sequentially as cells transition from myeloblast to promyelocyte, to segmented stages of differentiation. PMN granules are divided into three classes defined by their distinctive granule proteins, namely, primary granules which contain myeloperoxidase (MPO) and neutrophil elastase (NE), secondary granules with lactoferrin, and tertiary granules which contain gelatinase (also known as matrix metalloproteinase-9, or MMP-9). PMN granules are formed by sequential transcription and packaging of proteins during bone marrow development {Rorvig, 2013 #216, 18, 19). Consistent with this notion, proteins synthesized after PMN release from the bone marrow are not found in the granules. In addition, PMNs contain a population of secretory vesicles produced by endocytosis of plasma membrane, yielding a compartment of ready-to-use receptors (20).

LIFESPAN AND RECRUITMENT TO THE PERIPHERY

Transendothelial and transepithelial migrations. After mature PMNs are mobilized from the bone marrow into the bloodstream, they may exit the bloodstream if they are recruited to a peripheral tissue incurring injury or infection. This involves a coordinated multi-step process by which PMNs flowing in the bloodstream are slowed down by adhesion molecules expressed by endothelial cells, after which they roll, then firmly adhere to the endothelium and proceed with diapedesis to cross the endothelium and make their way into tissues (21) **(Figure 1.1)**.

Rolling is initiated first through the activation of endothelial cells by inflammatory stimuli such as tumor necrosis factor (TNF)-α and IL-1β. As PMNs roll along the

endothelium, their surface adhesion molecule P-selectin ligand-1 (PGSL-1) binds to P- and E-selectin on the endothelium. This is followed by binding of lymphocyte function-associated antigen (LFA)-1 expressed on the PMN surface to intercellular adhesion molecule (ICAM)-1 on the endothelium, which slows and arrests PMNs. This in turn promotes intercellular communication through the engagement of chemokine receptors and increased inside-out signaling (15, 22). Recent studies also suggest that as PMNs adhere and crawl along the endothelium, they actively scan for an optimal site for transendothelial migration into tissues, a process controlled in part by an intravascular gradient of chemoattractants (23). PMNs then migrate by passing through intercellular junctions between endothelial cells. In order to make their way through the extracellular matrix of the tissue toward the site of injury or infection, PMNs then unleash granule proteases such as MMP-9 and NE.

As occurs frequently in the case of mucosal injuries or infection, PMNs transiting through tissues continue to travel through the tissue interstitium and epithelium, and into the luminal space. In order to cross the epithelium, PMNs must migrate via the paracellular route through intercellular junctional complexes. This migratory process is facilitated by transient interactions with junction proteins like occludins, claudins and junctional adhesion molecules (JAM), and through adherens junctions. When excessive, transepithelial PMN migration can result in increased permeability and loss of barrier function (24).

Regulation of lifespan in homeostasis and inflammation. PMNs are conventionally viewed as short-lived effectors, with an average lifespan of 4-8 hours in blood. However, a recent deuterium pulse-chase study suggested an average lifespan of human blood PMNs as long as 5.4 days in normal homeostasis (25). While the assumptions and computational model leading to these results are hotly debated, the notion that PMNs last for less than a

day needs revisiting nonetheless, since bacterial products and inflammatory mediators have long been known to extend PMN lifespan during inflammatory responses (26). PMN lifespan is also increased significantly by transepithelial migration, which delays apoptotic signaling via down-regulation of pro-apoptotic receptors (e.g., Fas-L), and enzymes (e.g., caspases) (27, 28). Reconsidering the question of PMN lifespan in the periphery also pushes to reconsider their function, as PMNs can exert not only acute, but also chronic influences on the microenvironment in peripheral tissues,. This is particularly important in mucosae, in which PMNs interact with the epithelium and with other cells of the adaptive and innate immune system.

In chronic inflammatory diseases such as rheumatoid arthritis (RA), chronic obstructive pulmonary disease (COPD), and chronic granulomatous disease (CGD), the lifespan of PMNs has been shown to be significantly augmented (29). In fact, in several acute and chronic diseases, the length of inflammatory bouts is in part controlled by an altered lifespan of PMNs in tissues (30, 31). This illustrates the mutual relationship between inflammation and PMN survival, which in chronic diseases can impact disease severity. PMN lifespan is also modulated by cell density and inflammatory mediators including cytokines, chemokines, and damage-associated molecular patterns (DAMPs) released by host cells during infection and tissue damage (29). One example of such mediators is leukotriene B4 (LTB4), a significant driver of inflammation in diseases such as cystic fibrosis (CF), asthma, and gout. In addition to its well-known role as a PMN chemoattractant, LTB4 can delay apoptosis of inflammatory PMNs by increasing degradation of the pro-apoptotic factor Bad (29, 32). Another example is granulocyte-colony stimulating factor (G-CSF), a growth factor released by endothelial and epithelial cells to induce increased bone marrow granulopoiesis, and which also acts as a pro-survival signal by increasing the expression of

proliferating cell nuclear antigen (PCNA) in PMNs, thereby inhibiting pro-apoptotic caspases (33).

Apoptosis and clearance. The kinetics of PMN clearance from the periphery were studied in labeling studies, in which it was observed that PMNs injected in bloodstream have a lifespan of 7 hours before being cleared in the liver (8, 34). One caveat of these studies is linked to potential changes in surface properties of injected PMNs leading to artefactual trapping and/or clearance. This has motivated the use of deuterium pulse-chase and mathematical modeling methods, themselves fraught with controversy (35). Regardless, one critical mechanism of PMN clearance relies on surface expression of the chemokine receptor CXCR4. In mice, senescent blood PMNs increase expression of CXCR4, which leads to their sequestration in the bone marrow and subsequent apoptosis, after which they are phagocytosed by stromal macrophages (34, 36-39). Interestingly, CXCR4 is expressed highly in maturing PMNs, acting as a retention mechanism to promote proper differentiation in the bone marrow. The same receptor appears to be co-opted as aging blood PMNs return to the bone marrow for clearance. As mentioned above, tissue PMNs can also be phagocytosed by scavenger macrophages and DCs, which modulates the production of PMNs in the bone marrow (8).

PMN heterogeneity and phenotypes. PMNs were once thought to be terminally differentiated cells after their maturation and release from the bone marrow. However, once in the periphery, under both homeostatic and inflammatory conditions, distinct PMN subsets emerge. These are defined by their function, distinct surface phenotype, relative density, and tissue localization **(Figure 1.2)** (6, 40). One such subset that emerges in the

blood under homeostatic conditions corresponds to *aged PMNs* ($CD62L^{low}$, $CXCR4^{+}$) (41). Aged PMNs home to the bone marrow, display a distinct pattern of gene expression that follows circadian rhythm, and enact a peripheral signal regulating hematopoiesis (42). Under acute inflammatory conditions, another distinct PMN subset emerges termed *low-density neutrophils (LDN)*. LDN are detected in various disease settings, and are considered to be pro-inflammatory in most occurences. However, in certain cancers, they can act as myeloid-derived suppressor cells (MDSCs), inhibiting T cell function (43, 44). Another distinct subset of mature PMNs emerges upon LPS stimulation, and is defined by distinctive relative expression of CD16 and CD62L. Interestingly, these *$CD16^{high}$ $CD62L^{low}$ PMNs* have high cell surface CD11b and production of ROS, which contribute to their immunomodulatory functions and ability to suppress T cells (45, 46). Finally, following the M1 and M2 nomenclature used to describe pro- and anti-inflammatory macrophages, respectively, N1 and N2 subsets of PMNs have been observed in certain cancers as one mechanism of tumor-immune evasion and suppression, primarily regulated by TGF-β secretion (47-49). Despite the heterogeneity of PMN subsets described in the literature, it is still not clear whether or not these subsets represent distinct developmental and/or functional paths, as their ontogeny has not been fully elucidated.

CORE FUNCTIONS

Reactive oxygen species (ROS) release. PMNs are capable of producing ROS upon assembly of the multi-protein nicotinamide adenine dinucleotide phosphate (NADPH) oxidase complex on both plasma and phagosomal membranes, resulting in a respiratory burst that uses oxygen and NADPH to produce superoxide, which is the parent ion for downstream production of other ROS, including hydrogen peroxide (50, 51). The primary

granule enzyme MPO can combine hydrogen peroxide with halide ions to form hypohalous acids such as hypochlorous acid (HOCl, the active component of bleach), which act to destroy phagocytosed microbes (52). Interestingly, assembly of the NADPH oxidase complex NOX2 in close proximity to phagosomes is associated with fusion of both primary and secondary granules in PMNs (53).

Degranulation. A key mechanism by which PMNs combat microbes is the mobilization of cytosolic granules containing receptors, enzymes and antimicrobial effectors. This degranulation process depends on the movement and subsequent fusion of granules with the plasma membrane or phagosomal compartment. Cytosolic movements of granules are regulated by rearrangements of the actin cytoskeleton and microtubules, which require ATP and are modulated by changes in intracellular Ca^{2+} (54). Secretory vesicles, tertiary, secondary and primary granules are released hierarchically and vary in the degree to which they are able to be mobilized to the cell surface (55). Secretory vesicles are the first and easiest to mobilize (generally upon priming or diapedesis of PMNs while still in the bloodstream), followed by tertiary granules during diapedesis and tissue migration, and secondary granules during tissue and transepithelial migration, while primary granules are the most difficult to mobilize (56). This is of critical importance since primary granules contain the most toxic mediators, (e.g., NE and MPO), which can exert severe damage to neighboring cells if these granules are mobilized to the plasma membrane and the mediators are released extracellularly (20). *In vitro*, the bacteria-derived formyl peptide fMLF can trigger the release of secretory vesicles, while the phorbol ester phorbol myristate acetate (PMA) induces release of secretory vesicles and tertiary granules, with limited release of secondary and primary granules (57-59).

Generally, pro-degranulation stimuli work by activating protein tyrosine kinases and phospholipases, which in turn trigger the release of Ca^{2+}. The fusion of granules to membranes is dependent upon Soluble N-ethylmaleimide-sensitive factor Attachment protein Receptors (SNAREs), and their downstream interactions with Rab GTPases, and regulated via the reorganization of the actin cytoskeleton (60). One particular Rab GTPase, Rab27a, has been implicated in the regulation of the exocytosis of tertiary and secondary granules (61). Much remains to be understood regarding how PMNs control the targeted release of their various types of granules. This is a highly critical area of research, since excessive PMN degranulation underlies numerous intractable inflammatory diseases (e.g., RA, COPD, CF), such that specific targeting of degranulation pathways may provide a new modality for therapeutic development (62).

Phagocytosis. PMNs depend on phagocytosis to take up extracellular microbes and cell debris into an intracellular compartment called the phagosome (63). This process is triggered by interactions between pathogen-associated molecular pattern molecules (PAMPs) on the surface of microbes, or damage-associated molecular pattern molecules (DAMPs) on host cell debris with cognate pattern-recognition receptors (PRRs) at the surface of the PMNs (64). Phagocytosis can also be triggered by complement or immunoglobulin (Ig) molecules, which serve as bridges (opsonins) between tagged microbes and cognate opsonoreceptors on PMNs (65). Once the phagosome has been formed by receptor-mediated endocytosis, intracellular granules become available for fusion with this intracellular compartment, thus delivering large amounts of antimicrobial and proteolytic effectors therein (66). The NADPH oxidase enzyme complex also assembles at the phagosomal membrane, which decreases intraphagosomal pH and enhances the activity of proteases (51).

Neutrophil extracellular traps (NETs). Recent studies have identified a new modality by which PMNs can release the content of their granules extracellularly. This process depends on the fusion of primary granules with the nucleus, leading to the release of a mesh of DNA, histones, NE and MPO that together form neutrophil extracellular traps, or NETs, which are endowed with antimicrobial functions (67). While NET formation from nuclear DNA results in the death of PMNs, it has been reported that the DNA scaffold of NETs can also originate from mitochondria, after which PMNs may remain alive (68). NET release has been observed in the context of infection by *S. aureus* and other bacteria, against which PMNs are able to rapidly release NETs while still maintaining their phagocytic and migratory capabilities. NET release is also regulated by NE and MPO, which translocate to the nucleus after forming a complex with DNA and degrading F-actin filaments in the cytosol (69, 70).

The pathophysiological roles of NETs are still under debate. While NETs may trap pathogens and limit their growth, they may also lead to the persistence of DNA-protein complexes that can trigger autoimmune reactions in RA, systemic lupus erythematosus (SLE), and atherosclerosis. In addition, our current understanding of the mechanisms that control and drive NETosis is limited by the use of activators for its *in vitro* induction. Indeed, triggers of NETosis *in vivo* differ from those used *in vitro*. Interestingly, some pathogens have developed mechanisms to escape NET-mediated killing, such as DNAse release to degrade the DNA scaffold of NETs (71-73).

METABOLIC AND TRANSCRIPTIONAL REGULATION

Fulfilling the energy needs of PMNs. PMN function requires a large amount of energy in the form of ATP (74). In order to provide this energy, PMNs metabolize nutrients via either fast or slow metabolic turnover **(Figure 1.3)** (75). A core mechanism providing energy for

cell function is glycolysis - the process by which glucose is converted in the cytoplasm to pyruvate and then lactate, yielding a rapid, but limited burst of ATP production (2 ATP per glucose). Pyruvate may also be shuttled to the mitochondria and converted to acetyl-CoA to enter the tricarboxylic acid (TCA) cycle. The TCA cycle produces NADH that then fuels oxidative phosphorylation (OxPhos), a slow but high yield ATP-producing route (depending on various electron transport processes in the mitochondria, yielding up to 28 ATP per glucose). Both glycolysis and OxPhos pathways are not solely catabolic, but also provide intermediates for ribose, fatty acids, and non-essential amino acid biosynthesis (74, 76, 77).

The main energy source for PMN chemotaxis and other functions is glycolysis (78). Compared to other immune cells, PMNs have fewer mitochondria, leading to the assumption that OxPhos plays a small role in their energy metabolism (79). Consistently, inhibitors of OxPhos have little effect on PMN function (78, 80, 81). Using the recently developed Seahorse platform, it was confirmed that PMNs have little to no dependency on OxPhos, and that glycolysis is not increased when mitochondrial ATP synthase is inhibited, although it is highly induced upon activation of the oxidative burst (75, 82).

Glycolysis and pentose phosphate pathway. Warburg described a metabolic switch occurring in tumors under normoxic conditions, in which glycolysis dominates despite the availability of oxygen for OxPhos (83). In PMNs, glucose consumption increases dramatically upon activation by the TLR4 agonist LPS, followed by an increase in oxygen consumption after assembly of the NADPH oxidase complex (84). Indeed, glycolysis in PMNs is a major source of NADPH, which is the rate-limiting substrate used by NADPH oxidase in combination with oxygen to generate superoxide. As discussed above, superoxide and downstream ROS are critical mediators for PMN killing of bacteria and other pathogens

(85, 86). Consistent with the notion that PMNs strongly depend on glycolysis for adequate function, PMN migration, phagocytosis, and bacterial killing capacity are all severely impaired upon exposure to glycolysis inhibitors such as 2-deoxyglucose (2-DG) (87, 88).

Increased glucose uptake in PMNs and macrophages upon LPS stimulation promotes both the glycolytic pathway, as detailed above, and the pentose phosphate pathway (PPP) (89-91). The PPP pathway is a critical source of 5-carbon sugars, which drive nucleotide biosynthesis (notably NADPH), fatty acid synthesis, and the reduction/recycling of the intracellular antioxidant and signaling intermediate glutathione (GSH) (75). Glucose shuttled through the PPP can be re-appropriated into the glycolysis upstream of pyruvate, where it can increase lactate production, or enter the TCA cycle (91). In macrophages, an important regulator of this pathway has been identified. Specifically, LPS stimulation of macrophages decreases the expression of carbohydrate kinase-like (CARKL) protein, which results in increased glucose flow through the PPP (90). Alternatively, increased CARKL expression antagonizes glycolytic flux through the PPP, thereby decreasing the rate of glycolysis and downstream induction of ROS and inflammatory cytokines (90). Additionally, shunting of glucose towards the PPP appears to be an important mechanism to control NET production through modulation of the NADPH oxidase complex, which also appears to be a key modulator of NETosis (89).

Oxidative metabolism. As stated earlier, PMNs possess a relatively small number of mitochondria. Thus, it is not surprising that mitochondrial respiration/OxPhos accounts for 5 percent or less of the glucose consumed by PMNs, unlike other immune cells in which OxPhos is the dominant pathway for glucose metabolism (81). However, because of its molar efficiency in generating ATP from glucose (ATP:glucose ratio of about 28:1 for

OxPhos, compared to 2:1 for glycolysis), OxPhos still provides nearly half the ATP in PMNs (92, 93). Additionally, modulation of mitochondrial membrane potential affects redox balance, apoptosis, and NETosis in PMNs (94). Despite initial observations suggesting that mitochondria contribute little to energy production in PMNs, more recent work has revisited this assumption by showing that PMNs possess a developed mitochondrial system. In PMNs, chemical uncouplers of the electron transport chain in mitochondria disrupt their rate of migration, while having no effect on respiratory burst or phagocytic capacity (81). These and other observations suggest that mitochondria may play a more important role than generally thought in PMN metabolism and function, although more research is needed to further clarify this role.

Lipid metabolism. PMNs and other immune cells can use not only glucose, but also others nutrient sources such as lipids which provide energy through the breakdown of fatty acids via fatty acid oxidation (FAO) (95). FAO is a metabolic process whereby fatty acyl-CoA molecules are used to shuttle acetyl-CoA in the TCA cycle to generate ATP by OxPhos. Lipid biosynthesis and utilization are important regulators of PMN function. In DCs, the balance between fatty acid synthesis and oxidation plays an important role in governing their function. Citrate for example is a rate-limiting substrate for fatty acid synthesis, which is required for DCs to increase cell size and support anabolic activities (96, 97). In macrophages, a metabolic shift towards fatty acid synthesis and away from FAO drives the development of pro-inflammatory functions, and it is possible that other myeloid cell subsets such as PMNs increase the production of important inflammatory mediators in part via increased lipid biosynthesis (98, 99). More recently, autophagy was discovered to be an important regulation of lipid metabolism in PMNs (100). Autophagy-deficient PMN

precursors displayed decreased mitochondrial respiration, but excessive glycolysis and lipid drop accumulation. It was only through administration of exogenous free fatty acids that mitochondrial respiration could be rescued. This finding shows that in PMNs, autophagy is an important regulator of FAO and oxidative metabolism to support energy production during development and differentiation (101).

mTOR and AMP kinase. The mechanistic target of rapamycin (mTOR) is a serine/threonine kinase pathway composed of two complexes (mTORC1 and mTORC2) that serves as an important nutrient sensor coordinating cellular responses to changes in the supply of amino acids, glucose, and other nutrients (102). The mTOR pathway supports increased anabolic activity in highly proliferating cells (e.g., embryonic or tumor cells), or other metabolically demanding situations such as acute immune cell activation following TLR stimulation (103). For example, activation of the mTOR pathway triggers increased synthesis of nucleic acids, proteins, and lipids which are subjected to a highly increased turnover during immune activation.

In PMNs, treatment with the mTORC1 complex inhibitor rapamycin leads to strong inhibition of chemotaxis and migration (104). Consistently, PMN chemotaxis and migration are tightly controlled by changes in the actin cytoskeleton occurring at the leading edge of PMNs under signaling by Rho GTPases and the Akt2 kinase, both known mTOR targets (105-107). Furthermore, inhibition of mTOR also impacts NETosis through the modulation of the transcription factor hypoxia inducible factor 1 alpha (HIF-1α, see below) and autophagy (107, 108). Counterbalancing mTOR signaling, the energy-sensing enzyme AMP-activated protein kinase (AMPK) serves to conserve energy when nutrients are limiting by inhibiting anabolic activity and enhancing catabolic pathways such as FAO. *In vitro*, PMN

treatment with a pharmacological activator of AMPK, 5-aminoimidazole-4-carboxamide-1-β-D-ribofuranoside (AICAR), concomitantly with LPS stimulation, inhibits the degradation of IκBα and nuclear translocation of NFκB and subsequent synthesis and release of TNF-α and IL-6 (109). *In vivo*, AICAR treatment in a model of acute lung injury decreases the amount of inflammatory cytokines, PMN accumulation, and overall injury, consistent with *in vitro* findings (109).

HIF-1α and glycolysis in PMNs. The transcription factor HIF-1α is an important molecular checkpoint in metabolism, translocating to the nucleus when cells are exposed to low extracellular oxygen, and subsequently binding to transcriptional sequences of genes encoding glycolytic enzymes and other important metabolic regulators (110). Functionally, HIF-1α promotes the switch to glycolysis that supports the ability of immune cells to produce ATP when oxygen is limited but energy demands are increased dramatically. In PMNs, HIF-1α supports a metabolic switch to glycolysis (111). Specifically, HIF-1α transcriptionally activates the glucose transporter Glut1 and the glycolytic enzyme phosphoglycerate kinase (PGK), upregulating glycolysis under conditions of hypoxia and/or infection. Importantly, activated PMNs consume oxygen at a very high rate, due to NADPH oxidase activity, which triggers profound local hypoxia in the inflammatory microenvironment (112). In turn, sustained HIF-1α signaling induced by this local hypoxia not only influences the metabolic status of PMNs, but also delays their apoptosis through combined HIF-1α and NF-κB signaling (113).

Transcriptional control and plasticity of PMN function. As described earlier, PMN production in the bone marrow is a highly coordinated, stepwise process controlled by

various transcription factors. In particular, C/EBPϵ acts a key transcription factor induced by C/EBPα and G-CSF to regulate the production of mature PMNs. Mature PMNs themselves are conventionally thought to be quiescent cells endowed with a short lifespan and highly condensed chromatin, and therefore not prone to profound transcriptional and functional changes. Importantly, the artillery of cytosolic granules mobilized upon activation are also pre-packaged in mature PMNs, and do not require *de novo* transcription and translation. Nevertheless, recent advances in tools for transcriptional analysis have forced researchers to revisit this paradigm, demonstrating that mature PMNs are endowed with surprising transcriptional plasticity when exposed to environmental signals in peripheral tissues, resulting in profound alterations in gene expression as PMNs transition from the circulation to sites of inflammation (114). Exposure to bacteria also alters PMN expression of genes for cytokines, surface receptors, and apoptosis-related proteins (115-118). In an added twist, polymorphisms in regulatory regions (also known as expression quantitative trait loci, or eQTLs) have been shown recently to exert significant allelic control on PMN gene expression during both bone marrow maturation and peripheral activation, leading to significant inter-individual differences (119). Thus, PMNs are transcriptionally plastic, both within and among individuals.

PMNs IN CYSTIC FIBROSIS AIRWAY INFLAMMATION

Cystic fibrosis (CF) pathogenesis. CF is the most frequent lethal genetic disease among Caucasians, resulting from mutations in the CF transmembrane conductance regulator (*cftr*) gene (120). Roughly 1 in 25 Caucasians is an heterozygous carrier of one wild-type and one mutated *cftr* allele, leading to an incidence of homozygous CF patients of about 1 in 2,500 live births (121). The CFTR protein is a cAMP-dependent channel for small anions that is

expressed mainly in exocrine epithelia throughout the body, and its loss leads to multiorgan disease in CF patients. In CF airways, CFTR dysfunction is associated with PMN-dominated inflammation, defective mucus clearance, and chronic microbial infection, leading to luminal obstruction and proteolysis and distension of the lung lamina propria, also known as bronchiectasis (122). The classic paradigm for CF airway disease pathogenesis holds that CFTR dysfunction results in defective chloride efflux and sodium hyperabsorption by the airway epithelium, which in turn dehydrates the airway surface liquid and promotes microbial stasis, followed by PMN recruitment. CFTR dysfunction has also been shown to hamper the normal reabsorption of luminal glucose and amino acids by the epithelium (123).

PMN contribution to CF airway inflammation. It is widely accepted that the presence of PMNs and PMN-derived products contributes significantly to CF airway disease progression (124). The unique microenvironment of CF airways triggers a pro-inflammatory loop that supports the early, massive, and sustained recruitment of PMNs into the lumen (125). Recruited PMNs produce reactive oxygen species (ROS) and release granule enzymes like NE and other proteases that play a major role in tissue destruction. Consistently, NE activity in the airway fluid is the strongest known predictor of CF lung function (125). Powerful proteolytic and oxidative activities of PMNs progressively overwhelm normal repair capacities, resulting in progressive destruction and lung failure (122). To this day, it is still not fully understood how and why PMNs are initially recruited to the CF lung. PMN chemoattractants such as LTB4 are known to be elevated in CF airway fluid, especially in patients infected with opportunistic *P. aeruginosa* bacteria (126). Early in the disease, detectable levels of the PMN chemoattractant chemokine IL-8/CXCL8 have been reported in infants as early as 4 weeks, concomitant with PMN recruitment to the lungs (127).

However, it remains unclear why CF airway PMNs undergo profoundly dysregulated exocytosis of their granule components, notably primary granules, leading to the hyperactive exocytosis of NE and MPO (128), and also the release of DNA by NETosis (129).

PMN conditioning and dysfunction in CF airways. Several studies have suggested the existence of intrinsic defects in PMNs from CF patients, following the identification of CFTR mRNA and protein in PMNs, albeit at low levels. It has been suggested, in particular, that CF PMNs may have reduced chloride transport into the phagosome, resulting in impaired intracellular killing (130, 131). In addition, CF PMNs have been shown to spontaneously produce higher levels of ROS, which may function to not only mediate lung damage, but also further enhance recruitment of blood PMNs (132). CF PMNs have also been reported to migrate at an increased rate toward IL-8 (133). Contradicting the notion that intrinsic PMN defects underlie CF disease is the fact that CF patients do not present with systemic infections typically seen in primary immunodeficiencies. Instead, CF infections are localized to the lungs, suggesting a specific effect of the CF airway microenvironment (134). This microenvironment is influenced by PMNs themselves. For example, high levels of extracellular NE can induce synthesis and secretion of IL-8 by the airway epithelium, reduce ciliary beating frequency, and promote tissue damage (135). NE is also known to cleave important cell surface receptors such as phagocytic and complement receptors on PMNs themselves (136). Thus, excessive NE release coupled with an overwhelmingly high bacterial load in CF airways may severely dampen the efficiency of PMN-mediated phagocytosis (137, 138).

Recent research by our group has ushered a new paradigm for CF pathogenesis emphasizing a major role for live PMNs in causing airway damage. Indeed, we discovered

that a large subset of live PMNs present in CF airway fluid displays high surface expression of the primary granule marker CD63, reflecting high active release of NE-rich primary granules (139). Live CF airway PMNs also show robust pro-survival signaling with stable activation of the mTOR pathway (140), increased metabolite transporter expression, and increased glucose uptake (141), suggesting metabolic adaptation to nutrient-rich conditions in CF airway fluid. Based on these *in vivo* data, we hypothesize that CF airway fluid not only induces the migration of PMNs into the airway lumen, but also orchestrates their dysfunction therein, following active processes that may be modulated by specific drugs.

Animal models of CF airway disease. Since the cloning of the *cftr* gene in 1989, several murine models of CF disease have been developed (142-(142). These models generally recapitulate well pathological defects seen in the intestine, pancreas, and liver of CF patients. However, with the exception of some evidence for decreased mucociliary clearance in the airways, none of the existing murine models of CF properly mimic PMN-dominated lung inflammation as seen in humans **(Table 1.2)** (143, 144). Because of these limitations, CF models were developed in larger animals, such as the pig, ferret, and rabbit (145-147).

The pig model was developed using gene targeting technology allowing for the generation of *CFTR*$^{-/-}$ and ΔF508 homozygous animals, the latter reproducing the most common mutation of the *cftr* gene in humans. Phenotypically, these animals show deficient anion transport, develop intestinal symptoms, and pancreatic insufficiency like their mouse counterparts. Initial studies in that model suggested that CF pigs, similarly to murine models, do not present with a dominant lung phenotype like that seen in human disease (147). However, recent work suggests that CF pigs display defective antibacterial airway defenses

within hours of birth and after a few months begin to exhibit low-grade lung inflammation, although the contribution of PMNs to this phenotype is not as obvious as in patients (148).

In ferrets, CFTR deficiency causes the majority of animals to die within the first 48 hours of life due to intestinal complications, doubled by severe pancreatic insufficiency (149). While CF ferrets are susceptible to lung infections, there is no clear consensus on the development of a dominant pathological lung phenotype (144, 149). Recent data from a study of newborn CF ferrets identified early innate immune anomalies, abnormal airway surface liquid height, and defective secretion of antimicrobial proteins (150). While large CF animal models open new avenues for basic research and drug testing, their use is limited due to the major cost linked to their maintenance. This critical limitation emphasizes a need to establish orthogonal *in vitro* models to study CF.

***Ex vivo* and *in vitro* models of CF airway disease.** An early example of *ex vivo* CF models is the approach relying on the development of human fetal lung xenografts in immunodeficient mice (151-153). In that model, mature CF xenografts displayed expected deficiencies in ion transport and robust signs of inflammation compared to non-CF control xenografts, revealing primary defects in the regulation of lung defenses both prior to, and after infection (154, 155). Another approach to the development of CF models is based on the generation of 3D organoid cultures from induced pluripotent stem cells (IPSCs) (156) or foregut stem cells (157) that attempt to approximate the histological complexity of the lung microenvironment *in vivo*. Recent advances have allowed for further refinements of such organoid cultures by mimicking physiological conditions of shear stress and tension under fluid flow (158). Another approach relies on "organ-on-a-chip" systems based on microfluidic technology that can support co-culture of lung cells with other cells, including

but not limited to, PMNs. One such model has been developed to study small airway inflammation using differentiated bronchiolar epithelial cells cultured with inflammatory cytokines and immune cells to recapitulate key features of airway inflammation as it occurs in COPD and CF (159, 160). Thanks to the use of primary human cells, and the ability to optimize experimental conditions to recapitulate key features of human disease, such models can overcome some of the challenges inherent to animal models and serve as screening tools to identify new therapeutics relevant to human disease.

CONCLUSION

Recent insights into PMN biology reviewed in this chapter highlight key mechanisms that control the functional, transcriptional, and metabolic plasticity of these cells in conditions of infection and inflammation. These and other mechanisms play a pivotal role in determining the impact of PMNs on disease, and suggest potentially important avenues for novel PMN-targeted therapies. This is especially important in currently intractable airway inflammatory diseases such as CF, in which PMNs play a dominant role and are recognized as key drivers of disease pathogenesis, albeit without any adequate short- or long-term treatment option.

Table 1.1. PMN development in the bone marrow. Distinct changes occur in nuclear morphology, granule production, and surface expression of protein markers of maturation as PMNs transition from myeloblasts to fully segmented, mature PMNs (3, 6).

Cells	Nuclear Morphology	Granules	Cell Surface Markers
Myeloblasts	High nuclear to cytoplasmic ratio; prominent nucleoli	Small peroxidase-negative granules	CD33, CD13, CD15
Promyelocytes	Round nucleus	Primary granules appear	CD33, CD13, CD15
Myelocytes	Indented nucleus	Secondary granules appear	CD33, CD13, CD15, CD14, CD11b
Metamyelocytes	Kidney-bean shaped nucleus	Tertiary granules appear; Large and dense primary granules	CD33, CD13, CD15, CD14, CD11b
Band Cells	Condensed band shaped nucleus; smooth nuclear membrane	Secretory vesicles start to develop	CD33, CD13, CD15, CD14, CD11b, CD10, CD66b
Segmented PMNs	Condensed multi-lobed nucleus (2-5 lobes); irregular nuclear membrane with indentations	Full set of granules and vesicles	CD33, CD13, CD15, CD14, CD11b, CD10, CD66b, CD16, CD62L

Table 1.2. Animal models of cystic fibrosis. This table have been modified and adapted from: **(161) (162) (142)**

Phenotypes	Human	Pig	Ferret	Rabbit	Mouse
Spontaneous lung infection	Yes	Yes	Yes	Yes	None
Sustained neutrophil recruitment	Severe	Mild	Mild	Mild	None
Pancreatic insufficiency	Yes	Yes	Yes	Yes	None
Intestinal complications	Yes	mild to severe intestinal blockage	mild to severe intestinal blockage	mild to severe intestinal blockage	mild to severe intestinal blockage
Liver and gallbladder disease	Billary cirrhosis	Billary cirrhosis	Liver disease	Liver disease	Liver disease
Fertility	Severe vas deferens defect	Severe vas deferens defect	Severe vas deferens defect	ND	Impaired sperm transport

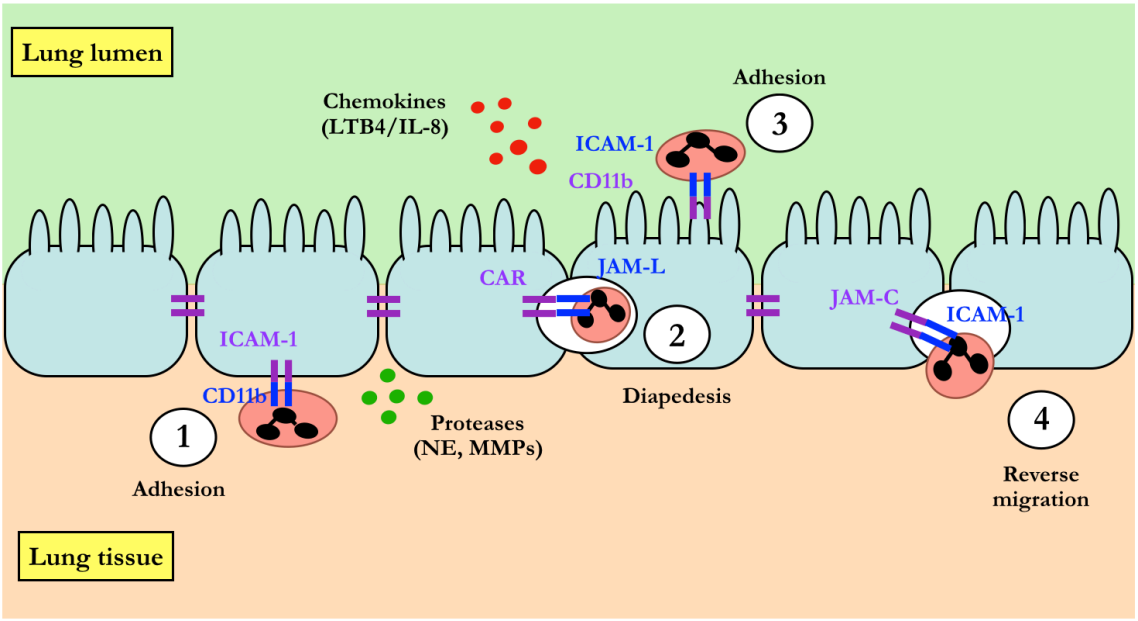

Figure 1.1. PMN transepithelial migration to the lung. PMNs recruited by cues present in the airway lumen undergo stepwise migration through the lung tissue via: 1) adhesion to the basal membrane of the epithelium, primarily through CD11b-ICAM-1 interactions; 2) diapedesis, which involves the release of proteases that facilitate PMN movement through adherens and tight junctions between epithelial cells, and PMN interactions with junction proteins such as CAR; 3) tethering and adhesion of recruited PMNs to the apical surface of the epithelium; and 4) possible reverse migration from the airway lumen back into the tissue and periphery through ICAM-1 and JAM-C junctional interactions.

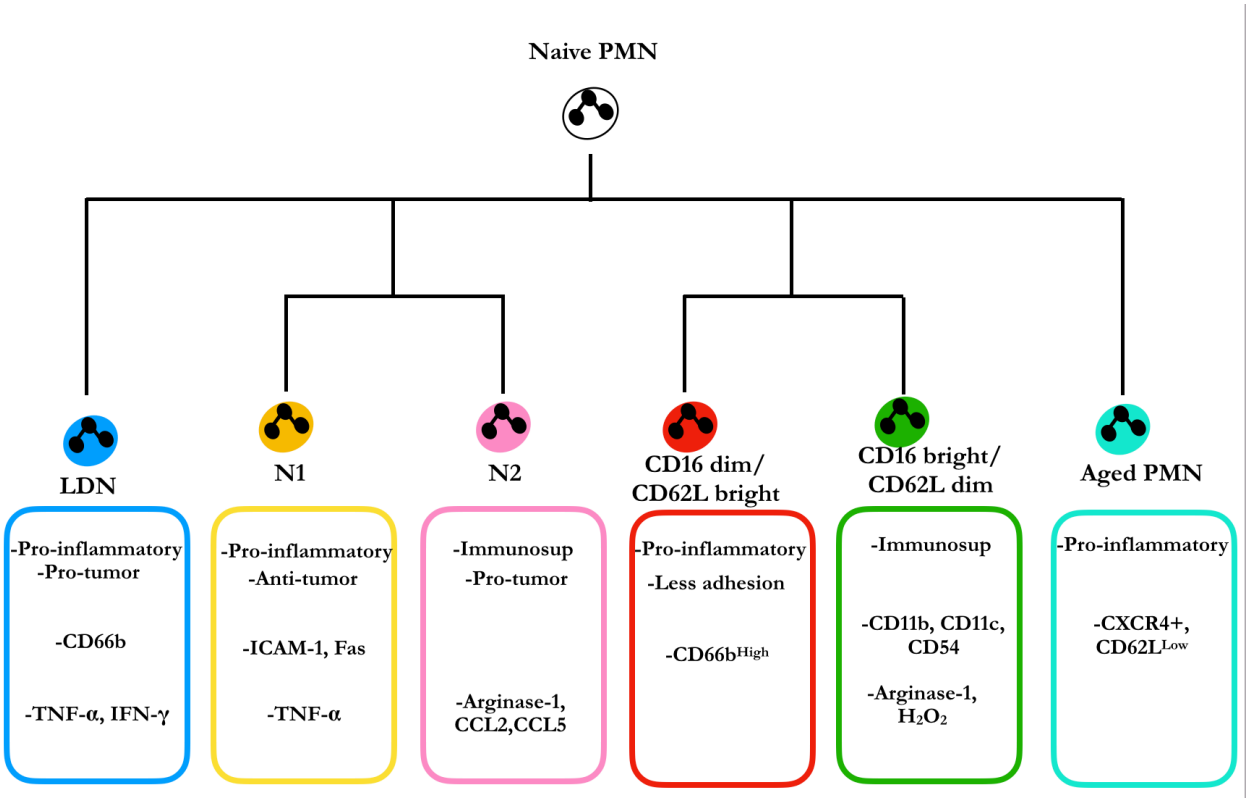

Figure 1.2. Heterogeneity and subtypes of PMNs. Peripheral PMNs demonstrate significant heterogeneity, with distinct subtypes appearing under both homeostatic and inflammatory conditions, and characterized by diverse pro-inflammatory and anti-inflammatory functions and cell surface markers. Immunosup: immunosuppressive (40).

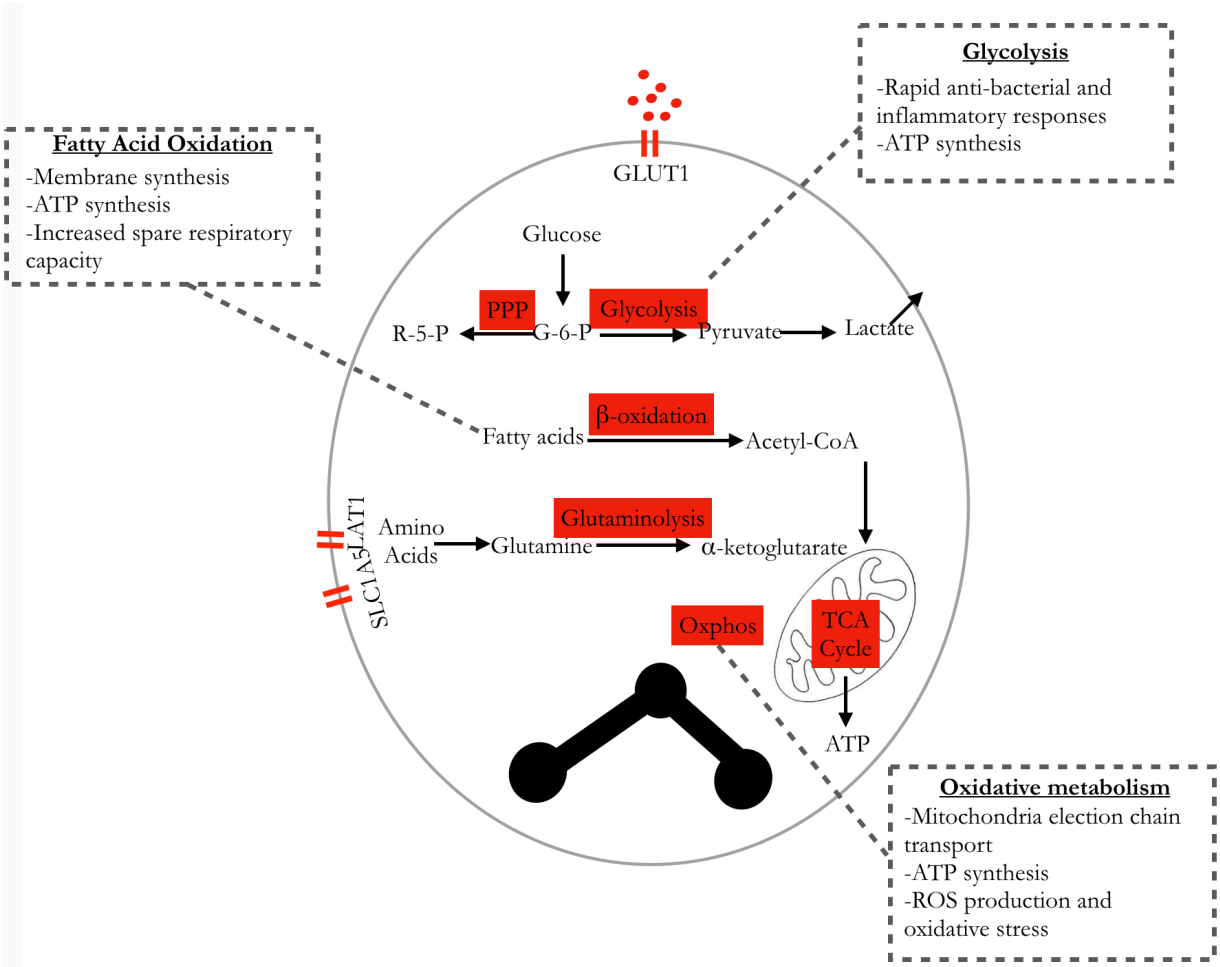

Figure 1.3. Metabolic pathways that support PMN function. PMNs are dependent on the flux of nutrients into the cell to generate the ATP needed to support both fast responses such as chemotaxis, as well as slower adaptations. 1) Glycolysis is the process by which glucose is converted to lactate producing two ATPs, or shuttled to the mitochondria to which fuel the tricarboxylic acid (TCA) cycle. 2) The pentose phosphate pathway (PPP) utilizes glucose to produce ribose, which aids in the biogenesis of nucleic acids, amino acids, and NADPH. 3) Fatty Acid Oxidation (FAO) allows for the generation of NADH and FADH, which are shuttled into the electron transport chain to generate ATP. 4) Oxidative metabolism uses pyruvate to drive oxidative phosphorylation, based on the translocation of protons across the mitochondrial inner membrane (163).

References

1. Furze RC, Rankin SM. Neutrophil mobilization and clearance in the bone marrow. *Immunology* 2008; 125: 281-288.

2. Summers C, Rankin SM, Condliffe AM, Singh N, Peters AM, Chilvers ER. Neutrophil kinetics in health and disease. *Trends Immunol* 2010; 31: 318-324.

3. Hoggatt J, Kfoury Y, Scadden DT. Hematopoietic Stem Cell Niche in Health and Disease. *Annu Rev Pathol* 2016; 11: 555-581.

4. da Silva FM, Massart-Leen AM, Burvenich C. Development and maturation of neutrophils. *Vet Q* 1994; 16: 220-225.

5. Gorgens A, Radtke S, Mollmann M, Cross M, Durig J, Horn PA, Giebel B. Revision of the human hematopoietic tree: granulocyte subtypes derive from distinct hematopoietic lineages. *Cell Rep* 2013; 3: 1539-1552.

6. Hong CW. Current Understanding in Neutrophil Differentiation and Heterogeneity. *Immune Netw* 2017; 17: 298-306.

7. Elghetany MT. Surface antigen changes during normal neutrophilic development: a critical review. *Blood Cells Mol Dis* 2002; 28: 260-274.

8. Shi J, Gilbert GE, Kokubo Y, Ohashi T. Role of the liver in regulating numbers of circulating neutrophils. *Blood* 2001; 98: 1226-1230.

9. Eash KJ, Greenbaum AM, Gopalan PK, Link DC. CXCR2 and CXCR4 antagonistically regulate neutrophil trafficking from murine bone marrow. *J Clin Invest* 2010; 120: 2423-2431.

10. Theilgaard-Monch K, Jacobsen LC, Borup R, Rasmussen T, Bjerregaard MD, Nielsen FC, Cowland JB, Borregaard N. The transcriptional program of terminal granulocytic differentiation. *Blood* 2005; 105: 1785-1796.

11. Friedman AD. Transcriptional control of granulocyte and monocyte development. *Oncogene* 2007; 26: 6816-6828.

12. Iwasaki H, Akashi K. Myeloid lineage commitment from the hematopoietic stem cell. *Immunity* 2007; 26: 726-740.

13. Kummalue T, Friedman AD. Cross-talk between regulators of myeloid development: C/EBPalpha binds and activates the promoter of the PU.1 gene. *J Leukoc Biol* 2003; 74: 464-470.

14. Rozman S, Yousefi S, Oberson K, Kaufmann T, Benarafa C, Simon HU. The generation of neutrophils in the bone marrow is controlled by autophagy. *Cell Death Differ* 2015; 22: 445-456.

15. Borregaard N. Neutrophils, from marrow to microbes. *Immunity* 2010; 33: 657-670.

16. Borregaard N, Cowland JB. Granules of the human neutrophilic polymorphonuclear leukocyte. *Blood* 1997; 89: 3503-3521.

17. Borregaard N, Sorensen OE, Theilgaard-Monch K. Neutrophil granules: a library of innate immunity proteins. *Trends Immunol* 2007; 28: 340-345.

18. Gullberg U, Bengtsson N, Bulow E, Garwicz D, Lindmark A, Olsson I. Processing and targeting of granule proteins in human neutrophils. *J Immunol Methods* 1999; 232: 201-210.

19. Rorvig S, Ostergaard O, Heegaard NH, Borregaard N. Proteome profiling of human neutrophil granule subsets, secretory vesicles, and cell membrane: correlation with transcriptome profiling of neutrophil precursors. *J Leukoc Biol* 2013; 94: 711-721.

20. Sengelov H, Follin P, Kjeldsen L, Lollike K, Dahlgren C, Borregaard N. Mobilization of granules and secretory vesicles during in vivo exudation of human neutrophils. *Journal of immunology* 1995; 154: 4157-4165.

21. Leick M, Azcutia V, Newton G, Luscinskas FW. Leukocyte recruitment in inflammation: basic concepts and new mechanistic insights based on new models and microscopic imaging technologies. *Cell Tissue Res* 2014; 355: 647-656.

22. Pick R, Brechtefeld D, Walzog B. Intraluminal crawling versus interstitial neutrophil migration during inflammation. *Mol Immunol* 2013; 55: 70-75.

23. Massena S, Christoffersson G, Hjertstrom E, Zcharia E, Vlodavsky I, Ausmees N, Rolny C, Li JP, Phillipson M. A chemotactic gradient sequestered on endothelial heparan sulfate induces directional intraluminal crawling of neutrophils. *Blood* 2010; 116: 1924-1931.

24. Orlova VV, Economopoulou M, Lupu F, Santoso S, Chavakis T. Junctional adhesion molecule-C regulates vascular endothelial permeability by modulating VE-cadherin-mediated cell-cell contacts. *J Exp Med* 2006; 203: 2703-2714.

25. Pillay J, den Braber I, Vrisekoop N, Kwast LM, de Boer RJ, Borghans JA, Tesselaar K, Koenderman L. In vivo labeling with 2H2O reveals a human neutrophil lifespan of 5.4 days. *Blood* 2010; 116: 625-627.

26. Colotta F, Re F, Polentarutti N, Sozzani S, Mantovani A. Modulation of granulocyte survival and programmed cell death by cytokines and bacterial products. *Blood* 1992; 80: 2012-2020.

27. Hu M, Miller EJ, Lin X, Simms HH. Transmigration across a lung epithelial monolayer delays apoptosis of polymorphonuclear leukocytes. *Surgery* 2004; 135: 87-98.

28. Le'Negrate G, Rostagno P, Auberger P, Rossi B, Hofman P. Downregulation of caspases and Fas ligand expression, and increased lifespan of neutrophils after transmigration across intestinal epithelium. *Cell Death Differ* 2003; 10: 153-162.

29. McCracken JM, Allen LA. Regulation of human neutrophil apoptosis and lifespan in health and disease. *J Cell Death* 2014; 7: 15-23.

30. Tracchi I, Ghigliotti G, Mura M, Garibaldi S, Spallarossa P, Barisione C, Boasi V, Brunelli M, Corsiglia L, Barsotti A, Brunelli C. Increased neutrophil lifespan in patients with congestive heart failure. *Eur J Heart Fail* 2009; 11: 378-385.

31. Droemann D, Aries SP, Hansen F, Moellers M, Braun J, Katus HA, Dalhoff K. Decreased apoptosis and increased activation of alveolar neutrophils in bacterial pneumonia. *Chest* 2000; 117: 1679-1684.

32. Barcellos-de-Souza P, Canetti C, Barja-Fidalgo C, Arruda MA. Leukotriene B(4) inhibits neutrophil apoptosis via NADPH oxidase activity: redox control of NF-kappaB pathway and mitochondrial stability. *Biochim Biophys Acta* 2012; 1823: 1990-1997.

33. Witko-Sarsat V, Mocek J, Bouayad D, Tamassia N, Ribeil JA, Candalh C, Davezac N, Reuter N, Mouthon L, Hermine O, Pederzoli-Ribeil M, Cassatella MA. Proliferating cell nuclear antigen acts as a cytoplasmic platform controlling human neutrophil survival. *The Journal of experimental medicine* 2010; 207: 2631-2645.

34. Saverymuttu SH, Peters AM, Keshavarzian A, Reavy HJ, Lavender JP. The kinetics of 111indium distribution following injection of 111indium labelled autologous granulocytes in man. *British journal of haematology* 1985; 61: 675-685.

35. Tofts PS, Chevassut T, Cutajar M, Dowell NG, Peters AM. Doubts concerning the recently reported human neutrophil lifespan of 5.4 days. *Blood* 2011; 117: 6050-6052; author reply 6053-6054.

36. Furze RC, Rankin SM. The role of the bone marrow in neutrophil clearance under homeostatic conditions in the mouse. *FASEB J* 2008; 22: 3111-3119.

37. Martin C, Burdon PC, Bridger G, Gutierrez-Ramos JC, Williams TJ, Rankin SM. Chemokines acting via CXCR2 and CXCR4 control the release of neutrophils from the bone marrow and their return following senescence. *Immunity* 2003; 19: 583-593.

38. Nagase H, Miyamasu M, Yamaguchi M, Imanishi M, Tsuno NH, Matsushima K, Yamamoto K, Morita Y, Hirai K. Cytokine-mediated regulation of CXCR4 expression in human neutrophils. *Journal of leukocyte biology* 2002; 71: 711-717.

39. Eash KJ, Means JM, White DW, Link DC. CXCR4 is a key regulator of neutrophil release from the bone marrow under basal and stress granulopoiesis conditions. *Blood* 2009; 113: 4711-4719.

40. Deniset JF, Kubes P. Neutrophil heterogeneity: Bona fide subsets or polarization states? *J Leukoc Biol* 2018.

41. Casanova-Acebes M, Pitaval C, Weiss LA, Nombela-Arrieta C, Chevre R, N AG, Kunisaki Y, Zhang D, van Rooijen N, Silberstein LE, Weber C, Nagasawa T, Frenette PS, Castrillo A, Hidalgo A. Rhythmic modulation of the hematopoietic niche through neutrophil clearance. *Cell* 2013; 153: 1025-1035.

42. Zhang D, Chen G, Manwani D, Mortha A, Xu C, Faith JJ, Burk RD, Kunisaki Y, Jang JE, Scheiermann C, Merad M, Frenette PS. Neutrophil ageing is regulated by the microbiome. *Nature* 2015; 525: 528-532.

43. Sagiv JY, Michaeli J, Assi S, Mishalian I, Kisos H, Levy L, Damti P, Lumbroso D, Polyansky L, Sionov RV, Ariel A, Hovav AH, Henke E, Fridlender ZG, Granot Z. Phenotypic diversity and plasticity in circulating neutrophil subpopulations in cancer. *Cell Rep* 2015; 10: 562-573.

44. Fu J, Tobin MC, Thomas LL. Neutrophil-like low-density granulocytes are elevated in patients with moderate to severe persistent asthma. *Ann Allergy Asthma Immunol* 2014; 113: 635-640 e632.

45. Pillay J, Kamp VM, van Hoffen E, Visser T, Tak T, Lammers JW, Ulfman LH, Leenen LP, Pickkers P, Koenderman L. A subset of neutrophils in human systemic inflammation inhibits T cell responses through Mac-1. *J Clin Invest* 2012; 122: 327-336.

46. Kamp VM, Pillay J, Lammers JW, Pickkers P, Ulfman LH, Koenderman L. Human suppressive neutrophils CD16bright/CD62Ldim exhibit decreased adhesion. *J Leukoc Biol* 2012; 92: 1011-1020.

47. Shaul ME, Levy L, Sun J, Mishalian I, Singhal S, Kapoor V, Horng W, Fridlender G, Albelda SM, Fridlender ZG. Tumor-associated neutrophils display a distinct N1 profile following TGFbeta modulation: A transcriptomics analysis of pro- vs. antitumor TANs. *Oncoimmunology* 2016; 5: e1232221.

48. Fridlender ZG, Sun J, Mishalian I, Singhal S, Cheng G, Kapoor V, Horng W, Fridlender G, Bayuh R, Worthen GS, Albelda SM. Transcriptomic analysis comparing tumor-associated neutrophils with granulocytic myeloid-derived suppressor cells and normal neutrophils. *PLoS One* 2012; 7: e31524.

49. Fridlender ZG, Sun J, Kim S, Kapoor V, Cheng G, Ling L, Worthen GS, Albelda SM. Polarization of tumor-associated neutrophil phenotype by TGF-beta: "N1" versus "N2" TAN. *Cancer Cell* 2009; 16: 183-194.

50. Robinson JM. Reactive oxygen species in phagocytic leukocytes. *Histochem Cell Biol* 2008; 130: 281-297.

51. Winterbourn CC, Kettle AJ, Hampton MB. Reactive Oxygen Species and Neutrophil Function. *Annu Rev Biochem* 2016; 85: 765-792.

52. Kettle AJ, Winterbourn CC. Myeloperoxidase: a key regulator of neutrophil oxidant production. *Redox Rep* 1997; 3: 3-15.

53. Anderson KE, Chessa TA, Davidson K, Henderson RB, Walker S, Tolmachova T, Grys K, Rausch O, Seabra MC, Tybulewicz VL, Stephens LR, Hawkins PT. PtdIns3P and Rac direct the assembly of the NADPH oxidase on a novel, pre-phagosomal compartment during FcR-mediated phagocytosis in primary mouse neutrophils. *Blood* 2010; 116: 4978-4989.

54. Burgoyne RD, Morgan A. Secretory granule exocytosis. *Physiol Rev* 2003; 83: 581-632.

55. Barrowman MM, Cockcroft S, Gomperts BD. Differential control of azurophilic and specific granule exocytosis in Sendai-virus-permeabilized rabbit neutrophils. *J Physiol* 1987; 383: 115-124.

56. Lacy P, Eitzen G. Control of granule exocytosis in neutrophils. *Front Biosci* 2008; 13: 5559-5570.

57. Sengelov H, Kjeldsen L, Diamond MS, Springer TA, Borregaard N. Subcellular localization and dynamics of Mac-1 (alpha m beta 2) in human neutrophils. *The Journal of clinical investigation* 1993; 92: 1467-1476.

58. Kjeldsen L, Bjerrum OW, Askaa J, Borregaard N. Subcellular localization and release of human neutrophil gelatinase, confirming the existence of separate gelatinase-containing granules. *Biochem J* 1992; 287 (Pt 2): 603-610.

59. Potera RM, Jensen MJ, Hilkin BM, South GK, Hook JS, Gross EA, Moreland JG. Neutrophil azurophilic granule exocytosis is primed by TNF-alpha and partially regulated by NADPH oxidase. *Innate Immun* 2016; 22: 635-646.

60. Jog NR, Rane MJ, Lominadze G, Luerman GC, Ward RA, McLeish KR. The actin cytoskeleton regulates exocytosis of all neutrophil granule subsets. *Am J Physiol Cell Physiol* 2007; 292: C1690-1700.

61. Herrero-Turrion MJ, Calafat J, Janssen H, Fukuda M, Mollinedo F. Rab27a regulates exocytosis of tertiary and specific granules in human neutrophils. *Journal of immunology* 2008; 181: 3793-3803.

62. Johnson JL, Ramadass M, He J, Brown SJ, Zhang J, Abgaryan L, Biris N, Gavathiotis E, Rosen H, Catz SD. Identification of Neutrophil Exocytosis Inhibitors (Nexinhibs), Small Molecule Inhibitors of Neutrophil Exocytosis and Inflammation: DRUGGABILITY OF THE SMALL GTPase Rab27a. *J Biol Chem* 2016; 291: 25965-25982.

63. Botelho RJ, Tapper H, Furuya W, Mojdami D, Grinstein S. Fc gamma R-mediated phagocytosis stimulates localized pinocytosis in human neutrophils. *J Immunol* 2002; 169: 4423-4429.

64. Lee WL, Harrison RE, Grinstein S. Phagocytosis by neutrophils. *Microbes Infect* 2003; 5: 1299-1306.

65. Schorlemmer HU, Hofstaetter T, Seiler FR. Phagocytosis of immune complexes by human neutrophils and monocytes: relative importance of Fc and C3b receptors. *Behring Inst Mitt* 1984: 88-97.

66. Nordenfelt P, Tapper H. Phagosome dynamics during phagocytosis by neutrophils. *J Leukoc Biol* 2011; 90: 271-284.

67. Brinkmann V, Reichard U, Goosmann C, Fauler B, Uhlemann Y, Weiss DS, Weinrauch Y, Zychlinsky A. Neutrophil extracellular traps kill bacteria. *Science* 2004; 303: 1532-1535.

68. Yipp BG, Petri B, Salina D, Jenne CN, Scott BN, Zbytnuik LD, Pittman K, Asaduzzaman M, Wu K, Meijndert HC, Malawista SE, de Boisfleury Chevance A, Zhang K, Conly J, Kubes P. Infection-induced NETosis is a dynamic process involving neutrophil multitasking in vivo. *Nature medicine* 2012; 18: 1386-1393.

69. Metzler KD, Fuchs TA, Nauseef WM, Reumaux D, Roesler J, Schulze I, Wahn V, Papayannopoulos V, Zychlinsky A. Myeloperoxidase is required for neutrophil extracellular trap formation: implications for innate immunity. *Blood* 2011; 117: 953-959.

70. Parker H, Dragunow M, Hampton MB, Kettle AJ, Winterbourn CC. Requirements for NADPH oxidase and myeloperoxidase in neutrophil extracellular trap formation differ depending on the stimulus. *J Leukoc Biol* 2012; 92: 841-849.

71. Beiter K, Wartha F, Albiger B, Normark S, Zychlinsky A, Henriques-Normark B. An endonuclease allows Streptococcus pneumoniae to escape from neutrophil extracellular traps. *Curr Biol* 2006; 16: 401-407.

72. Sumby P, Barbian KD, Gardner DJ, Whitney AR, Welty DM, Long RD, Bailey JR, Parnell MJ, Hoe NP, Adams GG, Deleo FR, Musser JM. Extracellular deoxyribonuclease made by group A Streptococcus assists pathogenesis by enhancing evasion of the innate immune response. *Proceedings of the National Academy of Sciences of the United States of America* 2005; 102: 1679-1684.

73. Walker MJ, Hollands A, Sanderson-Smith ML, Cole JN, Kirk JK, Henningham A, McArthur JD, Dinkla K, Aziz RK, Kansal RG, Simpson AJ, Buchanan JT, Chhatwal GS, Kotb M, Nizet V. DNase Sda1 provides selection pressure for a switch to invasive group A streptococcal infection. *Nature medicine* 2007; 13: 981-985.

74. Stienstra R, Netea-Maier RT, Riksen NP, Joosten LAB, Netea MG. Specific and Complex Reprogramming of Cellular Metabolism in Myeloid Cells during Innate Immune Responses. *Cell Metab* 2017; 26: 142-156.

75. Pearce EL, Pearce EJ. Metabolic pathways in immune cell activation and quiescence. *Immunity* 2013; 38: 633-643.

76. Ganeshan K, Chawla A. Metabolic regulation of immune responses. *Annu Rev Immunol* 2014; 32: 609-634.

77. Buck MD, Sowell RT, Kaech SM, Pearce EL. Metabolic Instruction of Immunity. *Cell* 2017; 169: 570-586.

78. Borregaard N, Herlin T. Energy metabolism of human neutrophils during phagocytosis. *The Journal of clinical investigation* 1982; 70: 550-557.

79. Maianski NA, Geissler J, Srinivasula SM, Alnemri ES, Roos D, Kuijpers TW. Functional characterization of mitochondria in neutrophils: a role restricted to apoptosis. *Cell Death Differ* 2004; 11: 143-153.

80. van Raam BJ, Verhoeven AJ, Kuijpers TW. Mitochondria in neutrophil apoptosis. *International journal of hematology* 2006; 84: 199-204.

81. Fossati G, Moulding DA, Spiller DG, Moots RJ, White MR, Edwards SW. The mitochondrial network of human neutrophils: role in chemotaxis, phagocytosis, respiratory burst activation, and commitment to apoptosis. *J Immunol* 2003; 170: 1964-1972.

82. Chacko BK, Kramer PA, Ravi S, Johnson MS, Hardy RW, Ballinger SW, Darley-Usmar VM. Methods for defining distinct bioenergetic profiles in platelets, lymphocytes, monocytes, and neutrophils, and the oxidative burst from human blood. *Lab Invest* 2013; 93: 690-700.

83. Vander Heiden MG, Cantley LC, Thompson CB. Understanding the Warburg effect: the metabolic requirements of cell proliferation. *Science* 2009; 324: 1029-1033.

84. Kramer PA, Ravi S, Chacko B, Johnson MS, Darley-Usmar VM. A review of the mitochondrial and glycolytic metabolism in human platelets and leukocytes: implications for their use as bioenergetic biomarkers. *Redox Biol* 2014; 2: 206-210.

85. Guthrie LA, McPhail LC, Henson PM, Johnston RB, Jr. Priming of neutrophils for enhanced release of oxygen metabolites by bacterial lipopolysaccharide. Evidence for increased activity of the superoxide-producing enzyme. *The Journal of experimental medicine* 1984; 160: 1656-1671.

86. Kelly B, O'Neill LA. Metabolic reprogramming in macrophages and dendritic cells in innate immunity. *Cell Res* 2015; 25: 771-784.

87. Weisdorf DJ, Craddock PR, Jacob HS. Granulocytes utilize different energy sources for movement and phagocytosis. *Inflammation* 1982; 6: 245-256.

88. Boxer LA, Baehner RL, Davis J. The effect of 2-deoxyglucose on guinea pig polymorphonuclear leukocyte phagocytosis. *Journal of cellular physiology* 1977; 91: 89-102.

89. Azevedo EP, Rochael NC, Guimaraes-Costa AB, de Souza-Vieira TS, Ganilho J, Saraiva EM, Palhano FL, Foguel D. A Metabolic Shift toward Pentose Phosphate Pathway Is Necessary for Amyloid Fibril- and Phorbol 12-Myristate 13-Acetate-induced Neutrophil Extracellular Trap (NET) Formation. *The Journal of biological chemistry* 2015; 290: 22174-22183.

90. Haschemi A, Kosma P, Gille L, Evans CR, Burant CF, Starkl P, Knapp B, Haas R, Schmid JA, Jandl C, Amir S, Lubec G, Park J, Esterbauer H, Bilban M, Brizuela L, Pospisilik JA, Otterbein LE, Wagner O. The sedoheptulose kinase CARKL directs

macrophage polarization through control of glucose metabolism. *Cell Metab* 2012; 15: 813-826.

91. El Kasmi KC, Stenmark KR. Contribution of metabolic reprogramming to macrophage plasticity and function. *Semin Immunol* 2015; 27: 267-275.

92. Foster JM, Terry ML. Studies on the energy metabolism of human leukocytes. I. Oxidative phosphorylation by human leukocyte mitochondria. *Blood* 1967; 30: 168-175.

93. Cheson BD, Curnette JT, Babior BM. The oxidative killing mechanisms of the neutrophil. *Prog Clin Immunol* 1977; 3: 1-65.

94. Rodriguez-Espinosa O, Rojas-Espinosa O, Moreno-Altamirano MM, Lopez-Villegas EO, Sanchez-Garcia FJ. Metabolic requirements for neutrophil extracellular traps formation. *Immunology* 2015; 145: 213-224.

95. Rodrigues HG, Takeo Sato F, Curi R, Vinolo MAR. Fatty acids as modulators of neutrophil recruitment, function and survival. *Eur J Pharmacol* 2016; 785: 50-58.

96. Everts B, Amiel E, Huang SC, Smith AM, Chang CH, Lam WY, Redmann V, Freitas TC, Blagih J, van der Windt GJ, Artyomov MN, Jones RG, Pearce EL, Pearce EJ. TLR-driven early glycolytic reprogramming via the kinases TBK1-IKKvarepsilon supports the anabolic demands of dendritic cell activation. *Nat Immunol* 2014; 15: 323-332.

97. O'Neill LA, Pearce EJ. Immunometabolism governs dendritic cell and macrophage function. *The Journal of experimental medicine* 2016; 213: 15-23.

98. O'Neill LA, Hardie DG. Metabolism of inflammation limited by AMPK and pseudo-starvation. *Nature* 2013; 493: 346-355.

99. Newsholme P, Curi R, Gordon S, Newsholme EA. Metabolism of glucose, glutamine, long-chain fatty acids and ketone bodies by murine macrophages. *Biochem J* 1986; 239: 121-125.

100. Riffelmacher T, Richter FC, Simon AK. Autophagy dictates metabolism and differentiation of inflammatory immune cells. *Autophagy* 2017: 1-8.

101. Riffelmacher T, Clarke A, Richter FC, Stranks A, Pandey S, Danielli S, Hublitz P, Yu Z, Johnson E, Schwerd T, McCullagh J, Uhlig H, Jacobsen SEW, Simon AK. Autophagy-Dependent Generation of Free Fatty Acids Is Critical for Normal Neutrophil Differentiation. *Immunity* 2017; 47: 466-480 e465.

102. Saxton RA, Sabatini DM. mTOR Signaling in Growth, Metabolism, and Disease. *Cell* 2017; 168: 960-976.

103. Byles V, Covarrubias AJ, Ben-Sahra I, Lamming DW, Sabatini DM, Manning BD, Horng T. The TSC-mTOR pathway regulates macrophage polarization. *Nature communications* 2013; 4: 2834.

104. Gomez-Cambronero J. Rapamycin inhibits GM-CSF-induced neutrophil migration. *FEBS letters* 2003; 550: 94-100.

105. He Y, Li D, Cook SL, Yoon MS, Kapoor A, Rao CV, Kenis PJ, Chen J, Wang F. Mammalian target of rapamycin and Rictor control neutrophil chemotaxis by regulating Rac/Cdc42 activity and the actin cytoskeleton. *Mol Biol Cell* 2013; 24: 3369-3380.

106. Liu L, Das S, Losert W, Parent CA. mTORC2 regulates neutrophil chemotaxis in a cAMP- and RhoA-dependent fashion. *Dev Cell* 2010; 19: 845-857.

107. Chen J, Tang H, Hay N, Xu J, Ye RD. Akt isoforms differentially regulate neutrophil functions. *Blood* 2010; 115: 4237-4246.

108. Itakura A, McCarty OJ. Pivotal role for the mTOR pathway in the formation of neutrophil extracellular traps via regulation of autophagy. *Am J Physiol Cell Physiol* 2013; 305: C348-354.

109. Zhao X, Zmijewski JW, Lorne E, Liu G, Park YJ, Tsuruta Y, Abraham E. Activation of AMPK attenuates neutrophil proinflammatory activity and decreases the severity of acute lung injury. *American journal of physiology Lung cellular and molecular physiology* 2008; 295: L497-504.

110. Phan AT, Goldrath AW. Hypoxia-inducible factors regulate T cell metabolism and function. *Mol Immunol* 2015; 68: 527-535.

111. Cramer T, Yamanishi Y, Clausen BE, Forster I, Pawlinski R, Mackman N, Haase VH, Jaenisch R, Corr M, Nizet V, Firestein GS, Gerber HP, Ferrara N, Johnson RS. HIF-1alpha is essential for myeloid cell-mediated inflammation. *Cell* 2003; 112: 645-657.

112. Palazon A, Goldrath AW, Nizet V, Johnson RS. HIF transcription factors, inflammation, and immunity. *Immunity* 2014; 41: 518-528.

113. Walmsley SR, Print C, Farahi N, Peyssonnaux C, Johnson RS, Cramer T, Sobolewski A, Condliffe AM, Cowburn AS, Johnson N, Chilvers ER. Hypoxia-induced neutrophil survival is mediated by HIF-1alpha-dependent NF-kappaB activity. *The Journal of experimental medicine* 2005; 201: 105-115.

114. Lakschevitz FS, Visser MB, Sun C, Glogauer M. Neutrophil transcriptional profile changes during transit from bone marrow to sites of inflammation. *Cell Mol Immunol* 2015; 12: 53-65.

115. Subrahmanyam YV, Yamaga S, Prashar Y, Lee HH, Hoe NP, Kluger Y, Gerstein M, Goguen JD, Newburger PE, Weissman SM. RNA expression patterns change dramatically in human neutrophils exposed to bacteria. *Blood* 2001; 97: 2457-2468.

116. Zhang X, Kluger Y, Nakayama Y, Poddar R, Whitney C, DeTora A, Weissman SM, Newburger PE. Gene expression in mature neutrophils: early responses to inflammatory stimuli. *Journal of leukocyte biology* 2004; 75: 358-372.

117. Fessler MB, Malcolm KC, Duncan MW, Worthen GS. A genomic and proteomic analysis of activation of the human neutrophil by lipopolysaccharide and its mediation by p38 mitogen-activated protein kinase. *The Journal of biological chemistry* 2002; 277: 31291-31302.

118. Kobayashi SD, Voyich JM, Buhl CL, Stahl RM, DeLeo FR. Global changes in gene expression by human polymorphonuclear leukocytes during receptor-mediated phagocytosis: cell fate is regulated at the level of gene expression. *Proceedings of the National Academy of Sciences of the United States of America* 2002; 99: 6901-6906.

119. Andiappan AK, Melchiotti R, Poh TY, Nah M, Puan KJ, Vigano E, Haase D, Yusof N, San Luis B, Lum J, Kumar D, Foo S, Zhuang L, Vasudev A, Irwanto A, Lee B, Nardin A, Liu H, Zhang F, Connolly J, Liu J, Mortellaro A, Wang de Y, Poidinger M, Larbi A, Zolezzi F, Rotzschke O. Genome-wide analysis of the genetic regulation of gene expression in human neutrophils. *Nature communications* 2015; 6: 7971.

120. Rowe SM, Miller S, Sorscher EJ. Cystic fibrosis. *N Engl J Med* 2005; 352: 1992-2001.

121. Hayes E, Pohl K, McElvaney NG, Reeves EP. The cystic fibrosis neutrophil: a specialized yet potentially defective cell. *Archivum immunologiae et therapiae experimentalis* 2011; 59: 97-112.

122. Gifford AM, Chalmers JD. The role of neutrophils in cystic fibrosis. *Current opinion in hematology* 2014; 21: 16-22.

123. Brennan AL, Gyi KM, Wood DM, Johnson J, Holliman R, Baines DL, Philips BJ, Geddes DM, Hodson ME, Baker EH. Airway glucose concentrations and effect on

growth of respiratory pathogens in cystic fibrosis. *Journal of cystic fibrosis : official journal of the European Cystic Fibrosis Society* 2007; 6: 101-109.

124. Laval J, Ralhan A, Hartl D. Neutrophils in cystic fibrosis. *Biol Chem* 2016; 397: 485-496.

125. Downey DG, Bell SC, Elborn JS. Neutrophils in cystic fibrosis. *Thorax* 2009; 64: 81-88.

126. Bodini A, D'Orazio C, Peroni D, Corradi M, Folesani G, Baraldi E, Assael BM, Boner A, Piacentini GL. Biomarkers of neutrophilic inflammation in exhaled air of cystic fibrosis children with bacterial airway infections. *Pediatric pulmonology* 2005; 40: 494-499.

127. Khan TZ, Wagener JS, Bost T, Martinez J, Accurso FJ, Riches DW. Early pulmonary inflammation in infants with cystic fibrosis. *American journal of respiratory and critical care medicine* 1995; 151: 1075-1082.

128. Koller DY, Urbanek R, Gotz M. Increased degranulation of eosinophil and neutrophil granulocytes in cystic fibrosis. *American journal of respiratory and critical care medicine* 1995; 152: 629-633.

129. Young RL, Malcolm KC, Kret JE, Caceres SM, Poch KR, Nichols DP, Taylor-Cousar JL, Saavedra MT, Randell SH, Vasil ML, Burns JL, Moskowitz SM, Nick JA. Neutrophil extracellular trap (NET)-mediated killing of Pseudomonas aeruginosa: evidence of acquired resistance within the CF airway, independent of CFTR. *PLoS One* 2011; 6: e23637.

130. Painter RG, Valentine VG, Lanson NA, Jr., Leidal K, Zhang Q, Lombard G, Thompson C, Viswanathan A, Nauseef WM, Wang G, Wang G. CFTR Expression in human neutrophils and the phagolysosomal chlorination defect in cystic fibrosis. *Biochemistry* 2006; 45: 10260-10269.

131. Zhou Y, Song K, Painter RG, Aiken M, Reiser J, Stanton BA, Nauseef WM, Wang G. Cystic fibrosis transmembrane conductance regulator recruitment to phagosomes in neutrophils. *J Innate Immun* 2013; 5: 219-230.

132. Brockbank S, Downey D, Elborn JS, Ennis M. Effect of cystic fibrosis exacerbations on neutrophil function. *Int Immunopharmacol* 2005; 5: 601-608.

133. Brennan S, Cooper D, Sly PD. Directed neutrophil migration to IL-8 is increased in cystic fibrosis: a study of the effect of erythromycin. *Thorax* 2001; 56: 62-64.

134. Rieber N, Hector A, Carevic M, Hartl D. Current concepts of immune dysregulation in cystic fibrosis. *Int J Biochem Cell Biol* 2014; 52: 108-112.

135. Nakamura H, Yoshimura K, McElvaney NG, Crystal RG. Neutrophil elastase in respiratory epithelial lining fluid of individuals with cystic fibrosis induces interleukin-8 gene expression in a human bronchial epithelial cell line. *The Journal of clinical investigation* 1992; 89: 1478-1484.

136. van den Berg CW, Tambourgi DV, Clark HW, Hoong SJ, Spiller OB, McGreal EP. Mechanism of neutrophil dysfunction: neutrophil serine proteases cleave and inactivate the C5a receptor. *J Immunol* 2014; 192: 1787-1795.

137. Morris MR, Doull IJ, Dewitt S, Hallett MB. Reduced iC3b-mediated phagocytotic capacity of pulmonary neutrophils in cystic fibrosis. *Clin Exp Immunol* 2005; 142: 68-75.

138. Singh PK, Schaefer AL, Parsek MR, Moninger TO, Welsh MJ, Greenberg EP. Quorum-sensing signals indicate that cystic fibrosis lungs are infected with bacterial biofilms. *Nature* 2000; 407: 762-764.

139. Tirouvanziam R, Gernez Y, Conrad CK, Moss RB, Schrijver I, Dunn CE, Davies ZA, Herzenberg LA, Herzenberg LA. Profound functional and signaling changes in

viable inflammatory neutrophils homing to cystic fibrosis airways. *Proc Natl Acad Sci U S A* 2008; 105: 4335-4339.

140. Makam M, Diaz D, Laval J, Gernez Y, Conrad CK, Dunn CE, Davies ZA, Moss RB, Herzenberg LA, Herzenberg LA, Tirouvanziam R. Activation of critical, host-induced, metabolic and stress pathways marks neutrophil entry into cystic fibrosis lungs. *Proc Natl Acad Sci U S A* 2009; 106: 5779-5783.

141. Laval J, Touhami J, Herzenberg LA, Conrad C, Taylor N, Battini JL, Sitbon M, Tirouvanziam R. Metabolic adaptation of neutrophils in cystic fibrosis airways involves distinct shifts in nutrient transporter expression. *J Immunol* 2013; 190: 6043-6050.

142. Rosen BH, Chanson M, Gawenis LR, Liu J, Sofoluwe A, Zoso A, Engelhardt JF. Animal and model systems for studying cystic fibrosis. *J Cyst Fibros* 2017.

143. Keiser NW, Engelhardt JF. New animal models of cystic fibrosis: what are they teaching us? *Curr Opin Pulm Med* 2011; 17: 478-483.

144. Fisher JT, Zhang Y, Engelhardt JF. Comparative biology of cystic fibrosis animal models. *Methods Mol Biol* 2011; 742: 311-334.

145. Rogers CS, Abraham WM, Brogden KA, Engelhardt JF, Fisher JT, McCray PB, Jr., McLennan G, Meyerholz DK, Namati E, Ostedgaard LS, Prather RS, Sabater JR, Stoltz DA, Zabner J, Welsh MJ. The porcine lung as a potential model for cystic fibrosis. *American journal of physiology Lung cellular and molecular physiology* 2008; 295: L240-263.

146. Li Z, Engelhardt JF. Progress toward generating a ferret model of cystic fibrosis by somatic cell nuclear transfer. *Reprod Biol Endocrinol* 2003; 1: 83.

147. Rogers CS, Stoltz DA, Meyerholz DK, Ostedgaard LS, Rokhlina T, Taft PJ, Rogan MP, Pezzulo AA, Karp PH, Itani OA, Kabel AC, Wohlford-Lenane CL, Davis GJ, Hanfland RA, Smith TL, Samuel M, Wax D, Murphy CN, Rieke A, Whitworth K, Uc A, Starner TD, Brogden KA, Shilyansky J, McCray PB, Jr., Zabner J, Prather RS, Welsh MJ. Disruption of the CFTR gene produces a model of cystic fibrosis in newborn pigs. *Science* 2008; 321: 1837-1841.

148. Stoltz DA, Meyerholz DK, Pezzulo AA, Ramachandran S, Rogan MP, Davis GJ, Hanfland RA, Wohlford-Lenane C, Dohrn CL, Bartlett JA, Nelson GAt, Chang EH, Taft PJ, Ludwig PS, Estin M, Hornick EE, Launspach JL, Samuel M, Rokhlina T, Karp PH, Ostedgaard LS, Uc A, Starner TD, Horswill AR, Brogden KA, Prather RS, Richter SS, Shilyansky J, McCray PB, Jr., Zabner J, Welsh MJ. Cystic fibrosis pigs develop lung disease and exhibit defective bacterial eradication at birth. *Science translational medicine* 2010; 2: 29ra31.

149. Sun X, Yan Z, Yi Y, Li Z, Lei D, Rogers CS, Chen J, Zhang Y, Welsh MJ, Leno GH, Engelhardt JF. Adeno-associated virus-targeted disruption of the CFTR gene in cloned ferrets. *The Journal of clinical investigation* 2008; 118: 1578-1583.

150. Keiser NW, Birket SE, Evans IA, Tyler SR, Crooke AK, Sun X, Zhou W, Nellis JR, Stroebele EK, Chu KK, Tearney GJ, Stevens MJ, Harris JK, Rowe SM, Engelhardt JF. Defective innate immunity and hyperinflammation in newborn cystic fibrosis transmembrane conductance regulator-knockout ferret lungs. *American journal of respiratory cell and molecular biology* 2015; 52: 683-694.

151. Peault B, Tirouvanziam R, Sombardier MN, Chen S, Perricaudet M, Gaillard D. Gene transfer to human fetal pulmonary tissue developed in immunodeficient SCID mice. *Hum Gene Ther* 1994; 5: 1131-1137.

152. Tirouvanziam R, Desternes M, Saari A, Puchelle E, Peault B, Chinet T. Bioelectric properties of human cystic fibrosis and non-cystic fibrosis fetal tracheal xenografts in SCID mice. *Am J Physiol* 1998; 274: C875-882.

153. Delplanque A, Coraux C, Tirouvanziam R, Khazaal I, Puchelle E, Ambros P, Gaillard D, Peault B. Epithelial stem cell-mediated development of the human respiratory mucosa in SCID mice. *J Cell Sci* 2000; 113 (Pt 5): 767-778.

154. Tirouvanziam R, de Bentzmann S, Hubeau C, Hinnrasky J, Jacquot J, Peault B, Puchelle E. Inflammation and infection in naive human cystic fibrosis airway grafts. *Am J Respir Cell Mol Biol* 2000; 23: 121-127.

155. Tirouvanziam R, Khazaal I, Peault B. Primary inflammation in human cystic fibrosis small airways. *Am J Physiol Lung Cell Mol Physiol* 2002; 283: L445-451.

156. Nichols JE, Niles JA, Vega SP, Cortiella J. Novel in vitro respiratory models to study lung development, physiology, pathology and toxicology. *Stem Cell Res Ther* 2013; 4 Suppl 1: S7.

157. Hannan NR, Sampaziotis F, Segeritz CP, Hanley NA, Vallier L. Generation of Distal Airway Epithelium from Multipotent Human Foregut Stem Cells. *Stem Cells Dev* 2015; 24: 1680-1690.

158. Konar D, Devarasetty M, Yildiz DV, Atala A, Murphy SV. Lung-On-A-Chip Technologies for Disease Modeling and Drug Development. *Biomed Eng Comput Biol* 2016; 7: 17-27.

159. Benam KH, Villenave R, Lucchesi C, Varone A, Hubeau C, Lee HH, Alves SE, Salmon M, Ferrante TC, Weaver JC, Bahinski A, Hamilton GA, Ingber DE. Small airway-on-a-chip enables analysis of human lung inflammation and drug responses in vitro. *Nat Methods* 2016; 13: 151-157.

160. Benam KH, Konigshoff M, Eickelberg O. Breaking the In Vitro Barrier in Respiratory Medicine: Engineered Microphysiological Systems for COPD and Beyond. *Am J Respir Crit Care Med* 2017.

161. Lavelle GM, White MM, Browne N, McElvaney NG, Reeves EP. Animal Models of Cystic Fibrosis Pathology: Phenotypic Parallels and Divergences. *Biomed Res Int* 2016; 2016: 5258727.

162. McCarron A, Donnelley M, Parsons D. Airway disease phenotypes in animal models of cystic fibrosis. *Respir Res* 2018; 19: 54.

163. O'Neill LA, Kishton RJ, Rathmell J. A guide to immunometabolism for immunologists. *Nat Rev Immunol* 2016; 16: 553-565.

Chapter 2

Pathological Conditioning of Human Neutrophils Recruited to the Airway Milieu in Cystic Fibrosis

Sections of this chapter have been accepted for publication as a highlighted "Frontline Science" original research article in the Journal of Leukocyte Biology

PATHOLOGICAL CONDITIONING OF HUMAN NEUTROPHILS RECRUITED TO THE AIRWAY MILIEU IN CYSTIC FIBROSIS

Osric A. Forrest[1,2], Sarah A. Ingersoll[1,2], Marcela K. Preininger[1,2], Julie Laval[1,2], Dominique H. Limoli[1,2], Milton R. Brown[1,2], Frances E. Lee[3], Brahmchetna Bedi[4], Ruxana T. Sadikot[3,4], Joanna B. Goldberg[1,2], Vin Tangpricha[3,4], Amit Gaggar[5,6], and Rabindra Tirouvanziam[1,2]

[1]Department of Pediatrics, Emory University, Atlanta, GA, USA, [2]Center for CF & Airways Disease Research, Children's Healthcare of Atlanta, Atlanta, GA, USA, [3]Department of Medicine, Emory University, Atlanta, GA, USA, [4]Atlanta VA Medical Center, Decatur, GA, USA, [5]Department of Medicine, University of Alabama at Birmingham, Birmingham, AL, USA, [6]Birmingham VA Medical Center, Birmingham, AL, USA

ABSTRACT

Rationale: Recruitment of neutrophils to the airways, and their pathological conditioning therein, drive tissue damage and coincide with the loss of lung function in patients with cystic fibrosis (CF). So far, these key processes have not been adequately recapitulated in models, hampering drug development. Here, we hypothesized that the migration of naïve blood neutrophils into CF airway fluid *in vitro* would induce similar functional adaptation to that observed *in vivo*, and provide a model to identify new therapies.

Methods: We used multiple platforms (flow cytometry, bacteria-killing, and metabolic assays) to characterize functional properties of blood neutrophils recruited in a transepithelial migration model using airway milieu from CF subjects as an apical chemoattractant.

Main findings: Similarly to neutrophils recruited to CF airways *in vivo*, neutrophils migrated into CF airway milieu *in vitro* display depressed phagocytic receptor expression and bacterial killing, but enhanced granule release, immunoregulatory function (arginase-1 activation), and metabolic activities including high Glut1 expression, glycolysis, and oxidant production. We also identify enhanced pinocytic activity as a novel feature of these cells. *In vitro* treatment with the leukotriene pathway inhibitor acebilustat reduces the number of transmigrating neutrophils, while the metabolic modulator metformin decreases metabolism and oxidant production, but fails to restore bacterial killing. Interestingly, we describe similar pathological conditioning of neutrophils in other inflammatory airway diseases.

Conclusions: We successfully tested the hypothesis that recruitment of neutrophils into airway milieu from patients with CF *in vitro* induces similar pathological conditioning to that observed *in vivo*, opening new avenues for targeted therapeutic intervention.

INTRODUCTION

Cystic fibrosis (CF) is the most frequent fatal recessive disease in Caucasians, caused by mutations in the CF transmembrane conductance regulator (cftr) gene (1). Most of the morbidity and mortality in CF is due to airway disease, with a triad of obstruction, infection, and inflammation driven by polymorphonuclear neutrophils (PMNs) recruited from blood (2). Inflammation occurs early in CF airway disease and persists through the patients' lifetime (3). The first symptoms of airway damage are detected in small airways of CF infants (4), with bronchiectasis coinciding with both PMN presence in the lumen, and extracellular neutrophil elastase (NE) activity (5). Extracellular NE activity is also a predictor of lung function in CF adults (6). Currently, no therapy exists to counter PMNs and PMN-derived NE in CF disease.

In prior *in vivo* studies, we showed that NE is primarily released via exocytosis by live PMNs (7, 8). In the CF airway milieu, PMNs also lose the surface phagocytic receptor CD16 (8), and modulate T-cell inhibitory molecules arginase-1 (Arg1) and programmed death-ligand 1 (PD-L1) (9). These functional changes occur in the context of anabolic signaling (7), with increased surface Glut1 expression and glucose uptake (10), and track with high extracellular lactate levels (11) high oxygen consumption and reactive oxygen species (ROS) production (12), and redox imbalance (13). Critically, such changes are not discernable in blood PMNs, and PMNs maintain diploid DNA content while undergoing changes in CF airways (7-10).

Together, changes undergone by PMNs in the CF airway milieu constitute a distinct fate, characterized by enhanced primary granule release leading to NE exocytosis, immunoregulatory function, and metabolic activities, henceforth dubbed the "GRIM" fate. Because of the major impact on CF airway disease of NE (14) and other GRIM PMN-

dependent factors, these cells constitute a *bona fide* target for therapy (15). However, a key limitation has been the absence of models recapitulating the GRIM fate (16, 17).

Importantly, PMN-driven inflammation is not only a hallmark of CF, but also of chronic obstructive pulmonary disease (COPD) and other chronic lung diseases (LD) such as severe asthma [18, 19], although the precise functional adaptations that recruited PMNs undergo in these contexts have been described in less details. Here, we describe a simple, yet robust *in vitro* model based on blood PMN transepithelial migration into airway milieu from patients with CF and other chronic inflammatory airway diseases, which recapitulates the multifaceted functional adaptations corresponding to the GRIM fate *in vivo* (17). Using this model, drug effects on effector and metabolic pathways relevant to the GRIM fate of human airway PMNs can be tested *in vitro*, opening new avenues for drug development.

METHODS

Human subjects. The protocol for collection and handling of human samples was approved by the Institutional Review Board at Emory University. Informed consent was obtained from all subjects for collection and use of their samples. CF was diagnosed by sweat chloride (60 mEq/L), using a quantitative iontophoresis test and/or documentation of two identifiable cftr mutations. COPD and LD patients were diagnosed using American Lung Association criteria. HC subjects were non-smokers, with no history of chronic disease. CF patients were assessed at either one or two visits more than 6 months apart. HC, COPD and LD subjects were assessed at one visit. **Table 2.1** presents demographic data for all subjects.

Sample processing and airway supernatant preparation. Blood was collected by venipuncture. Sputum was collected from CF patients by spontaneous expectoration, and from HC, COPD and LD subjects by induction. Blood and sputum were processed as previously described (8). In brief, blood was spun at 400 g to separate cells from platelet-rich plasma, which was further spun at 3,000 g to generate platelet-free plasma. Sputum was gently dissociated using repeated passage through an 18G needle after addition of 6 ml of PBS with 2.5 mM EDTA. Dissociated sputum was then spun at 800 g generating cell and fluid fractions. The fluid fraction was further spun at 3,000 g at 4ºC for 10 minutes to generate a purified, cell and bacteria-free, airway supernatant -ASN-, which was stored at -80ºC until use. Blood and airway cell fractions were re-suspended in PBS-EDTA and used for flow cytometric analysis. Blood was also used to prepare PMN fractions for in vitro experiments, as previously described (7). In brief, blood layered onto Polymorphprep (PMP, Nycomed Pharma) was centrifuged at 400 g with minimal brake for 45 minutes at room

temperature. The PMN layer was collected and erythrocytes removed by hypotonic lysis by 30-second incubation in water, after which PMNs were washed and resuspended in RPMI until use.

Transepithelial migration (TM) model. PMN transepithelial migration and subsequent inflammation occur first in the small airways of CF patients, i.e., the bronchiolar region, which is lined with a microvilli-covered epithelial monolayer dominated by Club cells (3-5). Therefore, to mimic PMN transmigration into the small airway lumen, we selected the H441 human Club cell line (20) to grow epithelial monolayers at air-liquid interface (ALI). To enable PMN loading in the lamina propria and transepithelial migration **(Fig. 2.1A)**, we used Alvetex (Reinnervate) 200 μm-thick inert 3D scaffolds with >90% porosity (pore sizes of 36-40 μm, with interconnects of 12-14 μm). In brief, inserts were activated with 70% ethanol, coated overnight at 37ºC with rat-tail collagen I (3 mg/mL, Sigma) and seeded with H441 cells at $2.5x10^5$ cells per 12-well insert. Cells were first grown in submerged cultures with DMEM/F12 supplemented with 10% heat-inactivated serum, penicillin, and streptomycin. After 2 days, cells were supplemented basally with serum-free DMEM/F12 with 10% Ultroser G (Pall Life Sciences) to establish ALI. Cultures were grown for 2 weeks at ALI and supplemented basally with fresh medium every 48 hours. For TM experiments, the ALI cultures were placed with the apical compartment exposed to RPMI, leukotriene B4 (LTB4, 100 nM), CXCL8 (100 ng/mL), formyl-methionine-leucine-phenylalanine (fMLF, 100 ng/mL), lipopolysaccharide (LPS, 500 ng/mL), or airway supernatant (ASN) from CF, HC, COPD, and LD subjects. TM experiments with 0.5-1 $\times 10^6$ PMNs loaded onto the 200 μm-thick basal compartment of the Alvetex scaffold (situated upside), and allowed to migrate at 37°C at 5% CO2 through the collagen and epithelial layers into the apical

compartment (situated downside, and bathed with either control medium with chemoattractant, or ASN). In some experiments, drugs were added to apical ASN and/or basal PMN suspensions. In other experiments, LPS-RS (competitive inhibitor of LPS binding to TLR4) was added to apical LPS or CF ASN. LPS and LPS-RS were purchased as ultrapure reagents from InvivoGen.

Flow cytometry. Blood and airway PMNs collected from human subjects and from our transmigration model were assessed by flow cytometry using standard templates for staining, acquisition and analysis, as described, enabling quantitative comparison of in vivo and in vitro samples throughout the whole study (21). Reagents used for the study included Live/Dead (Invitrogen), and antibodies against Arg1 (6G3, Hycult Biotech), as well as CD11b (M1/70), CD16 (3G8), CD41a (HIP8), CD45 (HI30), CD63 (H5C6), CD66b (G10F5), CD62L (DREG-56), and PD-L1 (29E.2A3) from BioLegend, and the ROS probe CellRox (ThermoFisher), using the gating strategy in **Fig. 2.7A**. Phosphorylated 5' adenosine monophosphate-activated protein kinase (AMPK) α1 levels were assessed using an antibody against phospho-Thr172 (Biorbyt) using a previously published protocol (7). For Glut1 detection, we used a specific receptor-binding domain probe (Metafora Biosciences), as detailed before (10). Data were acquired on a LSRII cytometer (BD Biosciences) and compensated, gated and analyzed in Flowjo (Treestar). Live PMNs were counted using CountBright beads (Life Technologies), and expression of all markers is reported as median fluorescence intensities.

Pinocytosis assay. Pinocytosis was assessed via Lucifer Yellow (LY, Biotium) uptake, as described previously (22), with some modifications. For *in vivo* samples, a NH_4Cl solution

(StemCell Technologies) was used to lyse erythrocytes from whole blood, yielding blood leukocytes. Airway cells were obtained as described above. Blood leukocytes and airway cells were then stained with probes for viability (Live/Dead) and antibody markers for PMNs (CD66b) and exocytosis (CD63), as described above. Cells were then incubated with LY diluted at 1 mg/mL in RPMI for 30 mins at 37ºC. For *in vitro* samples, PMNs were transmigrated to CFASN containing LY (1 mg/mL) for 2, 10, and 18 hours, after which the cells were washed with PBS-EDTA and stained with viability probes and antibodies, as above. Cells were then washed with RPMI and pinocytosis was measured by flow cytometry.

Bacteria-killing assay. *P. aeruginosa* strain PAO1 was grown in LB broth (BD Biosciences) at 37ºC with aeration to an optical density (600 nm) of 0.5. Bacteria were pelleted by centrifugation at 14,000 g for 5 min at room temperature, resuspended in 500 µl 10% autologous plasma in RPMI and opsonized for 30 minutes at 37°C. Opsonized bacteria were added to PMNs at a multiplicity of infection of 0.1. After an hour of incubation at 37°C, the cultures were lysed using 0.1% Triton for 2 minutes, after which the bacteria were serially diluted and plated in triplicate on LB plates and incubated at 37°C in a non-CO_2 incubator overnight. Viable bacterial CFUs were counted the following day and bacterial viability was calculated as a percentage of bacterial counts at time 0.

Metabolic assays. Real-time analysis of the extracellular acidification rate (ECAR) as a measure of glycolysis, and Oxygen Consumption Rate (OCR), were performed using a Seahorse XFp Extracellular Flux Analyzer (Agilent). In brief, PMNs were collected after transmigration, resuspended in Seahorse assay medium (DMEM-based, without serum, glucose or bicarbonate) and plated at 7.5 $\times 10^5$ cells/well on CellTak (BD Biosciences)-

coated Seahorse assay plates. PMNs were attached to the bottom of the wells by centrifugation at 350 g (without brake), and incubated for 45 minutes before the assay in a non-CO_2 incubator at 37ºC. The glycolysis stress test kit (Agilent) was used to obtain real-time measurements of ECAR and OCR upon sequential injections of glucose (10 mM) to induce glycolytic activity, oligomycin (complex V inhibitor, used at 3 μM) to shut down mitochondrial contribution to glucose consumption, 2-deoxyglucose (2-DG, 0.1 M) to competitively inhibit glucose use by hexokinase, and when indicated diphenyleneiodonium (DPI, 10 μM), an NADPH oxidase inhibitor. Extracellular lactate was measured in culture supernatants after Seahorse runs using the lactate assay kit (Biovision), according to manufacturer's instructions.

Murine PMN isolation and transmigration. Bone marrow PMNs were collected from the tibias and femurs of wild-type mice by flushing with RPMI with 10% FBS using a 25-gauge needle. Cells were then washed with PBS and allowed to migrate in our model to either CFASN or LTB4 for 5 or 10 hours. Recruited cells were stained with antibodies and analyzed by flow cytometry as detailed above for CD11b (M1/70) and Ly6G (1A8) expression to identity mature PMNs, and for CD63 (NVG-2) expression to assess primary granule release. Antibodies were from BioLegend.

Immunofluorescence and confocal microscopy. After 10 hours PTM with PMNs recruited to LTB4 or CF ASN, epithelialized Alvetex scaffolds were washed twice with PBS, and fixed with 4% paraformaldehyde in PBS for 15 minutes at room temperature. Fixed scaffolds were washed with PBS, then permeabilized with 0.5% Tween 20 in PBS (PBS-T), followed by two washes with PBS-T supplemented with 2% goat serum. After the last wash,

scaffolds were incubated overnight at 4°C with a polyclonal anti-ZO-1 antibody (ZMD.437, Thermo Fisher Scientific) diluted 1:250 in PBS with 2% goat serum. Scaffolds were then washed three times with PBS with 2% goat serum, and incubated for 1 hour at room temperature with a secondary anti-rabbit antibody (Invitrogen), followed by a 15 minute incubation with 0.5 μg/mL DAPI (BioLegend) as a nuclear stain. Scaffolds were then washed twice with PBS with 2% goat serum, and then twice more with PBS alone. Scaffolds were then dried and mounted on a glass slide, and stored for confocal imaging. Z-stack images were acquired using a Nikon A1plus confocal microscope with Apo TIRF 60X oil objective, and analyzed using the Imaris Image Analysis Software (Bitplane, version 8.2).

Dextran permeability assay. After 2 hours PTM with PMNs recruited to LTB4 or CF ASN, epithelialized Alvetex scaffolds were assessed for permeability to 4 kDa FITC dextran (Sigma) and Texas Red-70 kDa dextran (Thermo Fisher Scientific). Scaffolds were washed twice with HBSS plus calcium and magnesium (HBSS+), and incubated for 30 mins at 37°C to equilibrate them in this new medium. Then a 500 μl mix of 0.5 mg/mL 4 kDa FITC dextran and 0.25 mg/mL 70 kDa Texas Red dextran diluted in HBSS+ was added apically, and incubated for 30 mins at 37°C. Basal fluid was then sampled and measured for concentrations of both FITC and Texas Red dextrans in a clear bottom black well plate using the SpectraMax iD3 microplate reader (Molecular Devices). Relative percentage permeability of each scaffold was calculated against the maximum permeability condition to 4 kDa Dextran and 70kDa dextran obtained by treatment of an epithelialized Alvetex scaffold with 1% Triton X100 in HBSS+ for 2 hours.

Data analysis. Statistical analyses were performed using JMP12 (SAS Institute). Between-group and matched-pair statistical analyses used the Wilcoxon rank sum and signed-rank tests, respectively. Correlations were tested using the non-parametric Spearman test. A threshold of $p<.05$ was used to determine significance.

RESULTS

Core features of CF airway PMNs are recapitulated upon blood PMN transmigration in vitro. We designed a model **(Fig. 2.1A)** in which purified airway supernatant (ASN) from CF patients leads to the transepithelial migration of blood PMNs, yielding large numbers of "airway-like" PMNs that can be identified by flow cytometry **(Fig. 2.7A)**. PMNs transmigrated into CF ASN shed the CD62L receptor, as expected after transmigration **(Fig. 2.1B)**. Remarkably, these cells also recapitulated core phenotypes of PMNs recruited to the CF airway lumen *in vivo*, namely downmodulation of the phagocytic receptor CD16 **(Fig. 2.1C)**, and high CD63 expression **(Fig. 2.1D)**, reflecting active release of NE-rich granules [18]. While *in vivo* samples contain a mixed population of PMNs recruited to CF airways over hours/days, our model enables collection of transmigrated PMNs at precise intervals, so that the dynamic course of pathological conditioning can be resolved **(Fig. 2.7B)**. We assessed the status of the epithelial layer after PMN transmigration induced by LTB4 and CF ASN, and found that both conditions mostly preserved epithelial viability and junctionality **(Fig 2.8A)**, although permeability to low- and high-molecular weight dextran was expectedly increased compared to baseline **(Fig 2.8B)**.

Healthy control airway milieu promotes transmigration, but not pathological conditioning, of PMNs. PMNs transmigrated to HC and CF ASN showed similar loss of CD62L, while CD16 downregulation and CD63 upregulation were less pronounced at all time points for PMNs transmigrated to HC ASN **(Fig. 2.2A-C)**. In addition, HC ASN recruited PMNs in lesser numbers than CF ASN at 10 and 18 hours PTM **(Fig. 2.2D)**. These patterns recapitulate differences between HC and CF airway PMNs observed *in vivo* [8] (independently reproduced in **Fig. 2.9A-C)**. We also showed previously [9] that the

immunomodulatory receptor PD-L1 is uniformly increased *in vivo* on HC airway PMNs compared to HC blood PMNs, as also seen in our model, while CF airway PMNs cluster into PD-L1^{Lo} and PD-L1^{Hi} subsets, a bimodal pattern also recapitulated in our model **(Fig. 2.10A)**. In both HC and CF subjects, airway PMNs increase surface expression of Arg1 compared to blood PMNs [9], a pattern again recapitulated *in vitro* **(Fig. 2.10B)**.

Pathological conditioning induced by CF ASN on transmigrated PMNs is independent of their origin. Next, we investigated whether the origin of blood PMNs affected transmigration and pathological conditioning. We found that blood PMNs from HC and CF subjects do not markedly differ in their recruitment and exocytosis profile after transmigration to CF ASN **(Fig. 2.11D)**. Murine PMNs (from wiild-type animals) also undergo transmigration and primary granule hyperexocytosis in the context of CF ASN **(Fig. 2.11E)**. Thus, our data demonstrate a dominant role for CF ASN in causing pathological conditioning of transmigrated PMNs, irrespective of their origin.

CF airway milieu and transmigration are both critical to pathological conditioning of PMNs. A low dilution of CF ASN (1:3) leads to levels of primary granule exocytosis in transmigrated PMNs matching those seen in CF patients *in vivo*, while intermediate (1:30) and high (1:300) dilutions lead to two- and four-fold lower levels, respectively **(Fig. 2.2E)**. Diluting CF ASN also decreases transmigrated PMN count **(Fig. 2.2F)**. CF ASN contains multiple factors able to recruit and activate PMNs, including host chemoattractants [23] like LTB4 and CXCL8, and bacterial products [14] like fMLF and LPS. In our model, LTB4, CXCL8, and fMLF alone failed to induce primary granule exocytosis, despite promoting transmigration **(Fig. 2.2G-H)**. Importantly, direct incubation of blood PMNs in CF ASN

without transmigration failed to induce primary granule exocytosis, and delayed the downregulation of CD16 **(Fig. 2.2I-J)**. Thus, pathological conditioning of blood PMNs by CF ASN requires transmigration, and can be modulated by experimental dilution of the ASN.

Inhibition of LPS and LTB4 signaling does not impact the pathological conditioning of PMNs by the CF airway milieu. LPS alone failed to induce primary granule exocytosis or CD16 downregulation when used as an apical stimulus in the model **(Fig. 2.3A-B)**. LPS signals through Toll-like receptor 4, and blockade of this signaling cascade in PMNs using LPS-RS (24) did not affect primary granule exocytosis and CD16 modulation, whether in the context of CF ASN or LPS **(Fig. 2.3A-B)**. LPS-RS down-modulated surface CD11b expression and intracellular ROS accumulation in PMNs in the context of both LPS and CF ASN at 2 hours PTM, confirming the activating potential of LPS on airway PMNs, and the inhibitory mode of action of LPS-RS on LPS-induced activation. LTB4 is a critical host-derived chemoattractant orchestrating PMN migration through the lamina propria (25). Acebilustat blocks LTB4 production by inhibiting LTA4 hydrolase, the rate-limiting enzyme for LTB4 synthesis (26). In our model, acebilustat decreased the apical PMN count at 2, 10 and 18 hours PTM **(Fig. 2.3C)**, but it did not affect primary granule exocytosis or CD16 downregulation in PMNs **(Fig. 2.3D)**.

ASN from various airway diseases induce the GRIM fate upon transmigration. Severe asthma and bronchiolitis are examples of other diseases in which PMN dysfunction has been implicated as a potential pathogenic process (18). In our model, airway milieu from patients with these conditions leads to PMN transmigration and primary granule exocytosis, again

recapitulating *in vivo* data **(Fig.2.11A-C)**. In patients with COPD, disease symptoms, airway PMN dysfunction, and release of toxic by-products such as NE are similar to those observed in CF (19). In our model, COPD ASN leads to PMN recruitment and exocytosis of primary granules, mimicking in vivo data **(Fig. 2.11D-E)**. Similarly to what we observed for CF ASN, CD16 is also downregulated upon PMN transmigration to COPD ASN **(Fig. 2.11E)**.

Increased pinocytosis is a newly identified feature of PMNs transmigrated to the CF airway milieu, in vivo and in vitro. A prior study linked enhanced primary granule release by PMNs to pinocytosis (27). In CF patients, airway PMNs showed enhanced pinocytosis compared to blood PMNs, and pinocytic activity in CF airway PMNs correlated with primary granule release **(Fig. 2.4A)**. In our model, PMNs transmigrated to CF ASN increased their pinocytic activity over time, with a similar correlation with primary granule release to that observed *in vivo* **(Fig. 2.4B)**.

PMN transmigration to CF airway milieu leads to increased metabolism, but decreased bacterial killing. *In vivo*, CF airway PMNs undergo metabolic activation (7, 10). *In vitro*, PMNs transmigrated to CF ASN show increased glycolysis, as reflected by a higher extracellular acidification rate, and increased surface Glut1 expression, compared to those transmigrated to LTB4 **(Fig. 2.5A-D)**. PMNs transmigrated to CF ASN also showed a strong upregulation of their oxygen consumption rate, which was not sensitive to the inhibitor of mitochondrial oxidative phosphorylation oligomycin **(Fig. 2.5E-F)**, but was associated with an increased ROS production **(Fig. 2.5G)**. This is consistent with the notion that activated PMNs use oxygen for ROS production via either NADPH oxidase or mitochondrial complex I, with support from glycolysis (28, 29). Despite this metabolically

activated state, PMNs transmigrated to CF ASN showed lower ability to kill *P. aeruginosa* than those transmigrated to LTB4 **(Fig. 2.5 H)**. Thus, our model recapitulates a key paradox in CF, namely the inability to kill bacteria (14), despite PMN recruitment and their metabolic activation.

Metformin inhibits key pathological phenotypes of PMNs recruited to the CF airway milieu. Metformin is a metabolic modulator able to curb down glucose-dependent cell activation, ROS production, and inflammation (29, 30). Metformin had a mild effect on glycolysis, but strongly inhibited oxygen consumption in PMNs transmigrated to CF ASN **(Fig. 2.6 A-B)**. Metformin acts, in part, via activation of the metabolic checkpoint enzyme 5' adenosine monophosphate-activated protein kinase α1 (AMPKα1), by facilitating its phosphorylation (31). We observed that phosphorylated AMPKα1 levels were indeed reduced in CF airway compared to blood PMNs *in vivo*, and in PMNs transmigrated to CF ASN compared to LTB4 *in vitro*, and that treatment with metformin increased phosphorylated AMPKα1 levels in PMNs transmigrated to CF ASN **(Fig. 2.6C)**. This effect was associated with a reduction of ROS production and primary and secondary granule exocytosis **(Fig. 2.6D)**. Interestingly, metformin treatment did not rescue the ability of PMNs transmigrated to CF ASN to kill bacteria **(Fig. 2.6E)**.

DISCUSSION

Massive airway recruitment of PMNs, and their pathological conditioning resulting in heightened granule release, immunoregulatory, and metabolic activities ("GRIM" fate), and depressed bacterial killing, drive early and chronic lung damage in CF and other intractable diseases. These processes are incompletely understood and remain untapped as potential therapeutic targets, in large part due to the lack of adequate models. The model described here enables transepithelial recruitment and pathological conditioning yielding GRIM PMNs that feature characteristic hyperexocytosis of NE-rich granules, but also decreased surface CD16, increased Arg1 expression, bimodal PD-L1 expression, increased metabolic activity and decreased bacterial killing, all hallmarks of CF airway GRIM PMNs *in vivo*. In addition, we describe a new metabolic and functional feature of these cells *in vivo* and *in vitro*, which relates to their enhanced pinocytosis.

A dominant conditioning effect of CF airway secretions was noted in studies where these were acutely added to healthy or CF airway epithelium (32), and macrophages (33), although their effect on PMNs was not explored. In our model, apical CF ASN was necessary and sufficient to recruit and condition blood PMNs to adopt the GRIM fate, regardless of whether these PMNs originate from CF or HC subjects. Thus, our data demonstrate a dominant environmental effect of factors present in CF airway milieu onto recruited PMNs. However, they do not exclude a contribution of endogenous CFTR in PMNs (34, 35), although such an effect appears to be secondary relative to the induction of the pathogenic GRIM fate. Further studies are needed to fully delineate the still debated issue of whether endogenous CFTR is key to the function of PMNs recruited to CF airways *in vivo*, and in this model.

Our data show that PMN transmigration toward ASN from COPD and LD patients also lead to substantial primary granule exocytosis, similar to the results obtained with CF ASN, while HC ASN induced transmigration but not primary granule exocytosis. Thus, PMN pathological conditioning into the GRIM fate is not unique to CF. Murine PMNs also undergo transmigration and hyperexocytosis of NE-rich granules, suggesting that factors in CF ASN leading to PMN pathological conditioning are cross-specific. This result is reminiscent of the cross-specific recruitment of murine PMNs in human CF small airway xenografts (36). It also opens potential avenues for future studies using relevant mouse strains in our model to assess mechanisms of PMN plasticity and conditioning (14), and further delineate the role of endogenous CFTR using PMNs from wild-type and CFTR knockout or mutant mice.

CF ASN is characterized by an abnormal molecular composition (including altered lactate (11), small metabolite (37), and protein (38) contents), itself caused by altered epithelial function, and the sustained presence of bacteria and PMNs in the CF airway lumen (14). It is interesting to note that at concentrations similar to those used to promote PMN transmigration and conditioning in our model, CF ASN induces T-cell apoptosis (9). At lower concentrations, T-cells survive but their ability to activate and proliferate is dramatically reduced, due in part to Arg1 activity originating from GRIM PMNs. Both Arg1 and PD-L1, another prominent T-regulatory molecule, are modulated in the model in similar fashion to *in vivo* (9). Thus, CF ASN exerts paradoxical effects on PMNs and T-cells, promoting the former while demoting the latter, which further contributes to the build-up of a PMN-dominated inflammatory environment in the CF airway lumen.

The ability of CF ASN to license recruited PMNs metabolically toward increased Glut1 expression and glycolytic activity is of particular significance, since PMNs are generally

thought of as short-lived, yet thrive and undergo transcriptional changes (10) in this pathological milieu. In addition, GRIM PMNs obtained by transmigration into CF ASN show decreased killing of *P. aeruginosa* as compared to those transmigrated to LTB4, despite their metabolic licensing, which is consistent with CF pathology *in vivo* (14, 15). Further studies will focus on this paradox and screen for drugs capable of rewiring GRIM PMNs to enact proper bacterial clearance. The correlation between pinocytic activity and primary granule exocytosis in PMNs migrated to the CF airway lumen *in vivo* and *in vitro* also suggests a link between metabolic activity and abnormal granule mobilization (27), which warrants further study.

In typical Transwell models, PMNs are forced to squeeze one-by-one through pre-drilled 3 μm-wide cylindrical pores before reaching the epithelial basement membrane. By contrast, our model includes a highly porous lamina propria-like scaffold with 36-40 μm-wide pores that can each accommodate 20+ cells, thus enabling PMNs to congregate and migrate in physiologically relevant manner (25). Confocal imaging confirmed that LTB4- and CF ASN-induced PMN transmigration largely preserved the viability and typical peripheral ZO-1 staining pattern. Dextran permeability assays showed that both LTB4- and CF ASN-induced PMN transmigration led to an expected increase in transepithelial permeability. However, this increase in permeability remained well below that observed Triton X-treated monolayers (maximum permeability control). These results emphasize the physiological relevance and robustness of this experimental model.

While we plan to test the use of primary epithelial cells from CF patients in our model in future studies, the present set-up including a commercial 3D substrate, a small airway epithelial cell line, standard culture media, and human blood PMNs, provides a highly robust and reproducible platform to mass-produce airway-like PMNs for research. The CF

ASN used to induce PMN migration and pathological conditioning is a very abundant material easily collected from expectorations. Our model is advantageous not only because it integrates patient airway milieu as the apical stimulus; but also because blood PMNs from patients can be integrated as target cells; and because drugs can be readily added to blood and/or airway sides, mimicking systemic and airway routes of administration. These combined features provide the ability to de-risk drugs at an early stage, in conditions close to those seen *in vivo*.

Because of the long-held belief that PMNs die rapidly after migration into CF airways, PMN-targeted therapies have focused on reducing their recruitment via corticosteroids or non-steroidal anti-inflammatories (39). Because GRIM PMNs found in CF airways are alive when they release their toxic contents (7, 8), the pathological conditioning of PMNs, rather than their recruitment, may be a more effective target for new therapeutic agents to benefit patients with CF and other similar diseases (40). Our data obtained with the metabolic regulator metformin illustrate that point. Indeed, combined effects of metformin on GRIM PMN metabolism (i.e., oxygen consumption), ROS production, and degranulation, suggest that pathogenic functions in these cells are fueled by dysregulated metabolism, and that targeting metabolism in GRIM PMNs may be a relevant strategy for therapeutic intervention. Whether metformin is a relevant drug in the context of CF is questionable, however, since it did not rescue but rather seemed to further depress the ability of PMNs transmigrated to CF ASN to kill bacteria. Further studies are required to determine whether this adverse effect of metformin treatment may be linked to its ability to counter ROS production and degranulation, an otherwise beneficial effect of metformin considering the self-damaging impact of ROS and granule effectors unleashed by pathologically conditioned PMNs in CF airways.

Together, this study emphasizes the complex roles of GRIM PMNs, which represent a promising target for immunotherapy in CF and other human airway diseases. We also introduce a simple, robust and flexible *in vitro* model for basic studies and drug development efforts focused on this key pathogenic subset.

Table 2.1. Patient demographics.

Condition	N	Gender (F:M)	Age (years)	FEV1 (%pred)
CF	33	17:16	25 [24; 31]	50 [37; 61]
COPD	9	0:9	67 [59; 72]	40 [30; 47]
LD	5 (4 SA, 1 bronchiolitis)	3:2	34 [31; 58]	N/A

CF: cystic fibrosis; COPD: chronic obstructive pulmonary disease; FEV1 (%pred): forced expiratory volume in 1 second (%predicted); LD: lung disease other than CF or COPD; N/A: not available; SA: severe asthma. Numerical data presented as median [interquartile range]

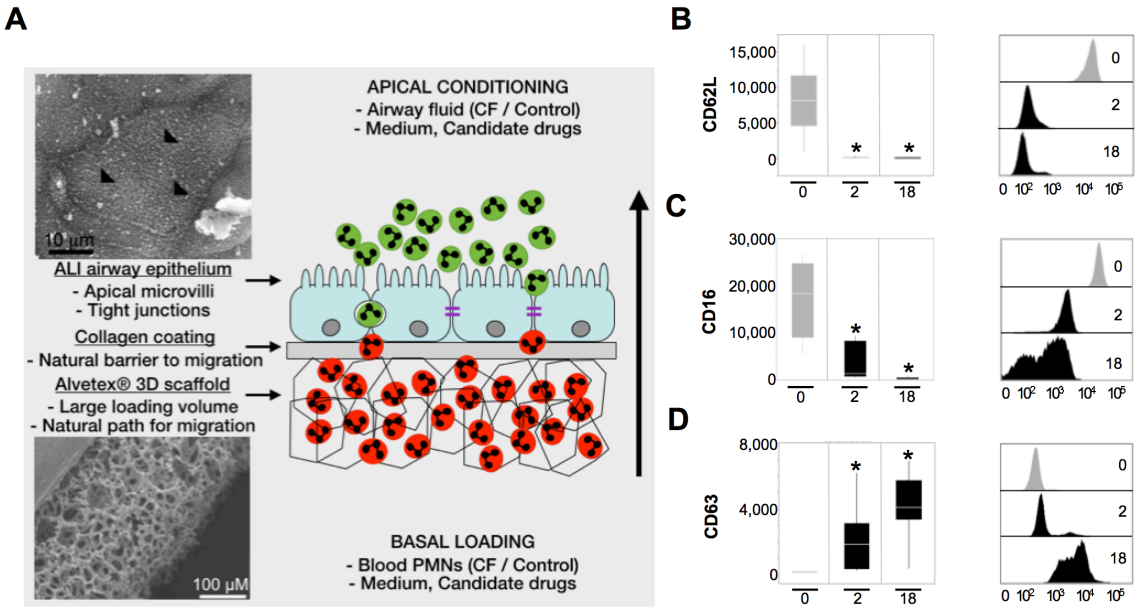

Figure 2.1. In vitro model mimicking human PMN transmigration and pathological conditioning in small airways. (A) We established a model emulating the small airway mucosa by growing the H441 Club-like human small airway cell line at air-liquid interface (upper left insert, arrowheads pointing to apical microvilli typical or Club cells) onto a continuous collagen layer covering a 200 µm thick, porous scaffold (lower left insert). The apical milieu impacts the conditioning of transmigrated PMNs, depending on its origin, e.g., airway supernatant (ASN) from CF or control subjects, or medium containing chemoattractants. Drugs can be tested in the model, via apical and/or basal addition. Transmigrated PMNs conditioned by the apical milieu of choice, exposed or not to candidate drugs, can be retrieved in large numbers and submitted to downstream assays. **(B-D)** Analysis of CD62L, CD16, and CD63 expression, respectively, shown in box plots (left panels) and representative histograms (right panels) for blood PMNs at 2 and 18 hours post-

transmigration (PTM) into CF ASN (black), compared to PMNs pre-transmigration (grey). * indicates $p < .05$ at 2 or 18 hours PTM vs. pre-transmigration ($n = 8$ experiments).

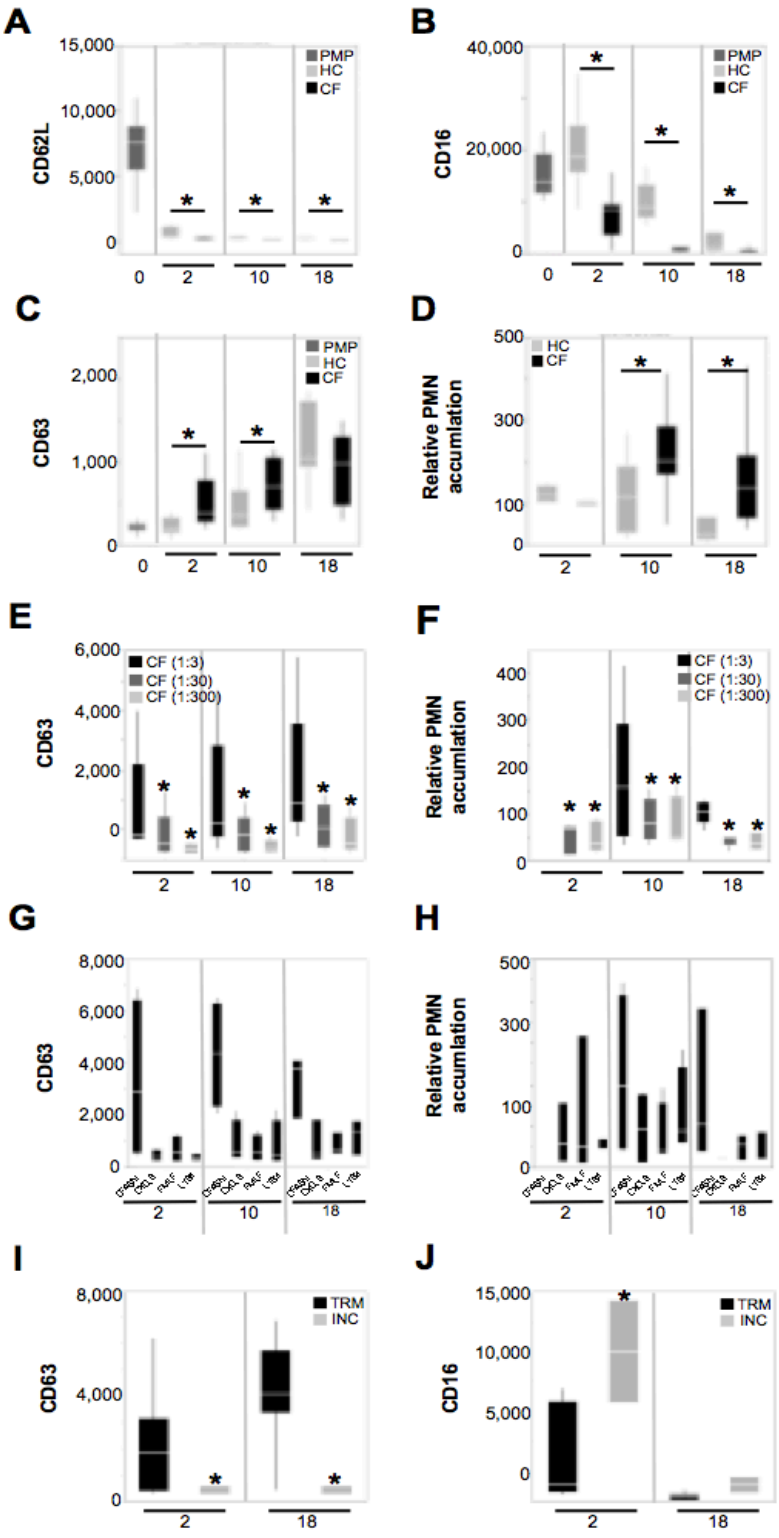
A
CD62L
15,000
10,000
5,000
0
PMP
HC
CF
0
2
10
18
B
CD16
40,000
20,000
0
C
CD63
2,000
1,000
D
Relative PMN accumulation
500
300
100
E
CF (1:3)
CF (1:30)
CF (1:300)
6,000
4,000
F
400
200
G
8,000
6,000
4,000
2,000
H
I
TRM
INC
J

Figure 2.2. CF ASN and transmigration are both required to induce pathological conditioning of PMNs *in vitro*. (A-D) Analysis of CD62L, CD16, and CD63 expression and relative PMN accumulation, respectively, for PMNs transmigrated to HC control (light grey) vs. CF ASN (black) at 2, 10 and 18 hours PTM, compared to PMNs pre-transmigration (grey). The relative PMN accumulation at each time point was calculated as % fold change compared to the number of PMNs transmigrated into CF ASN at 2 hours PTM (set at 100%). *indicates $p<.05$ for HC vs. CF ASN (n = 8 experiments). **(E-F)** Analysis of CD63 expression and relative PMN accumulation, respectively, for PMNs transmigrated to CF ASN at various dilutions, 2, 10, and 18 hours PTM. The relative PMN accumulation at each time point was calculated as % fold change compared to the number of PMNs transmigrated into CF ASN at the minimal dilution at 2 hours (set at 100%). * indicates $p<.05$ in matched pairs statistics between dilutions (n = 5 experiments). **(G-H)** Analysis of CD63 expression and relative PMN accumulation, respectively, for PMNs transmigrated to CF ASN, CXCL8 (100 ng/mL), fMLF (100 nM), or LTB4 (100 nM) at 2, 10, and 18 hours PTM. The relative PMN accumulation at each time point was calculated as % fold change compared to the number of PMNs transmigrated into CF ASN at the minimal dilution at 2 hours (set at 100%). * indicates $p<.05$ in matched pairs statistics between conditions (n = 5 experiments). **(I-J)** Analysis of CD63 and CD16 expression, respectively, for PMNs transmigrated to CF ASN (TRM, black), or incubated in it without transmigration (INC, grey) for 2 and 18 hours. * indicates $p<.05$ in matched pairs statistics between conditions (n = 5 experiments).

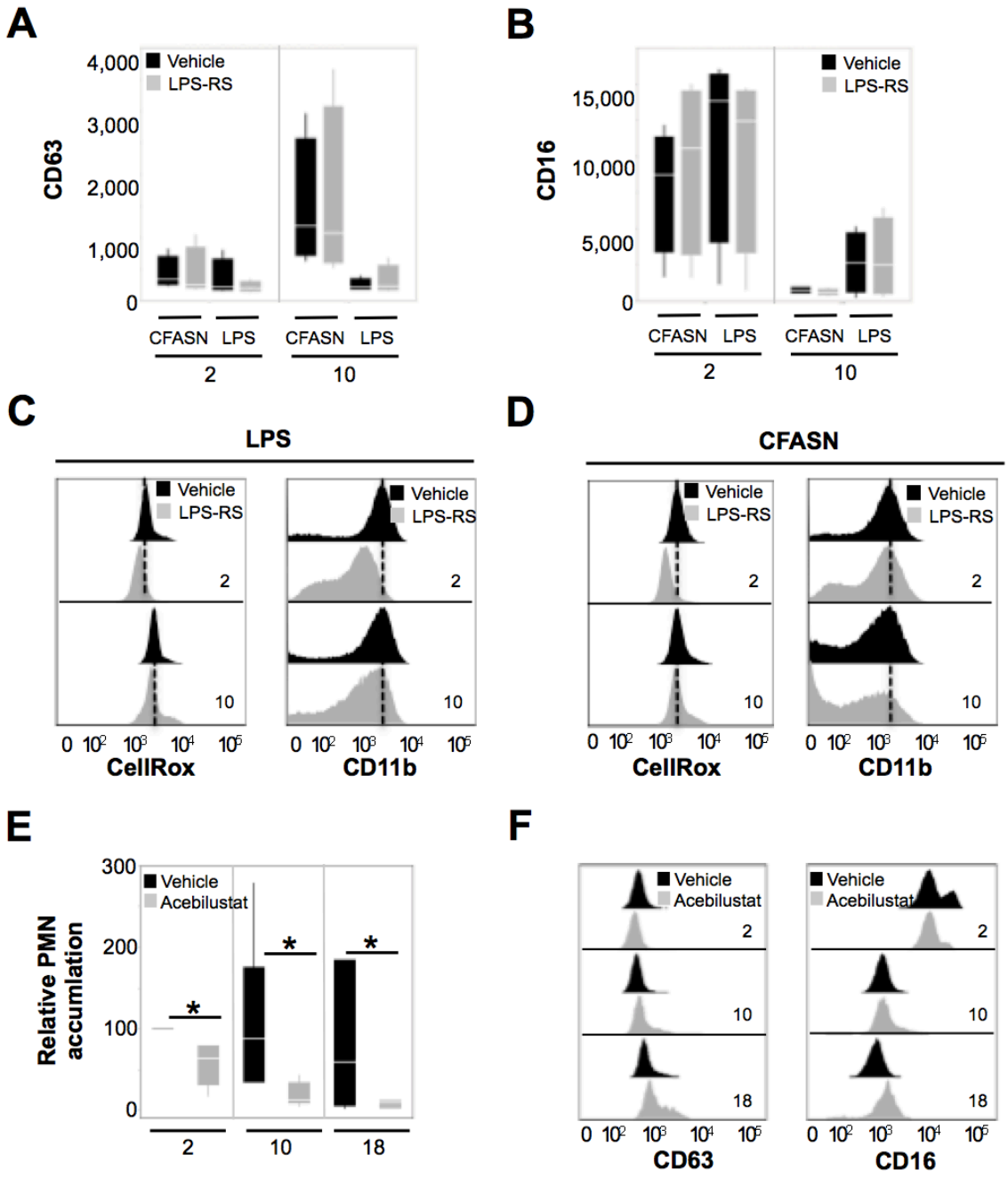

Figure 2.3. Inhibition of LPS and LTB4 signaling does not impact pathological conditioning of PMNs by CF ASN. (A-B) Analysis of CD63 and CD16 expression, respectively, for PMNs transmigrated to LPS (500 ng/mL) or CFASN, each tested in the context of vehicle control (black) or LPS blockade by LPS-RS (5 μg/mL, grey), 2 and 10 hours PTM (n = 5 experiments). **(C-D)** Analysis of CD11b expression and intracellular ROS

levels (CellRox probe) in PMNs transmigrated to LPS (500 ng/mL) or CFASN combined with either vehicle (black) or LPS-RS (5 μg/mL, grey) for 2 and 10 hours. Shown here in representative histograms. **(E-F)** Analysis of CD63 expression and relative PMN accumulation, respectively, for PMNs transmigrated to CF ASN with vehicle control (black) or the LTA4H inhibitor acebilustat (0.1 μM, grey) for 2, 10, and 18 hours PTM. The relative PMN accumulation at each time point was calculated as % fold change compared to the number of PMNs transmigrated to CF ASN with vehicle control at 2 hours (set at 100%). * indicates $p<.05$ when comparing PMNs transmigrated to CF ASN with vehicle control vs. acebilustat (n = 3 experiments).

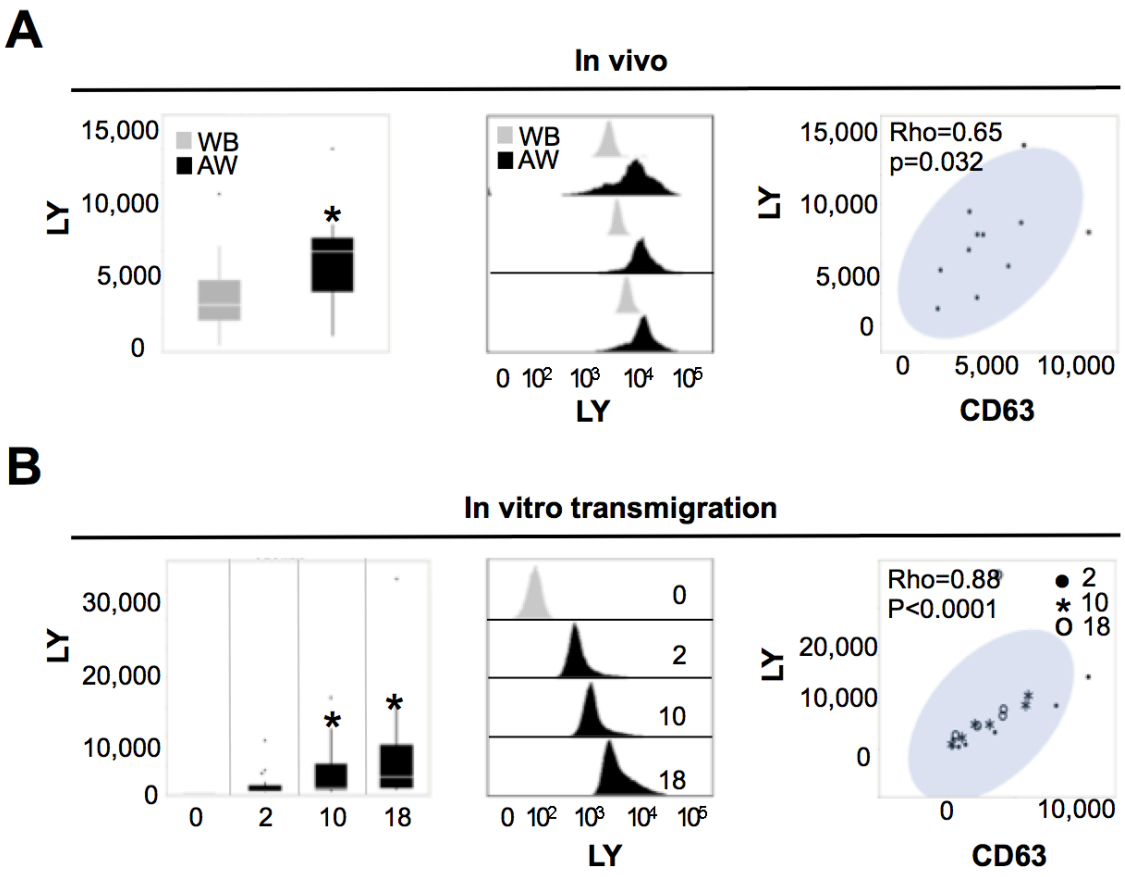

Figure 2.4. PMN transmigration to CF ASN *in vivo* and *in vitro* induces increased pinocytosis, concomitant with primary granule exocytosis. (A) Lucifer Yellow (LY) uptake was used to assess pinocytosis in whole blood (WB, grey) and airway (AW, black) PMNs from CF patients as illustrated in box plot (n =12 patients, left panel), and representative histograms (n = 3 patients, middle panel). Correlation of primary granule exocytosis (reflected by surface CD63) with pinocytosis (LY uptake) within CF airway PMNs *in vivo* was assessed using the Spearman test (n = 12 patients, right panel). **(B)** LY uptake was assessed on PMNs transmigrated to CF ASN at 2, 10, and 18 hours PTM as illustrated in box plot (n = 6 experiments, left panel), and representative histograms (middle panel). * indicates $p < .05$ comparing pinocytosis at 10 and 18 hours PTM vs. 2 hours PTM (left panel). Correlation of primary granule exocytosis (reflected by surface CD63) with

pinocytosis (LY uptake) within CF airway PMNs *in vitro* was assessed using the Spearman test (right panel, all time points, as labeled).

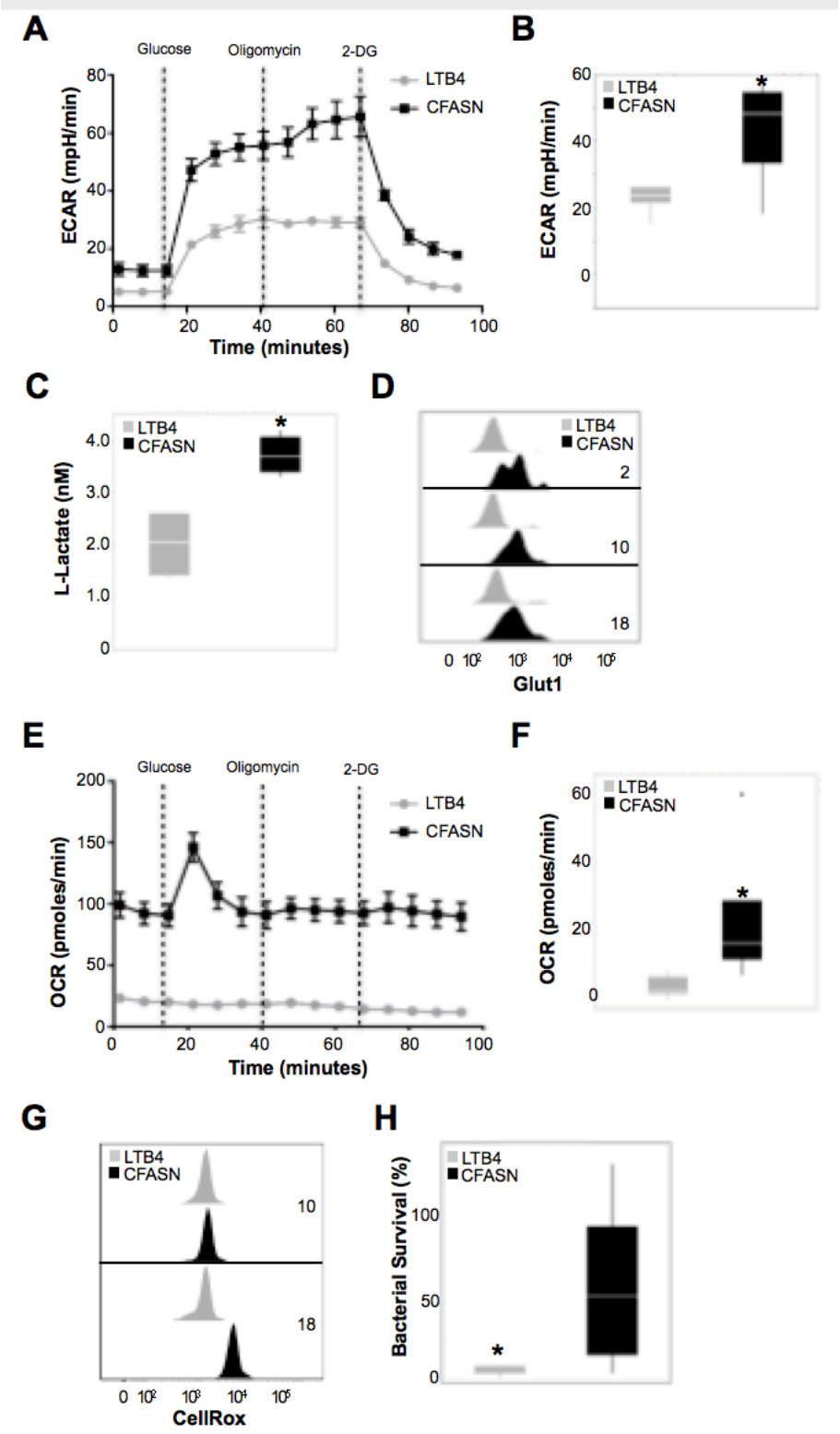
A
Glucose
Oligomycin
2-DG
LTB4
CFASN
ECAR (mpH/min)
Time (minutes)
B
LTB4
CFASN
ECAR (mpH/min)
C
LTB4
CFASN
L-Lactate (nM)
D
LTB4
CFASN
2
10
18
Glut1
E
Glucose
Oligomycin
2-DG
LTB4
CFASN
OCR (pmoles/min)
Time (minutes)
F
LTB4
CFASN
OCR (pmoles/min)
G
LTB4
CFASN
10
18
CellRox
H
LTB4
CFASN
Bacterial Survival (%)

Figure 2.5. PMN transmigration to CF ASN increases glycolysis, oxygen consumption, and ROS production, but impairs killing of *P. aeruginosa*. (A) Analysis of extracellular acidification rate (ECAR) by PMNs transmigrated to LTB4 (100 nM, grey) or CF ASN (black) for 10 hours, then washed, and placed in fresh assay medium in a Seahorse XFp system, with subsequent injections of glucose, oligomycin, and 2-DG (representative tracing). **(B)** Maximal ECAR value was measured after injection of glucose during Seahorse runs. **(C)** Extracellular L-lactate was measured in PMN supernatants after Seahorse runs. **(D)** Analysis of surface Glut1 glucose transporter expression in PMNs transmigrated to LTB4 (grey) or CF ASN (black) shown in representative histograms at 2, 10, and 18 hours PTM. **(E)** Analysis of oxygen consumption rate (OCR) by PMNs transmigrated to LTB4 (grey) or CF ASN (black) for 10 hours in a Seahorse XFp system (representative tracing, as above). **(F)** Maximal OCR value was measured after injection of glucose during Seahorse runs. **(G)** Analysis of intracellular ROS levels (CellRox probe) by PMNs transmigrated to LTB4 (grey) or CF ASN (black) shown in representative histograms at 10, and 18 hours PTM. **(H)** PMNs transmigrated to LTB4 (grey) or CF ASN (black) for 10 hours were washed and incubated with serum-opsonized *P. aeruginosa* (PAO1 strain), after which bacterial survival was assessed by colony count. Box plots (B, C, F, H) show * for $p<.05$ comparing PMNs transmigrated to CF ASN vs. LTB4 (n = 5 experiments).

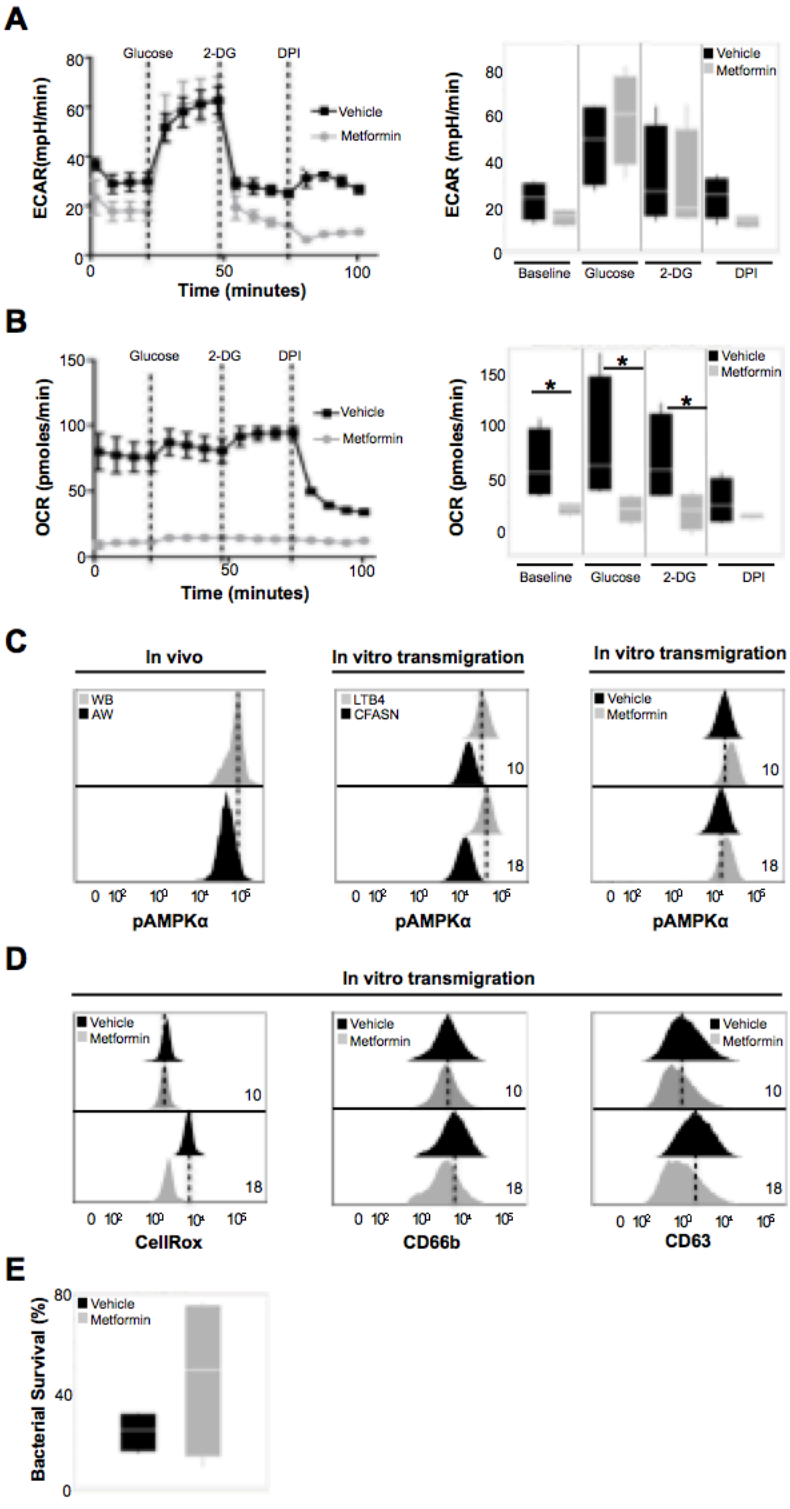
A
Glucose
2-DG
DPI
ECAR(mpH/min)
Vehicle
Metformin
Time (minutes)
ECAR (mpH/min)
Baseline
Glucose
2-DG
DPI
B
OCR (pmoles/min)
OCR (pmoles/min)
C
In vivo
In vitro transmigration
In vitro transmigration
WB
AW
LTB4
CFASN
pAMPKα
D
CellRox
CD66b
CD63
E
Bacterial Survival (%)

Figure 2.6. Metformin modulates oxygen consumption, ROS production, granule exocytosis, and bacterial killing capacity by PMNs transmigrated to CF ASN *in vitro*. (A-B) Analysis of ECAR and OCR, respectively, for PMNs pre-incubated for 4 hours with either metformin or vehicle control, and subsequently transmigrated to CF ASN with vehicle control (black) or CF ASN containing metformin (50 μM, grey) for 18 hours, followed by washing, and suspension in fresh assay medium in the Seahorse system. Shown are representative tracings (left panels), and box plots for peak ECAR and OCR at baseline and after glucose, DPI, and 2-DG injections (right panels), n = 4 experiments, with *indicating $p<.05$ comparing with vehicle control vs. metformin conditions. **(C)** Representative histograms are shown for the metformin target phosphorylated AMPKα1 (pAMPKα) in CF blood (grey) and airway (black) PMNs *in vivo* (left panel); in PMNs transmigrated to LTB4 and CF ASN at 10 and 18 hours PTM (middle panel); and in PMNs transmigrated to CF ASN with either vehicle or metformin treatment at 10 and 18 hours PTM (right panel). Hashed lines in all panels represent median in control conditions (n = 4 experiments). **(D)** Representative histograms are shown for intracellular ROS levels (CellRox probe, left panel), as well as CD66b (middle panel), and CD63 (right panel) expression assessed in PMNs transmigrated into CF ASN with either vehicle (black) or metformin (grey) treatment at 10 and 18 hours PTM, with hashed line in all panels representing median in control conditions (n = 3 experiments). **(E)** PMNs transmigrated for 18 hours into CF ASN combined with either vehicle control (black) or metformin (50 μM, grey) were washed and incubated with serum-opsonized *P. aeruginosa* (PAO1 strain), after which bacterial survival was assessed by colony count, as shown here in a box plot (n = 4 experiments).

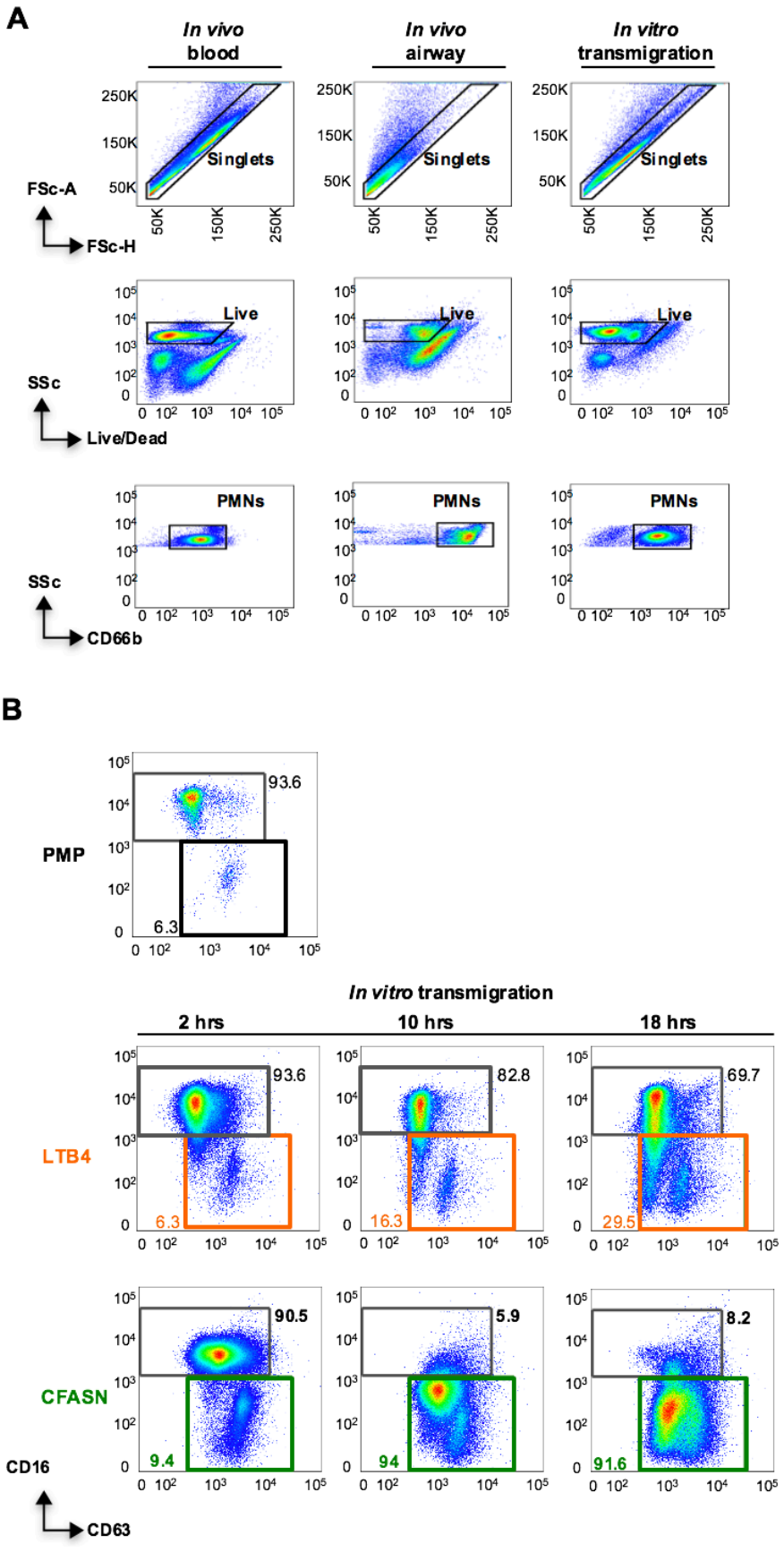
A
In vivo blood
In vivo airway
In vitro transmigration
Singlets
FSc-A
FSc-H
Live
SSc
Live/Dead
PMNs
CD66b
B
PMP
93.6
6.3
In vitro transmigration
2 hrs
10 hrs
18 hrs
LTB4
93.6
6.3
82.8
16.3
69.7
29.5
CFASN
90.5
9.4
5.9
94
8.2
91.6
CD16
CD63

Figure 2.7. *In vivo* and *in vitro* gating of live PMNs and two-dimensional analysis of pathological conditioning of PMNs. (A) To distinguish live PMNs *in vivo* from blood (left panels) and airway samples (middle panels), and *in vitro* from the apical compartment of our transmigration model (right panels), we used three-step flow cytometry gating, including (i) a singlet gate based on forward scatter area vs. height (top row); (ii) a viability gate based on side scatter and Live/Dead staining (middle row); and (iii) a PMN gate based on side scatter and CD66b staining (bottom row). **(B)** Shown are representative two-dimensional plots illustrating surface CD63 (surrogate for primary granule release) and CD16 (phagocytic receptor) expression in PMNs freshly isolated from blood by Polymorphprep (PMP, top panel), and after transmigration in the model for 2, 10 and 18 hours toward either LTB4 or CF ASN (bottom panels). Note the dramatic shift toward the pathological $CD63^{hi}CD16^{lo}$ phenotype in the context of CF ASN after 10 and 18 hours PTM (green boxes).

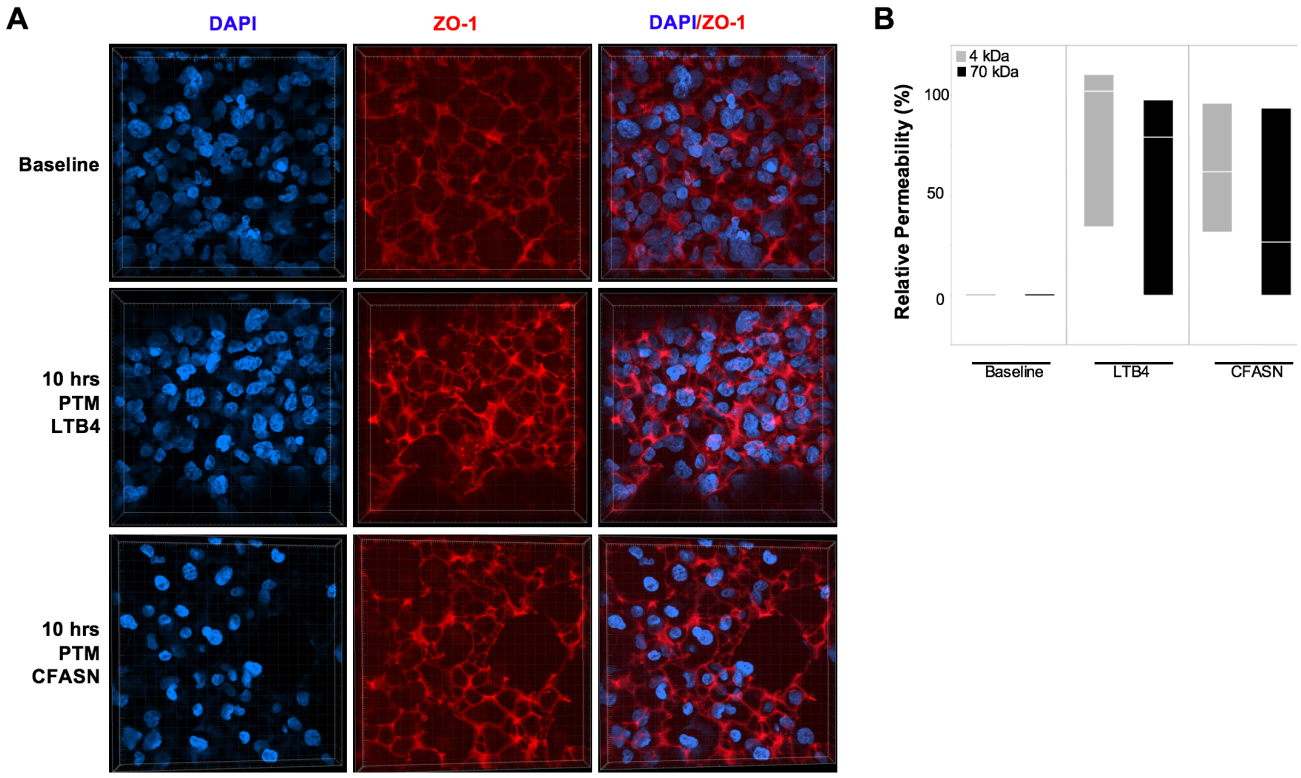

Figure 2.8. Assessment of epithelialized scaffolds after PMN transmigration. (A) Junctional ZO-1 (red) and nuclear DAPI (blue) staining was assessed after PMN transmigration to LTB4 and CFASN for 10 hours. Representative XYZ confocal images collected at 0.21 μm steps with a 60X oil objective are shown. **(B)** Permeability to 4kDa FITC and 70 kDa Texas Red dextran was assessed after PMN transmigration for 2 hours to LTB4 and CFASN (n = 3 independent repeats).

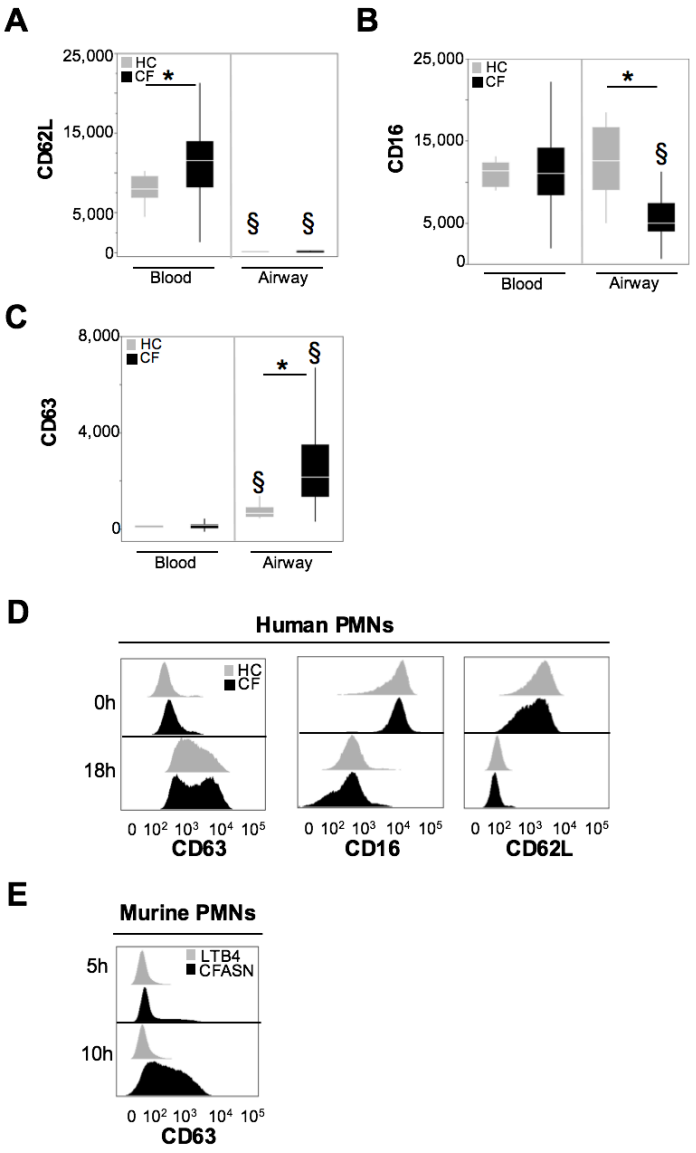

Figure 2.9. Impact of ASN and PMN origin on pathological conditioning. (A-C) *In vivo* analysis of CD63, CD16, and CD62L surface expression on PMNs from HC (grey, n = 9) and CF (black, n = 60 visits, n = 33 patients) blood and airway samples is illustrated in box plots. * indicates p<.05 in HC vs. CF between-group comparisons, while § indicates p<.05 in matched blood vs. airway within-group comparisons. **(D)** Surface expression of CD63, CD16, and CD62L was assessed pre- and post-transmigration to CF ASN (18 hours) comparing human PMNs from HC and CF subjects. **(E)** Naïve bone marrow PMNs isolated from wild-type mice were allowed to transmigrate towards either LTB4 (100 nM,

grey) or CF ASN (black), and assessed for CD63 surface expression at 5 and 10 hour PTM. Shown are representative histograms.

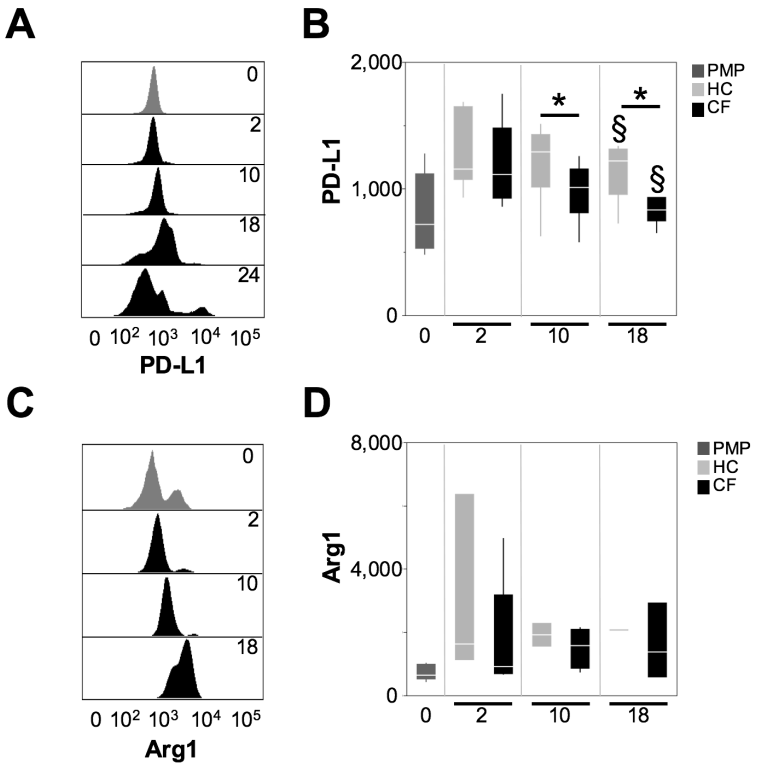

Figure 2.10. Transmigration to CF ASN induces Arg1 and PD-L1 expression patterns similar to *in vivo*. Surface expression of the T-modulatory molecules PDL1 **(A-B)** and Arg1 **(C-D)** by PMNs transmigrated to HC ASN (grey) or CF ASN (black) was assessed at 2, 10, and 18 hours PTM. PMNs from the Polymorphprep (PMP) pre-transmigration fraction are also shown as a control. Shown here are representative histograms **(A, C)** and boxplots (n = 5) **(B, D)**. * indicates $p<.05$ in HC vs. CF between-group comparisons, while § indicates $p<.05$ in matched blood vs. airway within-group comparisons.

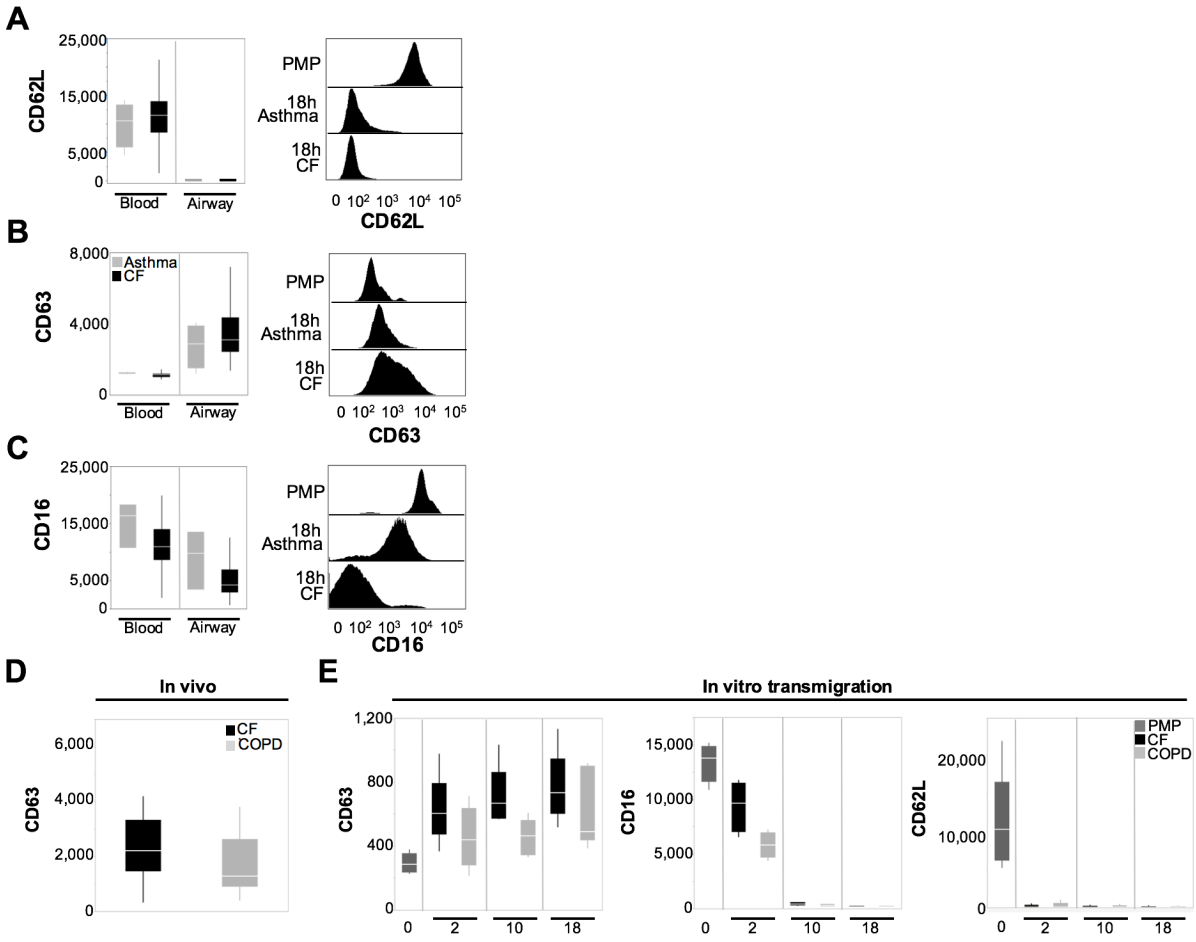

Figure 2.11. PMN reprogramming is seen in other lung diseases, similarly to CF. Surface expression of CD63 **(A)**, CD16 **(B)**, and CD62L **(C)** were assessed *in vivo* (left panels, box plots) in live PMNs from non-CF lung disease (LD, n = 5, grey) and CF (n = 60 visits, n = 33 subjects, black) blood and airway (sputum) samples. The same markers were assessed *in vitro* on PMNs transmigrated to LD or CF ASN at 18 hours PTM (right panels, representative histograms). LD and CF ASN dilutions were normalized based on urea levels. PMNs from the Polymorphprep (PMP) pre-transmigration fraction are also shown as a control. **.** *In vivo* analysis **(D)** of CD63 surface expression shows similar expression levels on CF (black, n = 60 visits, n = 33 patients) and COPD (grey, n = 9) airway PMNs**.** *In vitro* analysis **(E)** of CD63, CD16, and CD62L surface expression on HC blood PMNs

transmigrated into either COPD ASN (light grey), or CF ASN (black) in our model shows similar modulation of these markers in these two conditions after 2, 10 and 18 hours PTM, as compared to the pre-transmigration fraction shown at time 0 (PMP, dark grey).

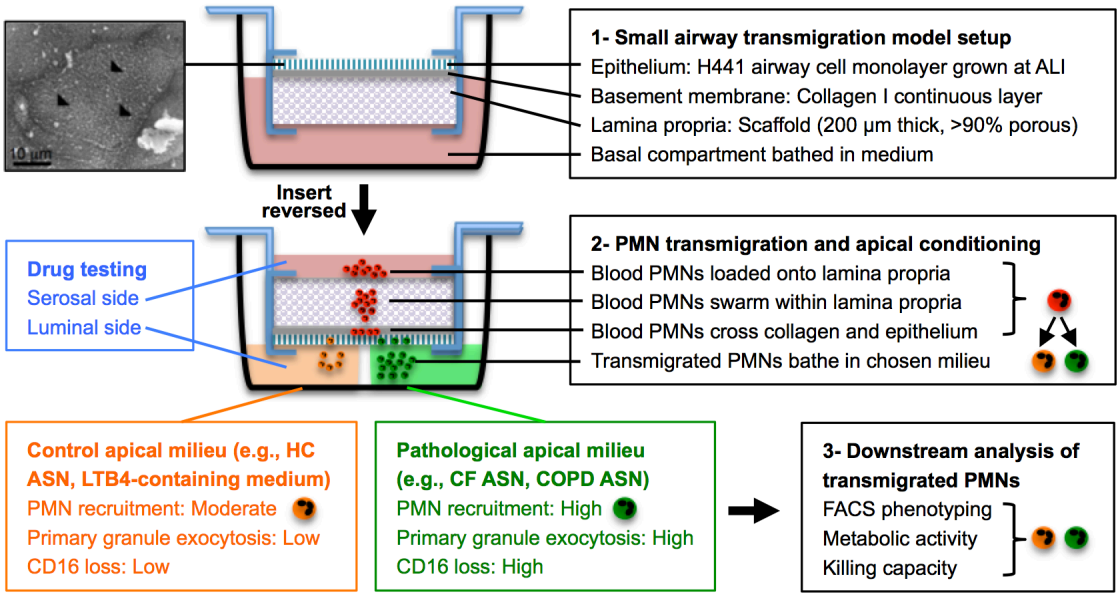

Figure 2.12. Schematic of pathologic conditioning of human PMNs in small airways. **(A)** Upon transmigration across H441 Club-like human small airway cell line at air-liquid interface (upper left insert) grown on a collagen layer coated 200 µm thick porous scaffold (lower left insert), to airway supernatant (ASN) from CF donors (green), PMN decrease CD16 expression while increasing primary granule release (CD63). This conditioning is not observed when PMNs are recruited to HC airway fluid or LTB4 (orange). The model is advantageous, because it allows for the screening of drugs via apical and/or basal addition. Transmigrated PMNs conditioned by the apical milieu of choice, exposed or not to candidate drugs, can be retrieved in large numbers and submitted to downstream assays.

REFERENCES

1. Cutting, G. R. (2015) Cystic fibrosis genetics: from molecular understanding to clinical application. Nat Rev Genet 16, 45-56.

2. Hartl, D., Gaggar, A., Bruscia, E., Hector, A., Marcos, V., Jung, A., Greene, C., McElvaney, G., Mall, M., Doring, G. (2012) Innate immunity in cystic fibrosis lung disease. J Cyst Fibros 11, 363-82.

3. Stoltz, D. A., Meyerholz, D. K., Welsh, M. J. (2015) Origins of cystic fibrosis lung disease. New Engl J Med 372, 351-62.

4. Tiddens, H. A., Donaldson, S. H., Rosenfeld, M., Pare, P. D. (2010) Cystic fibrosis lung disease starts in the small airways: can we treat it more effectively? Ped Pulmonol 45, 107-17.

5. Sly, P. D., Gangell, C. L., Chen, L., Ware, R. S., Ranganathan, S., Mott, L. S., Murray, C. P., Stick, S. M. (2013) Risk factors for bronchiectasis in children with cystic fibrosis. New Engl J Med 368, 1963-70.

6. Sagel, S. D., Sontag, M. K., Wagener, J. S., Kapsner, R. K., Osberg, I., Accurso, F. J. (2002) Induced sputum inflammatory measures correlate with lung function in children with cystic fibrosis. J Pediatr 141, 811-7.

7. Makam, M., Diaz, D., Laval, J., Gernez, Y., Conrad, C. K., Dunn, C. E., Davies, Z. A., Moss, R. B., Herzenberg, L. A., Herzenberg, L. A., Tirouvanziam, R. (2009) Activation of critical, host-induced, metabolic and stress pathways marks neutrophil entry into cystic fibrosis lungs. Proc Natl Acad Sci USA 106, 5779-83.

8. Tirouvanziam, R., Gernez, Y., Conrad, C. K., Moss, R. B., Schrijver, I., Dunn, C. E., Davies, Z. A., Herzenberg, L. A., Herzenberg, L. A. (2008) Profound functional and signaling changes in viable inflammatory neutrophils homing to cystic fibrosis airways. Proc Natl Acad Sci USA 105, 4335-9.

9. Ingersoll, S. A., Laval, J., Forrest, O. A., Preininger, M., Brown, M. R., Arafat, D., Gibson, G., Tangpricha, V., Tirouvanziam, R. (2015) Mature cystic fibrosis airway neutrophils suppress T cell function: evidence for a role of arginase 1 but not programmed death-ligand 1. J Immunol 194, 5520-8.

10. Laval, J., Touhami, J., Herzenberg, L. A., Conrad, C., Taylor, N., Battini, J. L., Sitbon, M., Tirouvanziam, R. (2013) Metabolic adaptation of neutrophils in cystic fibrosis airways involves distinct shifts in nutrient transporter expression. J Immunol 190, 6043-50.

11. Bensel, T., Stotz, M., Borneff-Lipp, M., Wollschlager, B., Wienke, A., Taccetti, G., Campana, S., Meyer, K. C., Jensen, P. O., Lechner, U., Ulrich, M., Doring, G., Worlitzsch, D. (2011) Lactate in cystic fibrosis sputum. J Cyst Fibros 10, 37-44.

12. Kolpen, M., Hansen, C. R., Bjarnsholt, T., Moser, C., Christensen, L. D., van Gennip, M., Ciofu, O., Mandsberg, L., Kharazmi, A., Doring, G., Givskov, M., Hoiby, N., Jensen, P. O. (2010) Polymorphonuclear leucocytes consume oxygen in sputum from chronic Pseudomonas aeruginosa pneumonia in cystic fibrosis. Thorax 65, 57-62.

13. Tirouvanziam, R., Conrad, C. K., Bottiglieri, T., Herzenberg, L. A., Moss, R. B., Herzenberg, L. A. (2006) High-dose oral N-acetylcysteine, a glutathione prodrug, modulates inflammation in cystic fibrosis. Proc Natl Acad Sci USA 103, 4628-33.

14. Cohen, T. S. and Prince, A. (2012) Cystic fibrosis: a mucosal immunodeficiency syndrome. Nat Med 18, 509-19.

15. Laval, J., Ralhan, A., Hartl, D. (2016) Neutrophils in cystic fibrosis. Biol Chem 397, 485-96.

16. Lavelle, G. M., White, M. M., Browne, N., McElvaney, N. G., Reeves, E. P. (2016) Animal models of cystic fibrosis pathology: phenotypic parallels and divergences. Biomed Res Int 2016, 5258727.

17. Margaroli, C. and Tirouvanziam, R. (2016) Neutrophil plasticity enables the development of pathological microenvironments: implications for cystic fibrosis airway disease. Mol Cell Pediatr 3, 38.

18. Bruijnzeel, P. L., Uddin, M., Koenderman, L. (2015) Targeting neutrophilic inflammation in severe neutrophilic asthma: can we target the disease-relevant neutrophil phenotype? J Leukoc Biol 98, 549-56.

19. Dransfield, M. T., Wilhelm, A. M., Flanagan, B., Courville, C., Tidwell, S. L., Raju, S. V., Gaggar, A., Steele, C., Tang, L. P., Liu, B., Rowe, S. M. (2013) Acquired cystic fibrosis transmembrane conductance regulator dysfunction in the lower airways in COPD. Chest 144, 498-506.

20. Kulaksiz, H., Schmid, A., Honscheid, M., Ramaswamy, A., Cetin, Y. (2002) Clara cell impact in air-side activation of CFTR in small pulmonary airways. Proc Natl Acad Sci USA 99, 6796-801.

21. Tirouvanziam, R., Diaz, D., Gernez, Y., Laval, J., Crubezy, M., Makam, M. (2011) An integrative approach for immune monitoring of human health and disease by advanced

flow cytometry methods. In: Advanced Optical Flow Cytometry. V. Tuchin, Ed. Wiley-VCH Verlag GmbH & Co. KGaA 333-362.

22. Fittschen, C. and Henson, P. M. (1994) Linkage of azurophil granule secretion in neutrophils to chloride ion transport and endosomal transcytosis. J Clin Invest 93, 247-55.

23. Mackerness, K. J., Jenkins, G. R., Bush, A., Jose, P. J. (2008) Characterisation of the range of neutrophil stimulating mediators in cystic fibrosis sputum. Thorax 63, 614-20.

24. Stevens, C. W., Aravind, S., Das, S., Davis, R. L. (2013) Pharmacological characterization of LPS and opioid interactions at the toll-like receptor 4. Br J Pharmacol 168, 1421-9.

25. Afonso, P. V., Janka-Junttila, M., Lee, Y. J., McCann, C. P., Oliver, C. M., Aamer, K. A., Losert, W., Cicerone, M. T., Parent, C. A. (2012) LTB4 is a signal-relay molecule during neutrophil chemotaxis. Dev Cell 22, 1079-91.

26. Elborn, J. S., Horsley, A., MacGregor, G., Bilton, D., Grosswald, R., Ahuja, S., Springman, E. B. (2017) Phase I studies of acebilustat: biomarker response and safety in patients with cystic fibrosis. Clin Transl Sci 10, 28-34.

27. Hong, C. W., Kim, T. K., Ham, H. Y., Nam, J. S., Kim, Y. H., Zheng, H., Pang, B., Min, T. K., Jung, J. S., Lee, S. N., Cho, H. J., Kim, E. J., Hong, I. H., Kang, T. C., Lee, J., Oh, S. B., Jung, S. J., Kim, S. J., Song, D. K. (2010) Lysophosphatidylcholine increases neutrophil bactericidal activity by enhancement of azurophil granule-phagosome fusion via glycine.GlyR alpha 2/TRPM2/p38 MAPK signaling. J Immunol 184, 4401-13.

28. Baillet, A., Hograindleur, M. A., El Benna, J., Grichine, A., Berthier, S., Morel, F., Paclet, M. H. (2017) Unexpected function of the phagocyte NADPH oxidase in supporting hyperglycolysis in stimulated neutrophils: key role of 6-phosphofructo-2-kinase. FASEB J 31, 663-673.

29. Zmijewski, J. W., Lorne, E., Zhao, X., Tsuruta, Y., Sha, Y., Liu, G., Siegal, G. P., Abraham, E. (2008) Mitochondrial respiratory complex I regulates neutrophil activation and severity of lung injury. Am J Respir Crit Care Med 178, 168-79.

30. Piwkowska, A., Rogacka, D., Jankowski, M., Dominiczak, M. H., Stepinski, J. K., Angielski, S. (2010) Metformin induces suppression of NAD(P)H oxidase activity in podocytes. Biochem Biophys Res Commun 393, 268-73.

31. Rena, G., Hardie, D. G., Pearson, E. R. (2017) The mechanisms of action of metformin. Diabetologia 60, 1577-1585.

32. Ribeiro, C. M., Hurd, H., Wu, Y., Martino, M. E., Jones, L., Brighton, B., Boucher, R. C., O'Neal, W. K. (2009) Azithromycin treatment alters gene expression in inflammatory, lipid metabolism, and cell cycle pathways in well-differentiated human airway epithelia. PloS One 4, e5806.

33. Lubamba, B. A., Jones, L. C., O'Neal, W. K., Boucher, R. C., Ribeiro, C. M. (2015) X-Box-binding protein 1 and innate immune responses of human cystic fibrosis alveolar macrophages. Am J Respir Crit Care Med 192, 1449-61.

34. Painter, R. G., Valentine, V. G., Lanson, N. A., Jr., Leidal, K., Zhang, Q., Lombard, G., Thompson, C., Viswanathan, A., Nauseef, W. M., Wang, G., Wang, G. (2006) CFTR Expression in human neutrophils and the phagolysosomal chlorination defect in cystic fibrosis. Biochemistry 45, 10260-9.

35. Pohl, K., Hayes, E., Keenan, J., Henry, M., Meleady, P., Molloy, K., Jundi, B., Bergin, D. A., McCarthy, C., McElvaney, O. J., White, M. M., Clynes, M., Reeves, E. P., McElvaney, N. G. (2014) A neutrophil intrinsic impairment affecting Rab27a and degranulation in cystic fibrosis is corrected by CFTR potentiator therapy. Blood 124, 999-1009.

36. Tirouvanziam, R., Khazaal, I., Peault, B. (2002) Primary inflammation in human cystic fibrosis small airways. Am J Physiol Lung Cell Mol Physiol 283, L445-51.

37. Esther, C. R., Jr., Coakley, R. D., Henderson, A. G., Zhou, Y. H., Wright, F. A., Boucher, R. C. (2015) Metabolomic evaluation of neutrophilic airway inflammation in cystic fibrosis. Chest 148, 507-15.

38. Peters-Hall, J. R., Brown, K. J., Pillai, D. K., Tomney, A., Garvin, L. M., Wu, X., Rose, M. C. (2015) Quantitative proteomics reveals an altered cystic fibrosis in vitro bronchial epithelial secretome. Am J Respir Cell Mol Biol 53, 22-32.

39. Cantin, A. M., Hartl, D., Konstan, M. W., Chmiel, J. F. (2015) Inflammation in cystic fibrosis lung disease: Pathogenesis and therapy. J Cyst Fibros 14, 419-30.

40. Gernez, Y., Tirouvanziam, R., Chanez, P. (2010) Neutrophils in chronic inflammatory airway diseases: can we target them and how? Eur Respir J 35, 467-9.

Chapter 3

Extracellular Vesicles Activate Inflammasome Signaling in Cystic Fibrosis Airway Disease

Sections of this chapter have been prepared for submission as an Original Article

to the American Journal of Respiratory Cell and Molecular Biology

EXTRACELLULAR VESICLES ACTIVATE INFLAMMASOME SIGNALING IN CYSTIC FIBROSIS AIRWAY DISEASE

Osric A. Forrest[1,2], Sanjana Rao[1,2], Yiwen Li[1,2], Sarah A. Ingersoll[1,2], Avril A. Robertson[3], Nelson C. Di Paolo[1], Julie Laval[1,2], Milton R. Brown[1,2], Dmitry M. Shayakhmetov[1], Matthew A. Cooper[3], Vin Tangpricha[4,5], and Rabindra Tirouvanziam[1,2*]

[1]Department of Pediatrics, Emory University, Atlanta, GA, USA; [2]Center for CF & Airways Disease Research, Children's Healthcare of Atlanta, Atlanta, GA, USA; [3]Institute for Molecular Biomedicine, University of Queensland, Brisbane, QLD, Australia; [4]Department of Medicine, Emory University, Atlanta, GA, USA; [5]VA Medical Center, Atlanta, GA, USA .

INTRODUCTION

Interleukin-1β (IL-1β) is a key regulator of both sterile and infection-induced inflammatory responses (1, 2). The release of this pro-inflammatory mediator is a tightly regulated process that requires two distinct signals; the first initiating the increased transcription of the pro-form of IL-1β and a second to induce cleavage and activation of a 17 kDa bioactive form that is secreted from the cell through a non-canonical pathway. The secretion of IL-1β and IL-18 is regulated by the assembly of a multi-protein signaling platform called the inflammasome. Inflammasome activation is generally initiated by binding of diverse stimuli to NOD-like receptors (NLRs), which serve as intracellular sensors. This in turn leads to the recruitment of an adaptor molecule, the apoptosis-associated speck-like protein containing a caspase activation and recruitment domain (CARD) (ASC), and the proteolytic cleavage and activation of the key effector molecule caspase-1. Caspase-1 activation is required for the cleavage and activation of IL-1β (3).

Inflammasome activation is a central response critical to myeloid cell-mediated immunity, but it has also been shown to form a key innate response in epithelial and endothelial cells (4-6). In macrophages, inflammasome activation is followed by pyroptotic cell death, which leads to the mass release of IL-1β and perpetuation of inflammation (7). However, in neutrophils, inflammasome activation can proceed without concomitant cell death, which illustrates that this pathway may be differentially regulated in various cell types (8, 9). Interestingly, IL-1β can also be activated in neutrophils in a caspase 1-independent manner through the activity of serine proteases such as neutrophil elastase (NE), which is located in primary granules (10, 11). Another interesting property lies in the ability of key components of the inflammasome (ASC, caspase-1) to be released by activated cells for uptake by bystander cells, thus serving as pyretic signals to perpetuate inflammasome

activation (12, 13). One mechanism of release for these proteins is through packaging in extracellular vesicles (EVs), which are released and endocytosed by neighboring cells to induce inflammatory signaling, cell injury, and death (14-16).

Inflammasome activation contributes to disease through binding and intracellular signaling induced by the IL-1 family of cytokines in a variety of inflammatory diseases. IL-1β in particular signals by binding to IL-1R1, a widely expressed activating IL-1 receptor (1, 17, 18). IL-1β signaling can be counteracted through various mechanisms, including competitive binding of IL-1 receptor antagonist (IL-1RA) to IL-1RI, or through binding of IL-1β to IL-R2, a decoy receptor expressed at the cell surface (19, 20).

In cystic fibrosis (CF), patients are affected by progressive lung disease which is dominated a pathological triad of airway obstruction by mucus, bacterial infection, and recruitment of polymorphonuclear neutrophils (PMNs) from blood (21). Inflammasome activation is thought to contribute significantly to the chronic recruitment of PMNs to CF airways, via both IL-1α from the diseased epithelium and IL-1β from activated myeloid cells (3, 22, 23). In myeloid cells, activation of caspase-1 is believed to be initiated in part by the gram negative bacterium *P. aeruginosa* which infects a majority of CF patients (24, 25). However, it remains unclear how inflammasome activation in PMNs in particular may contribute to the perpetuation of IL-1/IL-1R1 signaling and chronic inflammation in the airways of CF patients.

In this study, we focused specifically on the role of inflammasome activation in PMNs as a potential driving force in CF airway pathogenesis. We observed that the inflammasome pathway is activated in CF airway PMNs. In addition, we show that EVs from CF sputum can serve as activators of the inflammasome pathway in PMNs and

epithelial cells through the delivery inflammasome signaling mediators, working in a positive-feedback loop.

METHODS

Human subjects. Samples were collected from human donors according to Emory University IRB approved protocols for collection and handling of human samples. Informed consent was obtained from all subjects for collection and use of their samples. CF was diagnosed by sweat chloride (60 mEq/L), using a quantitative iontophoresis test and/or documentation of two identifiable cftr mutations.

Sample processing. Whole blood was collected by venipuncture using EDTA vacutainer tubes. Sputum was collected from CF patients by spontaneous expectoration, and from HC subjects by induction. Samples were processed according to a previous described protocol (26). Briefly, whole blood was spun at 400g to remove cells from the plasma, which was further spun at 3,000g to deplete platelets. Sputum samples were mechanically dissociated by repeated passage through an 18G needle after addition of 6 ml of PBS with 2.5 mM EDTA. The sputum was then spun at 800g to generate both cell and fluid fractions. The latter was spun at 3,000g at 4ºC for 10 minutes to generate airway supernatant (ASN), which was stored at -80ºC until use. Washed blood and sputum cells were re-suspended in PBS-EDTA for antibody staining and flow cytometry analysis.

PMN purification. PMNs were purified from whole blood samples from healthy control donors based on a previously described protocol (26). Blood was layered onto Polymorphprep (Nycomed Pharma) and centrifuged at 400g with minimal brake for 45 minutes at room temperature. The PMN layer was collected and remaining erythrocytes removed by hypotonic lysis.

ELISA assays. Commercial ELISA assays were used to quantify the levels of IL-1β, IL-1α, and IL-1RA (R&D), and IL-18 (Raybiotech) in sputum of CF and HC subjects.

Flow cytometry. Blood and airway cells from CF and HC subjects, and from our *in vitro* transmigration model, were stained with fluorescently labeled antibodies. These included antibodies against CD63 (H5C6), CD66b (G10F5), EpCAM (9C4), and ICAM-1(HA58) (from BioLegend), IL-R1, IL-1R2, and IL-1β (R&D Systems). Cells were also stained with the Live/Dead probe (Invitrogen) to ascertain viability. Data were acquired on a LSRII cytometer (BD Biosciences) and compensation and analysis were performed using the Flowjo software (Treestar).

Transepithelial migration (TM) model. PMNs were allowed to migrate in our previously published *in vitro* model of transepithelial migration mimicking conditions of the CF lung (Forrest et al., J. Leukocyte Biology, 2018, accepted). In brief, the H441 Club-like cell line was seeded on Alvetex scaffolds (Reinnervate) and grown at air-liquid interface (ALI). Subsequently, 0.5-1 × 10^6 purified PMNs from blood were allowed to migrate at 37°C under 5% CO_2 towards either leukotriene B4 (LTB4, 100nM, chemoattractant serving as transmigration control), or ASN from CF or HC subjects, placed apically. For some experiments, drugs were placed apically, mixed with the ASN.

Murine bone marrow cell isolation and transmigration. Bone marrow cells were collected from the tibias and femurs of wild-type mice by flushing with RPMI with 10% FBS using a 25-gauge needle. Cells were then washed with PBS and allowed to migrate in our

model to either CFASN or LTB4 for 5 or 10 hours. Recruited cells were stained with antibodies and analyzed by flow cytometry as detailed above for CD11b (M1/70) and Ly6G (1A8) (BioLegend) expression to identity mature PMNs, and for intracellular caspase-1 activity using the membrane-permeable FLICA probe (Immunochemistry, Ltd.).

Pinocytosis assay. Pinocytosis was assessed via Lucifer Yellow (LY, Biotium) uptake, as described previously (27). Briefly, murine bone marrow cells were transmigrated to CF ASN containing LY (1 mg/mL) for 5 and 10 hours, after which the cells were washed with PBS-EDTA and stained with viability probes and antibodies, as above. Cells were then washed with PBS-EDTA and fixed with Lyse/Fix Phosflow buffer (BD Biosciences) and pinocytosis was measured by flow cytometry.

In vitro inflammasome activation. *In vitro* inflammasome activation was performed according to a previously published protocol (28). In brief, purified PMNs from blood were stimulated with ultra-pure LPS (Invivogen) at 10 ng/ml in RPMI at 37 °C under 5% CO_2 for 4 hours, followed by treatment with nigericin (Sigma) at 5 μM for an additional 2 hours.

Isolation and characterization of EVs. EVs were isolated from plasma and CF ASN as follows. Samples were first spun at 20,000g for 15 mins to remove any cell debris after which they were loaded unto a 300 kDa molecular weight (MW) exclusion column (Vivaspin) and spun for 15 mins at 15,000g. EVs were further purified using the Exoflow kit (SBI) according to the manufacturer's guidelines. Briefly, anti-CD63 biotinylated antibodies were first conjugated to magnetic streptavidin-labeled beads. The retentate from the 300 kDa MW columns was then re-suspended in PBS and incubated with anti-CD63-bead complexes

overnight at 4°C, washed 3 times with wash buffer and then stained with Exostain-FITC and/or ExoOne stains (SBI), and the mmbrane-permeable fluorescent probe against intracellular active caspase-1 (FLICA, from Immunohistochemistry, Ltd.). Labeled EV-bead complexes were then assessed by flow cytometry using an LSRII FACS analyzer (BD).

Primary airway epithelial cell culture. Primary healthy control tracheal epithelial cells (NhTE) were grown on semi-permeable Transwell supports (Corning) in conditionally reprogrammed cell (CRC) culture medium by the CF@LANTA RDP Experimental Models Core at Emory University, as previously described (29), with some modifications. In brief, NhTE cells were first plated on human type IV placental collagen-coated 12-mm in CRC culture medium and fed every other day basolaterally for at least two weeks to allow for differentiation at ALI. All experiments were performed between 2 and 4 wk of ALI culture.

Immunofluorescence and confocal microscopy. After 24 or 48 hours of activation with isolated EVs and/or LPS plus nigericin, primary NhTE cells were stained with the active caspase-1 probe (FLICA) for 1 hour at 37 °C , after which the Transwells were washed twice with PBS, and fixed with 4% paraformaldehyde in PBS for 15 minutes at room temperature. Fixed Transwells were washed with PBS, permeabilized with 0.5% Tween 20 in PBS (PBS-T), followed by two washes with PBS-T supplemented with 2% goat serum. After the last wash, Transwells were incubated overnight at 4°C with a polyclonal anti-ZO-1 antibody (ZMD.437, Thermo Fisher Scientific) diluted 1:250 in PBS with 2% goat serum. Transwells were then washed three times with PBS with 2% goat serum, and incubated for 1 hour at room temperature with a secondary anti-rabbit antibody (Invitrogen), followed by a 15 minute incubation with 0.5 μg/mL DAPI (BioLegend) as a nuclear counterstain. Transwells

were then washed twice with PBS with 2% goat serum, and then twice more with PBS alone, then dried and mounted on a glass slide, and stored for confocal imaging. Z-stack images were acquired using an inverted FV1000 confocal microscope (Olympus), and analyzed using the Fiji image analysis software (National Institutes of Health).

Data analysis. Statistical analyses were performed using JMP12 (SAS Institute). Between-group and matched-pair statistical analyses used the Wilcoxon rank sum and signed rank tests, respectively, with a threshold of $p<.05$ to determine significance.

RESULTS

Inflammasome pathway mediators IL-1β, IL-1α and IL-18, and key receptor IL-1R1 are present in CF airways. We first sought to validate previous work linking soluble mediators of the inflammasome pathway to CF airways in our cohort of CF patients. Here saw that IL-1β, IL-1α, and IL-18, were elevated in the sputum of patients with CF compared to healthy control (HC) subjects **(Fig. 3.1A-C)**. This increase in inflammasome-mediated cytokine production was not accompanied by commensurate changes in IL-1RA levels comparing CF and HC sputum **(Fig. 3.1D)**. Next, we assessed if inflammasome activation in CF airway fluid also involved increased receptor expression on PMNs. By flow cytometry analysis of live blood and airway PMNs from CF subjects, we observed a significant increase in surface IL-1R1 in the latter, in both inpatient (exacerbation) and outpatient (stable) visits **(Fig. 3.2A)**, while surface IL-1R2 expression was unchanged **(Fig. 3.2B).**

PMNs recruited to CF airways *in vivo* and *in vitro* activate caspase-1 signaling. Next, we assessed activation of caspase-1, a key step in inflammasome activation, in PMNs recruited to CF airways. We observed increased intracellular caspase-1 activity based on FLICA staining of CF airway compared to blood PMNs **(Fig. 3.3A)**. This finding was confirmed by image cytometry, showing intracellular nucleation of caspase-1 specks in CF airway PMNs **(Fig. 3.3B)**. To further validate these *in vivo* findings, we used an *in vitro* transmigration model that recapitulates the recruitment and activation of PMNs in CF airways. Using this model system, we observed that PMNs recruited to CF airway fluid underwent increased intracellular caspase-1 activation **(Fig. 3.3C)**, which was partially inhibited by the NLRP3 inflammasome inhibitor MCC950 **(Fig 3.3D)**. Next, we assessed

whether caspase-1 activation in CF airway compared to blood PMNs *in vivo* was concomitant with increased production of IL-1β, which we confirmed by intracellular cytokine staining **(Fig. 3.3E).** Finally, we sought to determine the effect of exogenous activation of PMNs *in vitro* using LPS plus nigericin, a prototypical inflammasome agonistic treatment. We observed significant intracellular caspase-1 activity and primary granule release in activated PMNs **(Fig. 3.4A-B)**. Similar treatment of primary tracheal epithelial cells from non-CF controls (NhTE) showed increased ICAM-1 and secretion of IL-1α **(Fig. 3.4C-D)**. These findings confirm that both PMNs and epithelial cells are potentially contributing to inflammasome signaling.

Extracellular vesicles from CF sputum perpetuate inflammasome activation in PMNs. Building upon our observation that airway fluid from CF patients can induce inflammasome signaling in recruited PMNs *in vitro*, we next explored uptake of EVs the CF sputum as one potential inducing mechanism. First, we isolated EVs from CF sputum and from supernatants of PMNs treated *in vitro* with LPS plus nigericin to activate inflammasome signaling. We then incubated PMNs *in vitro* with those EVs, and observed both caspase-1 activation and secondary granule exocytosis in treated PMNs **(Fig. 3.5A**). Then, using our *in vitro* transmigration model, we observed that depleting the apical airway fluid of EVs using a size exclusion MW column decreased intracellular caspase-1 activity in recruited PMNs, and this dampening effect was counteracted by adding back purified EVs into the fluid **(Fig. 3.5B).** When using murine PMNs in our transmigration model, we found that those recruited to CF airway fluid, but not the chemoattractant control LTB4, displayed significant intracellular caspase-1 activity based on FLICA staining, which was concomitant with increased pinocytosis and uptake of Lucifer yellow **(Fig. 3.6A-B).** Interestingly, PMNs from

caspase-1$^{-/-}$knockout mice (genetically devoid of intrinsic caspase-1 activity) were also recruited to CF airway fluid in our transmigration model, and showed similar intracellular caspase-1 activity after recruitment, which strongly suggests uptake from the fluid **(Fig 3.6C-D).**

Extracellular vesicles from CF sputum perpetuate inflammasome activation in airway epithelial cells. We next assessed the effect of isolated EVs from CF sputum upon apical addition to primary airway epithelial ALI cultures. Using confocal microcopy, we observed that incubation of primary tracheal epithelial cells with isolated EVs induced intracellular caspase-1 activity **(Fig. 3.7A).** We validated this finding using flow cytometry and observed that epithelial not only took up labeled EVs during incubation **(Fig 3.7B),** but indeed quantitatively increased intracellular caspase-1 activity and surface expression of the activation marker intercellular adhesion molecule -1 (ICAM-1). This effect was particularly marked when EVs were incubated along with LPS, to mimic concomitant gram-negative infection which is common in CF **(Fig 3.7C-D).** Uptake by primary airway epithelial cells of EVs isolated from CF sputum also led to increased production of IL-1α and surface expression of the other activation marker epithelial cell adhesion molecule (EpCAM) **(Fig 4.4E-F)**.

DISCUSSION

Inflammasome signaling plays a key role in the pathogenesis of inflammatory disorders (1, 30). Inflammasome activation is a tightly regulated process that culminates in the oligomerization of a multi-protein complex controlling the downstream secretion of IL-1 cytokine family members IL-1α, IL-1β and IL-18. These cytokines regulate the recruitment of immune cells and support their continued activation, as exemplified in CF and asthma (2, 4, 31). Consequently, there is a great clinical need to better understand the molecular cues that control inflammasome activation in disease so we can effectively target potential deleterious effects occurring upon aberrant signaling. Findings presented here confirm the role of inflammasome activation in CF airway inflammation, and support a role for IL-1 family members in the recruitment and activation of PMNs, which are key drivers of pathogenesis. Finally, we uncovered a novel mechanism of inflammasome signaling in CF, dependent on the uptake of EVs present in the CF airway milieu by PMNs and epithelial cells.

Although the majority of prior work on inflammasome signaling has focused on monocytes and macrophages, several studies have established PMNs as an important source of IL-1β in inflammation and shown that these cells modulate inflammasome signaling differently from monocytes and macrophages (8, 10, 11, 32). In addition to IL-1β, PMNs are also a source of IL-18, which can be further cleaved by serine proteases also released during inflammation to render it more active (33). Moreover, PMNs appear resistant to pyroptotic cell death unlike monocytes and macrophages, and therefore can release IL-1β and remain viable (8). Our study confirms that inflammasome activation and IL-1β release by airway PMNs in CF do not require pyroptotic death of these cells.

Inflammasome activation is also a key part of innate effector responses of epithelial cells (34). For example, intestinal epithelial cells have been identified as potentially high producers of IL-1β (35). In alveolar epithelial cells, barrier integrity appears to be regulated in part by the NLRP3 inflammasome, although this effect is independent of IL-1β and IL-18 (36). Instead, recent studies have highlighted the role of epithelial-derived IL-1α in activating pro-inflammatory responses in fibroblasts, with a proposed role in mediating lung injury in the context of chronic inflammatory lung diseases (37-39). Epithelial-derived IL-1α has particular relevance to CF airway inflammation and PMN recruitment via IL-1R1 signaling.Indeed, prior work in the βENaC mouse model of CF airway inflammation has identified hypoxia-induced epithelial necrosis as a strong inducer of IL-1α secretion and downstream recrutiment of PMNs (22). These findings, along with data presented here highlight a role for epithelium-derived IL-1α in sputum and IL-1R1 mediated signaling at the surface of PMNs, as a potentially critical ligand / receptor pair in CF airway inflammation.

Another mechanism by which inflammasome activation may be perpetuated in CF airways is via the active release of inflammasome complex proteins caspase-1 and ASC, which are then phagocytosed by naïve cells. These in turn initiate inflammasome activation extrinsically, independent of typical signals needed for intrinsic inflammasome activation. Caspase-1 and ASC found free in the extracellular milieu, or in some cases packaged in EVs (12-14, 40). Our work here confirm that EVs which are known to contain active caspase-1, ASC, and even IL-1β can be taken up and induce inflammasome activation in PMNs and epithelial cells. Additionally, we show that PMNs secrete these EVs upon inflammasome activation *in vitro*, and by so doing may be a major source of these EVs, at the same time as they may serve as targets, within CF sputum. An open question is whether inflammasome regulators such as MCC950 (41) or recombinant IL-1RA (anakinra) (42) may be beneficial in

CF. In addition, our study identifies EVs as potential new targets to modulate inflammasome activation and airway inflammation in CF airways. Further studies are required to explore the therapeutic potential of EVs in more pointed fashion.

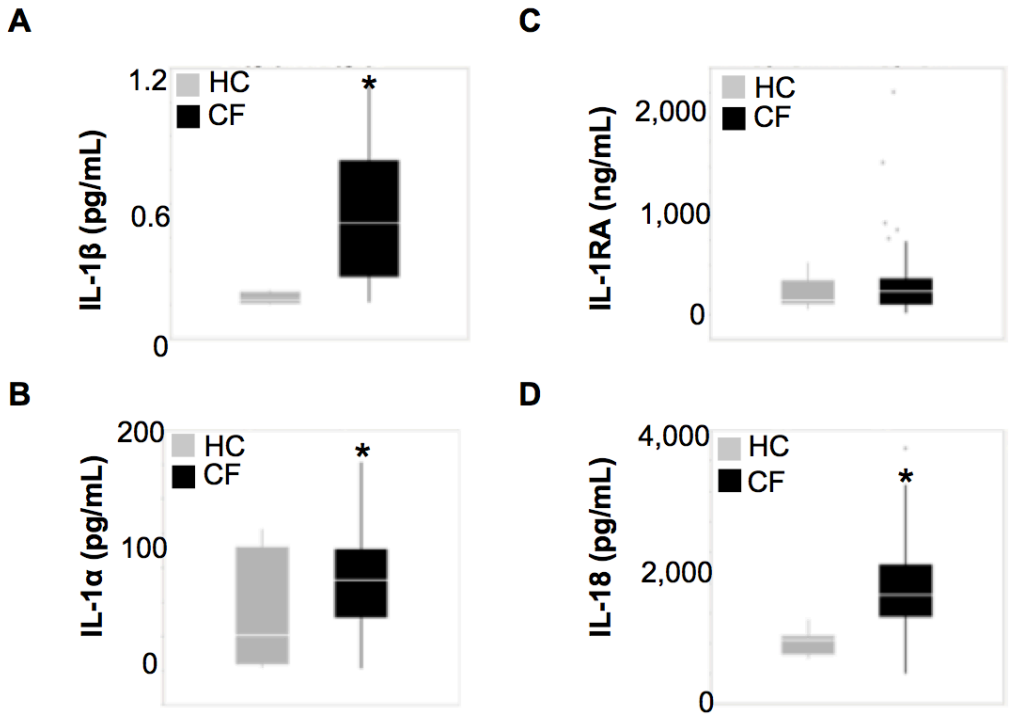

Figure 3.1. The IL-1β/IL-1α /IL-18 axis is activated in the CF airways. (A-D) L-1β, IL-1, IL-1RA, and IL-18 levels were measured in expectorated and induced sputum from CF (black) and HC (grey) subjects, respectively. *indicating $p<.05$ in between-group analysis comparing HC (N=9) and CF (N=20-30, depending on analyte).

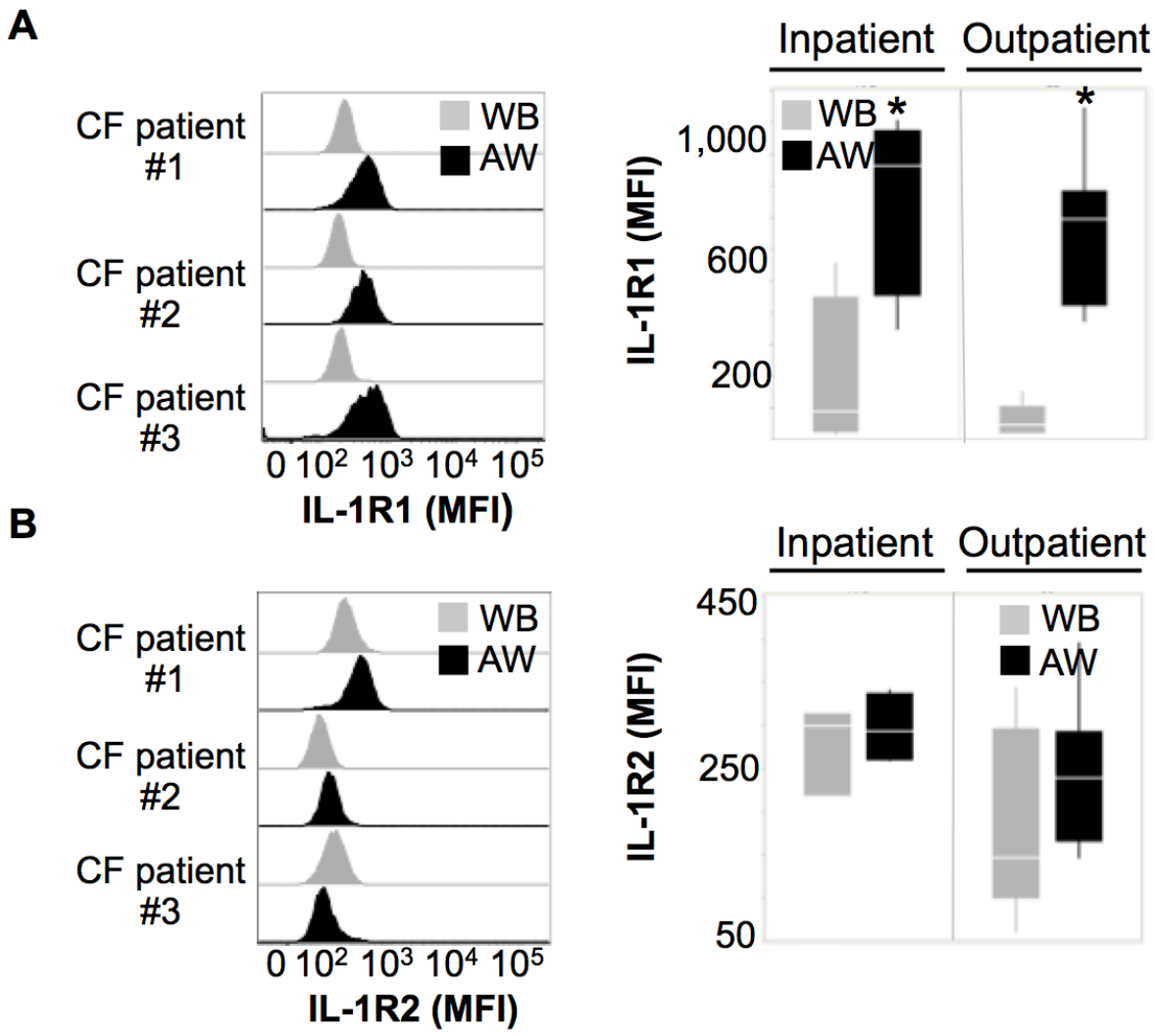

Figure 3.2. Surface IL-1R1 expression is increased on CF airway PMNs. Analysis of surface IL-1R1 **(A)** and IL1-R2 **(B)** expression on whole blood (WB, grey) and airway (AW, black) PMNs from CF patients (N=16) is shown as representative histograms (left panels), and as blox plots representing median fluorescence intensities of all samples (right panels). * indicates $p<.05$ in within-group analysis comparing whole blood and airway PMNs.

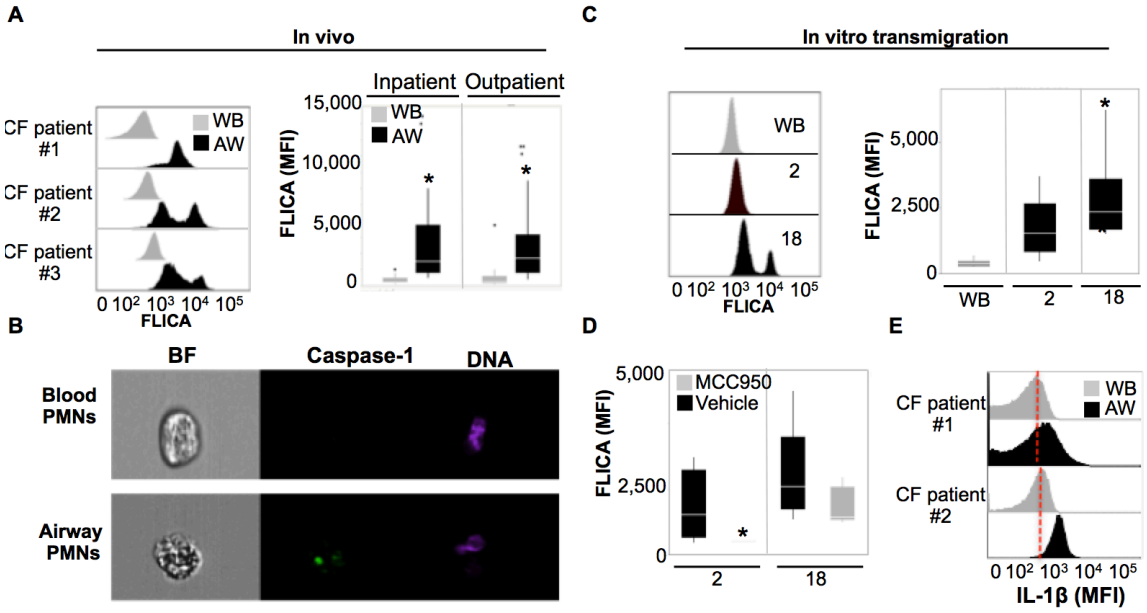

Figure 3.3. Intracellular caspase-1 activity and IL-1β are increased in CF airway PMNs. Intracellular caspase-1 activity was assessed in samples collected from CF patients (N=33) at both inpatient and outpatient visits (N=60 total) via analysis of FLICA staining of blood (grey) and airway (black) PMNs using flow cytometry **(A)**, shown here as representative histograms (left panel) and box plots (right panel), and confirmed by image cytometry **(B)**. **(C)** Intracellular caspase-1 activity was assessed in PMNs transmigrated *in vitro* into CF ASN (black). after 2, 10 and 18 hours post-transmigration (PTM), compared to whole blood control (WB, grey). **(D)** Intracellular caspase-1 activity was assessed in PMNs transmigrated *in vitro* into CF ASN (black). after 2 and 18 hours PTM in the presence of the NLRP3 inflammasome inhibitor MCC950 (grey), or vehicle control (black). *indicates $p<.05$ in within-group analysis comparing MCC950- to vehicle-treated conditions (N=9). **(E)** Intracellular IL-1β levels were assessed by flow cytometry in whole blood (WB, grey) and airway (AW, black) PMNs from CF patients, shown here as two sets of representative histograms.

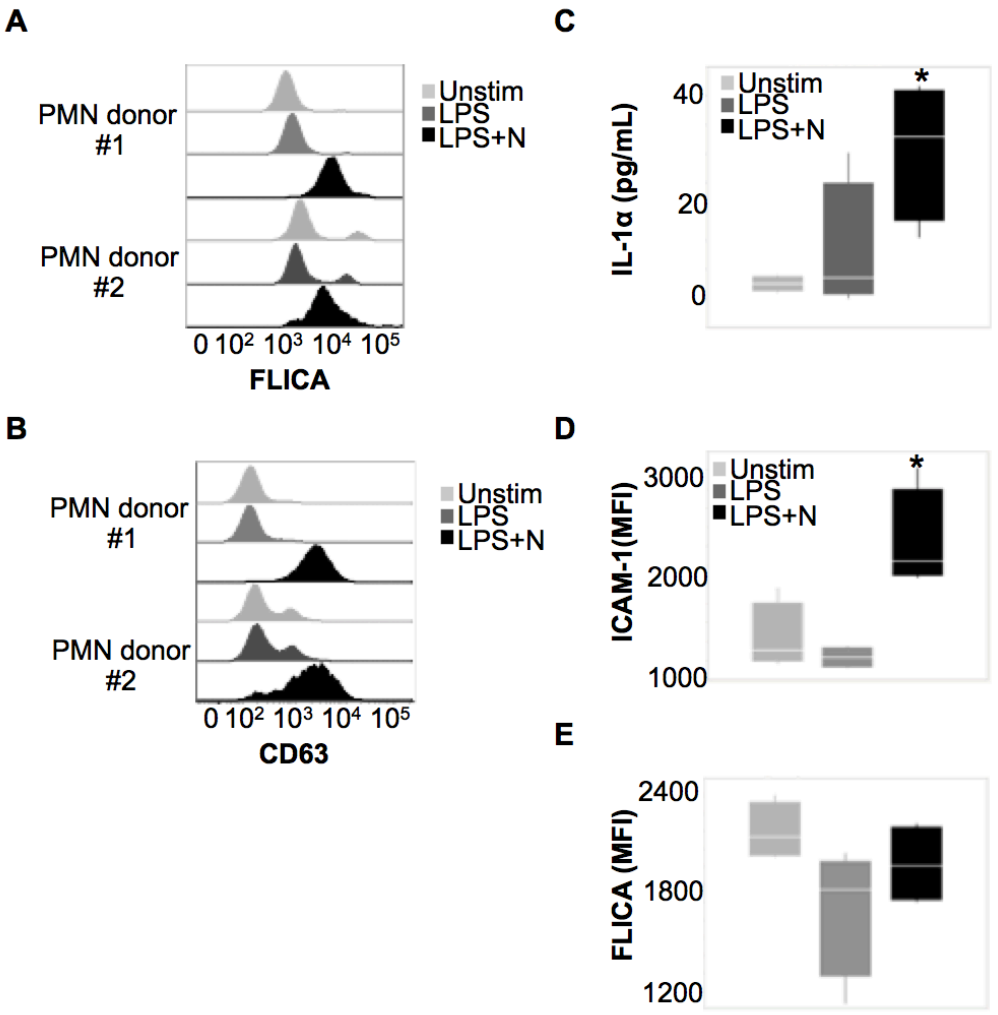

Figure 3.4. Treatment with LPS plus nigericin activates inflammasome signaling in PMNs and primary airway epithelial cells. PMNs were treated with LPS plus nigericin and assessed for intracellular caspase-1 activity with the FLICA probe **(A)**, and primary granule exocytosis reflected by surface CD63 expression **(B)** using flow cytometry, as shown here in representative histograms. Primary NhTE cells were treated with LPS plus nigericin, after which supernatants were analyzed for IL-1α by ELISA **(C)**, and cells were assessed for surface ICAM-1 **(D)**, and intracellular caspase-1 activity with the FLICA probe **(E)** using flow cytometry. *indicates $p<.05$ for within -group analysis comparing unstimulated *unstim) conditions to LPS, or LPS plus nigericin (LPS+N) treatment conditions (N=4).

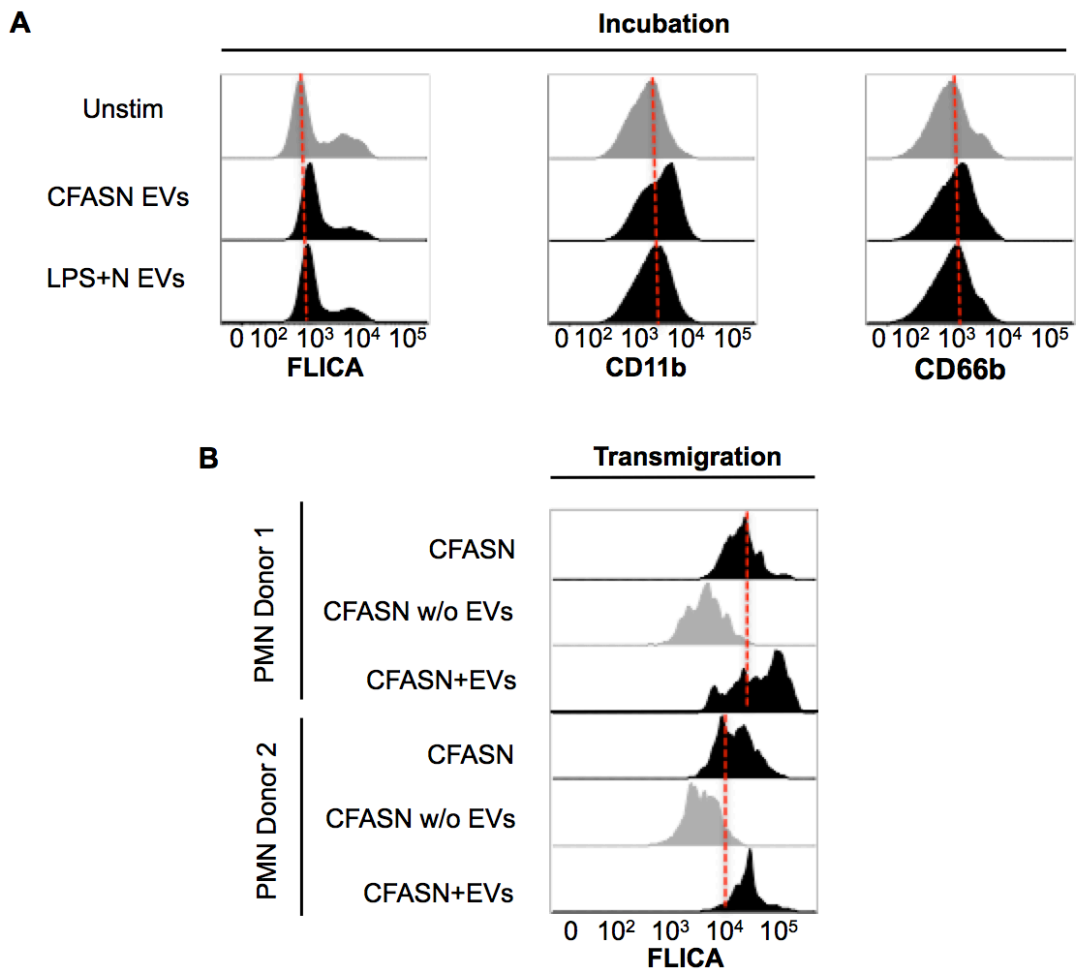

Figure 3.5. Extracellular vesicles activate inflammasome signaling in PMNs. (A) PMNs were incubated with EVs isolated from CF airway supernatant (CF ASN EVs) prepared from sputum or from *in vitro* culture supernatants from LPS plus nigericin-treated PMNs (LPS+N EVs). and assessed for intracellular caspase-1 activity with the FLICA probe, and surface CD11b and CD66b expression, as shown here in representative histograms. **(B)** PMNs were transmigrated *in vitro* into CF ASN, CF ASN depleted of EVs (CFASN w/o EVs), and CFASN with additional EVs (CFASN+EVs), and assessed for intracellular caspase-1 activity with the FLICA probe after 10 hours PTM, as shown here in representative histograms for 2 donors. Hashed red line represents median in control condition for each panel.

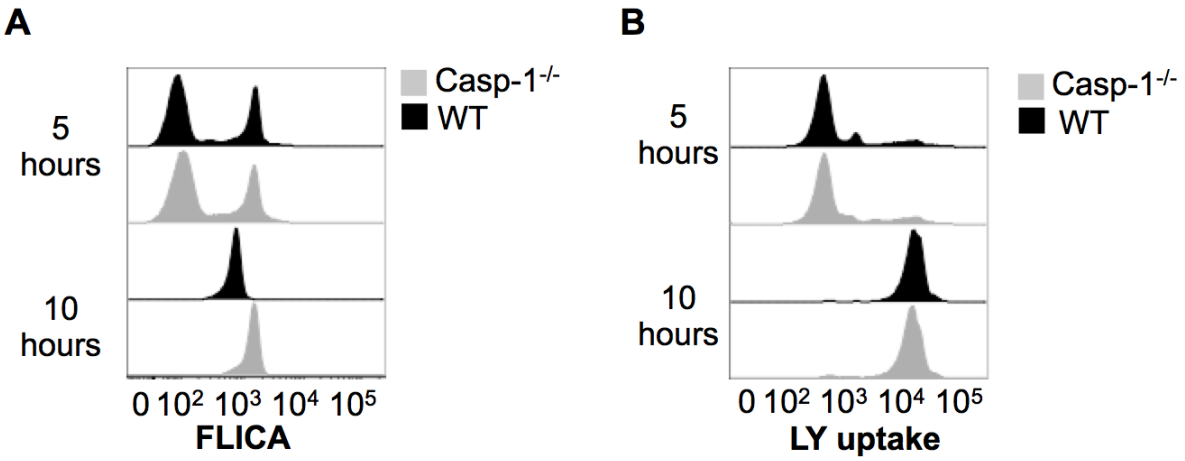

Figure 3.6. Mouse PMNs transmigrated to human CF airway fluid *in vitro* acquire intracellular caspase-1 activity. PMNs from WT or caspase-1 KO mice were recruited to CF ASN and assessed after 5 and 10 hours PTM for intracellular caspase-1 activity with the FLICA probe **(A)** and pinocytic activity using the LY uptake assay **(B)**, as shown here in representative histograms.

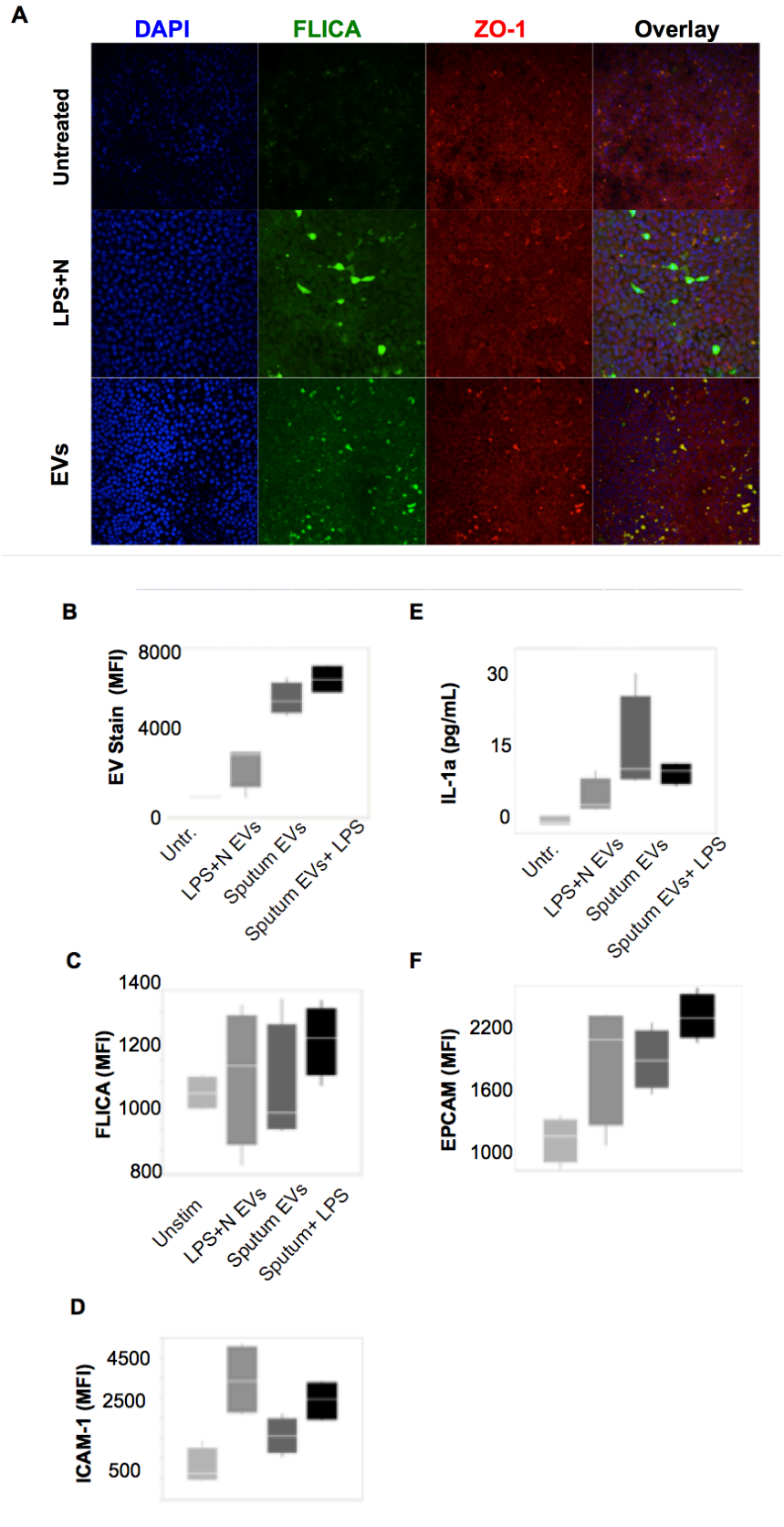
A
DAPI
FLICA
ZO-1
Overlay
Untreated
LPS+N
EVs
B
EV Stain (MFI)
8000
4000
0
Untr.
LPS+N EVs
Sputum EVs
Sputum EVs+ LPS
C
FLICA (MFI)
1400
1200
1000
800
Unstim
LPS+N EVs
Sputum EVs
Sputum+ LPS
D
ICAM-1 (MFI)
4500
2500
500
E
IL-1a (pg/mL)
30
15
0
Untr.
LPS+N EVs
Sputum EVs
Sputum EVs+ LPS
F
EPCAM (MFI)
2200
1600
1000

Figure 3.7. Extracellular vesicles activate inflammasome signaling in primary airway epithelial cells. Primary NhTE cells were incubated with control medium (Untreated), or with EVs isolated from the culture supernatant of PMNs treated with LPS plus nigericin *in vitro* (LPN+N), or EVs from CF sputum (EVs), after which they were assessed using confocal microscopy for intracellular caspase-1 activity with the FLICA probe, along with the junctional protein Z0-1, and the nuclear stain DAPI **(A).** Uptake of labeled EVs **(B)**, intracellular caspase-1 activity with the FLICA probe **(C),** surface ICAM-1 expression **(D)**, IL-1α levels in supernatant **(E)**, and surface EpCAM expression **(F)** were assessed.

REFERENCES

1. Lukens JR, Gross JM, Kanneganti TD. IL-1 family cytokines trigger sterile inflammatory disease. *Front Immunol* 2012; 3: 315.

2. dos Santos G, Kutuzov MA, Ridge KM. The inflammasome in lung diseases. *Am J Physiol Lung Cell Mol Physiol* 2012; 303: L627-633.

3. Sutterwala FS, Mijares LA, Li L, Ogura Y, Kazmierczak BI, Flavell RA. Immune recognition of Pseudomonas aeruginosa mediated by the IPAF/NLRC4 inflammasome. *J Exp Med* 2007; 204: 3235-3245.

4. Schroder K, Tschopp J. The inflammasomes. *Cell* 2010; 140: 821-832.

5. Kim SR, Kim DI, Kim SH, Lee H, Lee KS, Cho SH, Lee YC. NLRP3 inflammasome activation by mitochondrial ROS in bronchial epithelial cells is required for allergic inflammation. *Cell Death Dis* 2014; 5: e1498.

6. Thinwa J, Segovia JA, Bose S, Dube PH. Integrin-mediated first signal for inflammasome activation in intestinal epithelial cells. *J Immunol* 2014; 193: 1373-1382.

7. Brennan MA, Cookson BT. Salmonella induces macrophage death by caspase-1-dependent necrosis. *Mol Microbiol* 2000; 38: 31-40.

8. Chen KW, Gross CJ, Sotomayor FV, Stacey KJ, Tschopp J, Sweet MJ, Schroder K. The neutrophil NLRC4 inflammasome selectively promotes IL-1beta maturation without pyroptosis during acute Salmonella challenge. *Cell Rep* 2014; 8: 570-582.

9. Gaidt MM, Hornung V. Alternative inflammasome activation enables IL-1beta release from living cells. *Curr Opin Immunol* 2016; 44: 7-13.

10. Johnson JL, Ramadass M, Haimovich A, McGeough MD, Zhang J, Hoffman HM, Catz SD. Increased Neutrophil Secretion Induced by NLRP3 Mutation Links the

Inflammasome to Azurophilic Granule Exocytosis. *Front Cell Infect Microbiol* 2017; 7: 507.

11. Karmakar M, Katsnelson M, Malak HA, Greene NG, Howell SJ, Hise AG, Camilli A, Kadioglu A, Dubyak GR, Pearlman E. Neutrophil IL-1beta processing induced by pneumolysin is mediated by the NLRP3/ASC inflammasome and caspase-1 activation and is dependent on K+ efflux. *J Immunol* 2015; 194: 1763-1775.
12. Baroja-Mazo A, Martin-Sanchez F, Gomez AI, Martinez CM, Amores-Iniesta J, Compan V, Barbera-Cremades M, Yague J, Ruiz-Ortiz E, Anton J, Bujan S, Couillin I, Brough D, Arostegui JI, Pelegrin P. The NLRP3 inflammasome is released as a particulate danger signal that amplifies the inflammatory response. *Nat Immunol* 2014; 15: 738-748.
13. Venegas C, Kumar S, Franklin BS, Dierkes T, Brinkschulte R, Tejera D, Vieira-Saecker A, Schwartz S, Santarelli F, Kummer MP, Griep A, Gelpi E, Beilharz M, Riedel D, Golenbock DT, Geyer M, Walter J, Latz E, Heneka MT. Microglia-derived ASC specks cross-seed amyloid-beta in Alzheimer's disease. *Nature* 2017; 552: 355-361.
14. Exline MC, Justiniano S, Hollyfield JL, Berhe F, Besecker BY, Das S, Wewers MD, Sarkar A. Microvesicular caspase-1 mediates lymphocyte apoptosis in sepsis. *PLoS One* 2014; 9: e90968.
15. MacKenzie A, Wilson HL, Kiss-Toth E, Dower SK, North RA, Surprenant A. Rapid secretion of interleukin-1beta by microvesicle shedding. *Immunity* 2001; 15: 825-835.
16. Sarkar A, Mitra S, Mehta S, Raices R, Wewers MD. Monocyte derived microvesicles deliver a cell death message via encapsulated caspase-1. *PLoS One* 2009; 4: e7140.

17. Besnard AG, Togbe D, Couillin I, Tan Z, Zheng SG, Erard F, Le Bert M, Quesniaux V, Ryffel B. Inflammasome-IL-1-Th17 response in allergic lung inflammation. *J Mol Cell Biol* 2012; 4: 3-10.

18. Mahmutovic Persson I, Menzel M, Ramu S, Cerps S, Akbarshahi H, Uller L. IL-1beta mediates lung neutrophilia and IL-33 expression in a mouse model of viral-induced asthma exacerbation. *Respir Res* 2018; 19: 16.

19. Sims JE, Smith DE. The IL-1 family: regulators of immunity. *Nat Rev Immunol* 2010; 10: 89-102.

20. Nold MF, Mangan NE, Rudloff I, Cho SX, Shariatian N, Samarasinghe TD, Skuza EM, Pedersen J, Veldman A, Berger PJ, Nold-Petry CA. Interleukin-1 receptor antagonist prevents murine bronchopulmonary dysplasia induced by perinatal inflammation and hyperoxia. *Proc Natl Acad Sci U S A* 2013; 110: 14384-14389.

21. Cohen TS, Prince A. Cystic fibrosis: a mucosal immunodeficiency syndrome. *Nat Med* 2012; 18: 509-519.

22. Fritzsching B, Zhou-Suckow Z, Trojanek JB, Schubert SC, Schatterny J, Hirtz S, Agrawal R, Muley T, Kahn N, Sticht C, Gunkel N, Welte T, Randell SH, Langer F, Schnabel P, Herth FJ, Mall MA. Hypoxic epithelial necrosis triggers neutrophilic inflammation via IL-1 receptor signaling in cystic fibrosis lung disease. *Am J Respir Crit Care Med* 2015; 191: 902-913.

23. Rimessi A, Bezzerri V, Patergnani S, Marchi S, Cabrini G, Pinton P. Mitochondrial Ca2+-dependent NLRP3 activation exacerbates the Pseudomonas aeruginosa-driven inflammatory response in cystic fibrosis. *Nat Commun* 2015; 6: 6201.

24. Cohen TS, Prince AS. Activation of inflammasome signaling mediates pathology of acute P. aeruginosa pneumonia. *J Clin Invest* 2013; 123: 1630-1637.

25. Reiniger N, Lee MM, Coleman FT, Ray C, Golan DE, Pier GB. Resistance to Pseudomonas aeruginosa chronic lung infection requires cystic fibrosis transmembrane conductance regulator-modulated interleukin-1 (IL-1) release and signaling through the IL-1 receptor. *Infect Immun* 2007; 75: 1598-1608.

26. Tirouvanziam R, Gernez Y, Conrad CK, Moss RB, Schrijver I, Dunn CE, Davies ZA, Herzenberg LA, Herzenberg LA. Profound functional and signaling changes in viable inflammatory neutrophils homing to cystic fibrosis airways. *Proc Natl Acad Sci U S A* 2008; 105: 4335-4339.

27. Fittschen C, Henson PM. Linkage of azurophil granule secretion in neutrophils to chloride ion transport and endosomal transcytosis. *J Clin Invest* 1994; 93: 247-255.

28. Gross O. Measuring the inflammasome. *Methods Mol Biol* 2012; 844: 199-222.

29. Liu X, Ory V, Chapman S, Yuan H, Albanese C, Kallakury B, Timofeeva OA, Nealon C, Dakic A, Simic V, Haddad BR, Rhim JS, Dritschilo A, Riegel A, McBride A, Schlegel R. ROCK inhibitor and feeder cells induce the conditional reprogramming of epithelial cells. *Am J Pathol* 2012; 180: 599-607.

30. Brusselle GG, Provoost S, Bracke KR, Kuchmiy A, Lamkanfi M. Inflammasomes in respiratory disease: from bench to bedside. *Chest* 2014; 145: 1121-1133.

31. Tang A, Sharma A, Jen R, Hirschfeld AF, Chilvers MA, Lavoie PM, Turvey SE. Inflammasome-mediated IL-1beta production in humans with cystic fibrosis. *PLoS One* 2012; 7: e37689.

32. Karmakar M, Katsnelson MA, Dubyak GR, Pearlman E. Neutrophil P2X7 receptors mediate NLRP3 inflammasome-dependent IL-1beta secretion in response to ATP. *Nat Commun* 2016; 7: 10555.

33. Robertson SE, Young JD, Kitson S, Pitt A, Evans J, Roes J, Karaoglu D, Santora L, Ghayur T, Liew FY, Gracie JA, McInnes IB. Expression and alternative processing of IL-18 in human neutrophils. *Eur J Immunol* 2006; 36: 722-731.

34. Lei-Leston AC, Murphy AG, Maloy KJ. Epithelial Cell Inflammasomes in Intestinal Immunity and Inflammation. *Front Immunol* 2017; 8: 1168.

35. Mahida YR, Wu K, Jewell DP. Enhanced production of interleukin 1-beta by mononuclear cells isolated from mucosa with active ulcerative colitis of Crohn's disease. *Gut* 1989; 30: 835-838.

36. Kostadinova E, Chaput C, Gutbier B, Lippmann J, Sander LE, Mitchell TJ, Suttorp N, Witzenrath M, Opitz B. NLRP3 protects alveolar barrier integrity by an inflammasome-independent increase of epithelial cell adherence. *Sci Rep* 2016; 6: 30943.

37. Suwara MI, Green NJ, Borthwick LA, Mann J, Mayer-Barber KD, Barron L, Corris PA, Farrow SN, Wynn TA, Fisher AJ, Mann DA. IL-1alpha released from damaged epithelial cells is sufficient and essential to trigger inflammatory responses in human lung fibroblasts. *Mucosal Immunol* 2014; 7: 684-693.

38. Hill AR, Donaldson JE, Blume C, Smithers N, Tezera L, Tariq K, Dennison P, Rupani H, Edwards MJ, Howarth PH, Grainge C, Davies DE, Swindle EJ. IL-1alpha mediates cellular cross-talk in the airway epithelial mesenchymal trophic unit. *Tissue Barriers* 2016; 4: e1206378.

39. Scarpa M, Kessler S, Sadler T, West G, Homer C, McDonald C, de la Motte C, Fiocchi C, Stylianou E. The epithelial danger signal IL-1alpha is a potent activator of fibroblasts and reactivator of intestinal inflammation. *Am J Pathol* 2015; 185: 1624-1637.

40. Martin-Sanchez F, Gomez AI, Pelegrin P. Isolation of Particles of Recombinant ASC and NLRP3. *Bio Protoc* 2015; 5.

41. Coll RC, Robertson AA, Chae JJ, Higgins SC, Munoz-Planillo R, Inserra MC, Vetter I, Dungan LS, Monks BG, Stutz A, Croker DE, Butler MS, Haneklaus M, Sutton CE, Nunez G, Latz E, Kastner DL, Mills KH, Masters SL, Schroder K, Cooper MA, O'Neill LA. A small-molecule inhibitor of the NLRP3 inflammasome for the treatment of inflammatory diseases. *Nat Med* 2015; 21: 248-255.

42. Iannitti RG, Napolioni V, Oikonomou V, De Luca A, Galosi C, Pariano M, Massi-Benedetti C, Borghi M, Puccetti M, Lucidi V, Colombo C, Fiscarelli E, Lass-Florl C, Majo F, Cariani L, Russo M, Porcaro L, Ricciotti G, Ellemunter H, Ratclif L, De Benedictis FM, Talesa VN, Dinarello CA, van de Veerdonk FL, Romani L. IL-1 receptor antagonist ameliorates inflammasome-dependent inflammation in murine and human cystic fibrosis. *Nat Commun* 2016; 7: 10791.

Chapter 4

Resistin, A Novel Biomarker of Neutrophil-Driven Inflammation in Cystic Fibrosis Airway Disease

Part 1: Resistin is Elevated in Cystic Fibrosis Plasma and Sputum and Correlates Negatively with Lung Function

Part 2: Resistin is an Early Marker of Airway Disease in Children with Cystic Fibrosis

Parts of this work has been accepted for publication as an original article in the Journal of Cystic Fibrosis

PART 1: RESISTIN IS ELEVATED IN CYSTIC FIBROSIS PLASMA AND SPUTUM AND CORRELATES NEGATIVELY WITH LUNG FUNCTION

Osric A. Forrest[1,2], Daniel M. Chopyk[3], Yael Gernez[4], Milton R. Brown[1,2], Carol K. Conrad[4],Richard B. Moss[4], Vin Tangpricha[3,5], Limin Peng[6], Rabindra Tirouvanziam[1,2*]

[1]Department of Pediatrics, Emory University, Atlanta, GA, USA; [2]Center for CF & Airways Disease Research, Children's Healthcare of Atlanta, Atlanta, GA, USA; [3]Department of Medicine, Emory University, Atlanta, GA, USA; [4]Department of Pediatrics, Stanford University, Stanford, CA, USA; [5]Atlanta VA Medical Center, Decatur, GA, USA; [6]Department of Biostatistics and Bioinformatics, Emory University, Atlanta, GA, USA.

ABSTRACT

Background. Resistin is an immunometabolic mediator that is elevated in several inflammatory disorders. A ligand for Toll-like receptor 4, resistin modulates the recruitment and activation of myeloid cells, notably neutrophils. Neutrophils are major drivers of cystic fibrosis (CF) lung disease, in part due to the release of human neutrophil elastase- and myeloperoxidase-rich primary granules, leading to tissue damage. Here we assessed the relationship of resistin to CF lung disease.

Methods. *In vivo* levels of resistin in plasma and sputum of CF patients were measured in three cohorts spanning a wide range of disease. We also assessed the ability of neutrophils to secrete resistin upon activation *in vitro*. Finally, we constructed a multivariate model assessing the relationship between resistin levels and lung function.

Results. Plasma resistin levels were higher in CF than in healthy control subjects. Sputum resistin levels were strikingly high in CF, reaching 50-100 fold higher levels than in plasma. Among CF patients, higher plasma resistin levels were associated with allergic bronchopulmonary aspergillosis, and higher sputum resistin levels were associated with CF-related diabetes. Mechanistically, the *in vitro* release of neutrophil primary granules was concomitant with resistin secretion. Overall, sputum resistin levels were highly and negatively correlated with lung function in CF patients, independent of other variables (age, sex, and genotype).

Conclusions. Our data establish strong relationships between resistin levels in the plasma and sputum of CF patients that correlate with disease status, and identify resistin as a novel mechanistic link between neutrophilic inflammation and lung function decline in CF.

INTRODUCTION

Resistin was originally cloned as a 12.5KDa cysteine-rich adipokine in mice, and was implicated in mediating insulin resistance and diabetes (204, 205). Human resistin shares only 55% homology at the amino acid level with murine resistin, and has a divergent promoter region (206). It differs significantly from its mouse homolog in that its expression is found mainly in monocytes and neutrophils, not in adipocytes. Resistin has been linked to numerous inflammatory disorders including, but not limited to, rheumatoid arthritis, asthma, and cardiovascular disease (207-209). Resistin regulates inflammation in part by binding the lipopolysaccharide (LPS) receptor toll-like receptor 4 (TLR4), leading to modulation of nuclear factor kappa-light-chain-enhancer of activated B cells (NFkB), and mitogen-activated protein kinase signaling, and downstream cytokine secretion (210, 211). Resistin can also bind to other putative receptors, namely, adenylyl cyclase-associated protein 1, and decorin, which may also play important roles in the regulation of inflammation and metabolic disorders (212, 213).

A hallmark of cystic fibrosis (CF) lung disease is inflammation that starts shortly after birth, and progresses throughout the life of patients (214, 215). This inflammatory response is driven in large part by the recruitment and activation of polymorphonuclear neutrophils (PMNs) and subsequent extracellular release of their toxic granules laden with the protease human neutrophil elastase (HNE), myeloperoxidase, and other mediators. HNE, in particular, is a robust biomarker of CF lung disease, since its levels in airway fluid predict bronchiectasis risk in infants, and correlates strongly (negatively) with lung function in adults (216-218).

Here, we explored the role of resistin in CF because of its link to PMN-dominated inflammatory disorders. Using longitudinal and cross-sectional cohorts, we assessed the

relationship between resistin and clinical outcomes in CF. We show that resistin is elevated in CF plasma and sputum, correlates negatively with lung function, and can be reliably measured at various stages of disease. Our data establishes resistin as a biomarker of CF airway disease, and a contributor to chronic inflammation that may serve as a new target for intervention.

METHODS

Human Subjects. We conducted a retrospective analysis of CF patients from three IRB-approved studies (summarized in **Table 4.2**). Cohort 1 (detailed in **Table 4.3**) included CF patients from whom expectorated sputum and blood were collected at the time of hospitalization for an acute pulmonary exacerbation and upon follow-up visit either 3 or 12 months later. Cohort 2 (detailed in **Table 4.4**) included CF patients from whom induced sputum and blood were collected at 3 visits separated by 4-week intervals. Cohort 3 (detailed in **Table 4.5**) included CF patients divisible into three categories based on clinical diagnosis prior to enrollment: (i) patients with allergic bronchopulmonary aspergillosis diagnosed according to CF Foundation guidelines using elevated blood IgE levels (CF-ABPA); (ii) patients stably colonized by *Aspergillus fumigatus (*AF), indicated by two or more positive sputum cultures without hypersensitization (CF-AC); and (iii) patients without stable AF colonization or sensitization. For all studies, CF was diagnosed by sweat chloride of 60 mEq/l using a quantitative iontophoresis test and/or documented CFTR mutations. Healthy control (HC) subjects were also enrolled for plasma and induced sputum collection under an IRB-approved protocol.

Sample collection and processing. Blood was collected by venipuncture using EDTA tubes, and sputum samples were collected as previously described by either spontaneous expectoration (141), or induction using hypertonic saline (140), and processed at 4ºC. Briefly, sputum samples were mixed with PBS-EDTA (2.5 mM final), and submitted to gentle mechanical dissociation by passing through an 18G needle, after which the supernatant was purified by centrifugation at 800G and 3,000G (to remove cells, and bacteria and debris, respectively). Platelet-free plasma was generated by centrifugation at 400G and 3,000G (to

remove cells, and platelets, respectively). Purified sputum supernatant and platelet-free plasma were stored at -80ºC until use.

***In vitro* PMN stimulation.** PMNs were isolated from whole blood using a Polymorphprep gradient (Nycomed Pharma), as detailed previously (219). Briefly, blood was layered onto the gradient, spun at room temperature at 400G with minimal brake, after which the PMN layer was removed, and residual red blood cells were lysed by hypotonic shock. Isolated PMNs were then re-suspended in RPMI without FBS and stimulated at 37ºC with latrunculin B (LB, 5 μM) for 5 minutes, followed by formyl-methionine leucine phenylalanine (fMLF, 5 μM) for 10 minutes. Stimulated PMNs were then spun at 400G to remove culture supernatant, washed with PBS-EDTA, and stained with antibodies for CD63 (clone H5C6), CD66b (clone G10F5) from BioLegend, and the Live/Dead probe (Thermo Scientific), and analyzed by flow cytometry as detailed before (141). Culture supernatant was stored at -80ºC until use.

Fluid measurements. Resistin was measured in plasma and sputum fractions prepared from CF patients and HC subjects, and in culture supernatant from *in vitro* PMN stimulation experiments using an ELISA kit (R&D Systems) according to the manufacturer's protocol. IL-8 was measured in sputum with an ELISA kit (R&D Systems) according to the manufacturer's protocol. HNE activity was measured using a spectrophotometric assay, as previously described (15).

Neutrophil extracellular trap stimulation and quantification. MPO-DNA, NE-DNA, and resistin-DNA complexes were measured using an ELIA previously described here (220).

Briefly, purified PMNs were stimulated with 100 nM phorbol-myristate-acetate (PMA) for 4 hrs. Cell free supernatants and CF airway fluid were then treated with DNAse (2 U/mL) at RT for 15 mins and then stopped by adding 25 mM EGTA for final concentration 2.5 mM. Supernatants were diluted and added to a high-binding 96-well plate coated with either anti-MPO (Upstate), HNE (Calbiochem), or resistin (R&D) antibodies overnight and blocked with 5% BSA. Secondary, anti-DNA antibody conjugated to peroxidase (Roche) was added for 60 mins, then the plate was washed 3 times after which TMB substrate was added. The reaction as stopped and measured using a microplate reader.

Flow cytometry. Blood and airway cells from CF subjects were stained with fluorescently labeled antibodies. These included antibodies against CD63 (H5C6), CD66b (G10F5) (from BioLegend), Resistin (R&D), and TLR4/MD2 (7E3) (InvivoGen). Cells were also stained with the Live/Dead probe (Invitrogen) to ascertain viability and FcBlock (BioLegend). Data were acquired on a LSRII cytometer (BD Biosciences) and compensation and analysis were performed using the Flowjo software (Treestar).

Isolation and characterization of EVs. EVs were isolated from plasma and CF ASN as follows. Samples were first spun at 20,000g for 15 mins to remove any cell debris after which they were loaded unto a 300 kDa molecular weight (MW) exclusion column (Vivaspin) and spun for 15 mins at 15,000g. EVs were further purified using the Exoflow kit (SBI) according to the manufacturer's guidelines. Briefly, anti-CD63 biotinylated antibodies were first conjugated to magnetic streptavidin-labeled beads. The retentate from the 300 kDa MW columns was then re-suspended in PBS and incubated with anti-CD63-bead complexes overnight at 4^{o}C., washed 3 times with wash buffer and then stained with Exostain-FITC

stain (SBI), and an anti- Resistin antibody (R&D). Labeled EV-bead complexes were then analyzed by flow cytometry using an LSRII instrument (BD).

Statistical Analysis. Statistical analyses were performed using JMP12 and SAS 9.4 (SAS Institute). Significant differences were determined by using p-values <0.05. Multivariate models were constructed to assess the relationship between resistin and lung function (expressed as FEV1 %predicted). All models were adjusted for demographic information (age, sex, genotype).

RESULTS

Increased plasma and sputum resistin correlate negatively with lung function in CF. We first compared resistin levels in CF Cohort 1 and HC subjects. In both the plasma and sputum of CF patients, resistin levels were significantly elevated compared to HC subjects. The most striking difference was for sputum, in which resistin levels were more than 100-fold higher in CF than in HC subjects **(Fig. 4.1A)**. We then assessed the relationship between resistin levels and lung function in CF Cohort 1, and found that plasma and, even more so, sputum resistin levels showed a strong negative correlation with FEV1% of predicted for age **(Fig. 4.1B-C)**. Comparison of plasma and sputum resistin levels within the CF cohort showed that sputum levels were at least two orders of magnitude (50- to 100-fold) higher than plasma levels, whether collected during pulmonary exacerbations or in a stable condition three or twelve months later **(Fig 4.1D)**. Because of the proposed role of resistin in metabolic regulation, we tested if patients with CF-related diabetes (CFRD) showed differences in resistin levels compared to non-diabetic patients, and found higher levels of sputum resistin at inpatient visits in CFRD compared to non-diabetic patients **(Fig.**

4.1E-F). Age, sex, and CFTR genotype, did not significantly impact plasma and sputum resistin levels.

Resistin levels are stable in the short term in CF patients, and track with established markers of airway inflammation. In CF Cohort 2, induced sputum and plasma were collected from 16 patients at three consecutive stable visits 4 weeks apart, enabling us to assess short-term stability of resistin levels. There was no significant time effect (Wilcoxon signed-rank test for each pair of visits) on resistin levels in plasma and sputum over an 8-week period **(Fig. 4.2A-B)**. Sputum IL-8 and NE, two established markers of CF airway inflammation linked to PMN dysfunction, were also measured and showed strong positive correlations with sputum resistin at all time points **(Fig. 4.2C-D)**.

CF patients with allergic bronchopulmonary aspergillosis have elevated plasma resistin levels. In CF Cohort 3, we studied the relationship between resistin and ABPA. In plasma, CF-ABPA patients had higher levels of resistin compared to both Aspergillus-colonized (CF-AC), and non-colonized CF patients **(Fig. 4.3A)**. However, sputum resistin levels were similar in the three groups, and stable over two years **(Fig. 4.3B)**. We applied repeated measures linear model to assess the impact of sputum resistin on lung function (measured as FEV1, while adjusting for potential confounders, age, ABPA status, genotype, and the presence of PA. The repeated measures linear model appropriately accommodates the correlations among the measurements taken from the same subjects across different visits through a flexible AR(1) structure. The repeated measures analysis showed that higher sputum resistin is significantly associated with lower lung function ($p=0.024$) (**Table 4.6**).

Combined analysis across all patient cohorts reveals a strong negative correlation between sputum resistin and lung function. Next, we combined data from cohort 1-3 and used the data at the first visit (inpatient visit for Cohort 1 and enrollment visits for Cohorts 2 and 3). We conducted multivariate longitudinal analysis based on repeated measures linear model to investigate the association of resistin with lung function (measured as FEV1). The model included sputum resistin and plasma resistin, and adjusted for confounders including age, gender, genotype. It is found that sputum resistin is a strong independent predictor of lung function. Age, gender, and genotype do not show significant effects on FEV1. It is interesting to note that plasma resistin shows little prognostic power once sputum resistin is adjusted for. This may further confirm the prognostic value of sputum resistin on predicting the progression of lung function.

Neutrophils secrete resistin upon release of primary granules in vitro. Since levels of both resistin and NE are highly elevated in CF sputum, and correlate strongly with one another, we explored whether the release of NE-rich primary granules by PMNs, as we previously observed in CF airways (140), could also result in the extracellular release of resistin, thereby explaining the high levels observed in CF sputum fluid. Upon *in vitro* stimulation with LB and fMLF, PMNs increased both surface CD63 and CD66b compared with unstimulated PMNs, consistent with the induced release of primary and secondary granules **(Fig. 4.4A-B)**. This release was concomitant with increased levels of extracellular resistin in the supernatants of activated PMNs **(Fig. 4.4C)**. Consistently, we observed that sputum resistin levels were positively correlated with the count of degranulating PMNs in Cohort 1 at inpatient visits **(Fig. 4.5)**.

Resistin is compartmentalized on the surface of PMNs, NETs, and extracellular vesicles in the CF airways. Building upon our observation that resistin was elevated in CF sputum and plasma, we next sought to assess in which fraction of the sputum resistin is compartmentalized. Using flow cytometric analysis of live blood and airway PMNs from CF donors, we observed increased surface expression of resistin on CF airway PMNs **(Fig. 4.6A).** This increased surface expression of resistin was concomitant with active exocytosis, as these cells were dually positive for surface resistin and CD63, a marker of primary granule exocytosis **(Fig. 4.6B).** We next explored the expression of the putative resistin receptor TLR4 on the surface of CF airway PMNs by tracking TLR4/MD2 complexes that form when TLR4 is activated. From these analyses, we observed that CF airway PMNs had increased surface expression of TLR4/MD2 complexes compared to PMNs from blood **(Fig. 4.6C).** Additionally, we explored if resistin could also be present on NETs, similarly to other PMN granule proteins. Using ELISA assays for DNA-MPO, DNA-NE, and DNA-resistin complexes, we observed that soluble resistin was positively correlated with both DNA-MPO and DNA-NE complexes in the CF sputum **(Fig. 4.7A-B),** and that PMA-stimulated PMNs were able to produce DNA-resistin complexes *in vitro* (**Fig. 4.7C).** Finally, we assessed the surface expression of resistin on CD63 positive extracellular vesicles (EVs) isolated from the plasma and sputum of both healthy control and CF donors. We found that EVs from CF sputum had increased surface expression of resistin, as measured by ExoFlow analysis **(Fig. 4.8A).** Further analysis of samples after size exclusion filtration using 300kDa MW cut-off filters showed that resistin was detectable in both the eluate and retentate from CF sputum and varied in its relative abundance between these two fractions depending on patients **(Fig. 4.8B)**

DISCUSSION

In this study, we explored the relationship between the immunometabolic mediator resistin and CF disease, using both cross-sectional and longitudinal sample collections. We observed that resistin levels are elevated in both CF plasma and sputum compared to healthy controls. To our knowledge, this is the first published report linking resistin with CF disease, although resistin has been identified previously as a contributor to other human inflammatory diseases. Moreover, while resistin levels were reported to be elevated in the plasma of patients with asthma and COPD (221), its prominent presence in sputum suggests that is may serve as both a systemic and airway biomarker of CF disease. This notion is strengthened by the strong negative correlations of plasma and sputum resistin with CF lung function.

Myeloid cells, most notably PMNs, have been identified as a dominant source of resistin in humans. In human PMNs, resistin is stored in primary granules, which also contain the serine protease NE (222, 223). Resistin has been shown to increase PMN sensitivity to LPS-dependent activation through inhibition of AMP-activated protein kinase activity, acting essentially as a priming agent (224). Additionally, mice in which endogenous resistin was knocked out and human resistin knocked in have increased edema and extracellular secretion of pro-inflammatory cytokines and other byproducts of PMN activation upon acute lung injury (224). Our study suggests that similar processes are at play in CF patients, since sputum resistin levels correlate positively with the number of live sputum PMNs, NE, IL-8, and NE/MPO-positive NETs. While resistin is present, as expected, in the low molecular weight fraction of CF sputum supernatant, we also found it compartmentalized in part on the surface of EVs, suggesting a complex distribution. In addition, we showed that upon *in vitro* stimulation of PMNs both primary granules (as we

previously observed in CF airways (140)), and extremely high levels of resistin are released into the extracellular milieu. Thus, CF PMNs act both as a source, and potential target, of resistin signaling.

Although most published data on resistin suggest that it functions a pro-inflammatory mediator, in part by activating PMNs, some reports suggest that resistin may also reduce the rate of chemotaxis and oxidative burst in stimulated PMNs (225, 226). Consistently, in mice with human resistin knocked in exposed to an LPS-induced septic shock, resistin was found to bind competitively to TLR4. This in turn induced anti-inflammatory signaling through activation of the transcription factors signal transducer and activator of transcription 3 and TANK binding kinase 1, lowering systemic pro-inflammatory cytokine levels, and in turn, enhanced survival (227). Thus, resistin may ligate TLR4 and either activate it or protect it against overwhelming LPS-mediated signaling. This is further supported by the increased TLR4 signaling observed in CF airway PMNs. This increased signaling is possibly mediated by resistin on the surface of PMNs or via signaling mediated by EVs. Further studies are required to determine the mechanisms at play in CF.

CF-related diabetes (CFRD) is a common comorbidity observed in adults with CF, and linked to accelerated lung function decline, increased incidence and severity of exacerbations, and mortality risk (228, 229). Here, we observed that patients with CFRD had increased sputum resistin during inpatient visits compared to non-diabetic CF patients. This observation is consistent with the link between resistin and insulin signaling in diabetes (204, 230). A possible explanation is that resistin may act as a pro-inflammatory and metabolic mediator, simultaneously worsening lung PMN burden/activation and causing hyperglycemia during exacerbations in CF patients with glucose intolerance. Of note, we also found that patients with CF-ABPA had higher plasma resistin levels than those without

ABPA, and consequently, plasma resistin may contribute to worsening systemic inflammation and overall morbidity in that subgroup (231, 232). Further studies specifically designed to assess the relationship of systemic and airway resistin levels with CFRD and ABPA are warranted. Finally, by compiling data from the three cohorts included in this study, we constructed a statistical model that identified resistin as a strong correlate of CF lung function, independent of common factors known to affect disease severity such as age, sex, genotype, microbiology, and medication regimen.

Together, our data identify a strong relationship between plasma and sputum resistin levels and the severity of airway disease in CF patients. Resistin likely originates from excessive primary granule release by PMNs in CF airways (140). PMNs may also be the main target of resistin, making it a potential focus for future development of therapies to modulate CF airway inflammation. Further studies are warranted to identify other potential sources and targets of CF airway resistin, and characterize its potential as an independent disease biomarker.

Table 4.1. Multivariate logistical model showing the relationship between sputum and plasma resistin levels and FEV1 across all three patient cohorts.

Effect	Gender	Genotype	Estimate	Standard Error	DF	t Value	Pr > |t|
Intercept			128.71	16.527	62	7.79	<.0001
Age			-0.1916	0.1954	62	-0.98	0.3304
Gender	F		3.0193	4.45	62	0.68	0.5
Gender	M		0	.	.	.	.
Genotype		HO	0.8923	7.4469	62	0.12	0.905
Genotype		HZ	-2.5537	7.599	62	-0.34	0.738
Genotype		OT	0	.	.	.	.
Sputum resistin log10			-15.1227	3.4947	62	-4.33	<.0001
Plasma resistin log10			-10.087	8.1332	62	-1.24	0.2196

Table 4.2. Summary of demographic information for all three CF cohorts included in the study. Numerical data presented as median [interquartile range]. Abbreviations: F, female; FEV1 (%), functional expiratory volume in 1 second expressed in % predicted; HO= F508Del homozygous; HZ= heterozygous (comprising one F508Del mutation, and a second mutation); M, male; OT, two mutations other than F508Del.

Cohort	1	2	3
Subjects (n)	32	16	48
Age (Yrs)	22 [24,30]	32 [48,25]	18 [28.5,14]
Sex	18 [F]14 [M]	9 [F] 7 [M]	22 [F] 27 [M]
FEV1 (%)	51 [38,62]	61 [66,44]	88 [94,61]
Genotype	14 [HO] 14 [HZ] 1 [OT]	8 [HO] 6 [HZ] 2 [OT]	28 [HO] 13 [HZ] 8 [OT]
Sputum Collection	Expectorated	Induced	Induced

Table 4.3. Demographic information for CF Cohort 1. Abbreviations: F, female; FEV1 (%), functional expiratory volume in 1 second expressed in % predicted; HO= F508Del homozygous; HZ= heterozygous (comprising one F508Del mutation, and a second mutation); I: inpatient visit during active pulmonary exacerbation; M, male; O, outpatient visit; OT, two mutations other than F508Del; UNK: unknown.

Patient	Visit Type	Gender	Age (Yr)	CTFR Mutation 1	CTFR Mutation 2	Zygosity	FEV1(%)
1	I	M	27	dF508	L467P	HZ	22
2	I	M	41	UNK	UNK	ND	45
3	I	F	63	dF508	2184insA	HZ	21
4	I	F	40	dF508	dF508	HO	25
5	I	F	62	dF508	dF508	HO	21
6	I	F	47	dF508	N1303K	HZ	31
7	I	F	55	dF508	R347P	HZ	21
8	I	F	46	dF508	177delC>T	HZ	39
9	I	F	25	dF508	dF508	HO	29
10	I	F	61	dF508	R1162X	HZ	22
11	I	M	41	UNK	UNK	ND	22
12	I	M	49	dF508	R560T	HZ	22
13	I	F	35	dF508	dF508	HO	22
14	I	M	56	dF508	dF508	HO	23
15	I	M	51	dF508	dF508	HO	30
16	I	M	51	dF508	dF508	HO	17
17	I	M	51	dF508	dF508	HO	24
18	I	M	64	dF508	UNK	HZ	29
19	I	F	72	dF508	P67L	HZ	35
20	I	F	90	dF508	dF508	HZ	22
21	I	M	65	dF508	P67L	HZ	24
22	I	F	61	dI507	c.2988+IG>A	OT	24
23	I	F	101	dF508	dF508	HO	30
24	I	F	60	dF508	dF508	HO	24
25	I	F	59	dF508	S945L	HZ	23
26	I	M	29	dF508	UNK	HZ	36
27	I	M	37	dF508	dF508	HO	26
28	I	M	43	dF508	dF508	HO	20
29	I	M	65	dF508	dF508	HO	28
30	I	F	35	dF508	dF508	HO	31
31	I	F	37	dF508	UNK	HZ	29
32	I	F	30	UNK	UNK	ND	19
33	O	F	27	dF508	dF508	HO	31
34	O	M	22	dF508	L467P	HZ	25
35	O	M	45	UNK	UNK	ND	17
36	O	F	21	dF508	dF508	HO	50
37	O	F	31	dF508	N1303K	HZ	52
38	O	F	21	dF508	R347P	HZ	48
39	O	F	39	dF508	177delC>T	HZ	45
40	O	F	29	dF508	dF508	HO	24
41	O	F	23	dF508	R1162X	HZ	70
42	O	M	22	UNK	UNK	ND	93
43	O	M	22	dF508	R560T	HZ	57
44	O	F	22	dF508	dF508	HO	74
45	O	M	30	dF508	dF508	HO	71
46	O	M	18	dF508	dF508	HO	70
47	O	M	25	dF508	dF508	HO	50
48	O	M	30	dF508	UNK	HZ	71
49	O	F	35	dF508	P67L	HZ	78
50	O	M	25	UNK	UNK	ND	ND
51	O	F	24	dF508	c.2988+IG>A	HZ	70
52	O	F	30	dF508	dF508	HO	56
53	O	F	25	dF508	S945L	HZ	64
54	O	M	23	dF508	UNK	HZ	ND
55	O	M	26	dF508	dF508	HO	46
56	O	M	29	dF508	dF508	HO	69
57	O	M	31	dF508	dF508	HO	36
58	O	F	24	dF508	2184insA	HZ	50
59	O	M	46	dF508	A455E	HZ	79
60	O	M	24	dF508	dF508	HO	51
61	O	F	23	dF508	dF508	HO	59
62	O	F	25	dI507	c.2988+IG>A	OT	72
N=62	I=32 O=30	M=29 F=33	Age :40±17.9			HO=27 HZ=27 OT=2	FEV1%= 40±20

Table 4.4. Demographic information for CF Cohort 2. Abbreviations: F, female; FEV1 (%), functional expiratory volume in 1 second expressed in % predicted; HO= F508Del homozygous; HZ= heterozygous (comprising one F508Del mutation, and a second mutation); M, male; OT, two mutations other than F508Del.

Patient	Gender	Age (Yr)	Zygosity	FEV1(%)
1	M	22	HO	66
2	M	49	HO	67
3	F	27	HZ	48
4	M	11	HZ	65
5	M	25	HO	59
6	F	50	HZ	65
7	F	26	HO	52
8	F	50	HO	41
9	F	32	HZ	44
10	F	45	HZ	64
11	M	32	OT	73
12	F	38	HZ	59
13	M	32	HO	82
14	F	44	OT	74
15	F	12	HO	40
16	M	50	HO	41
N=16	M=7 F=9	Age=34±13	HO=8 HZ=6 OT=2	FEV1%=59±13

Table 4.5. Demographic information for CF Cohort 3. Abbreviations: CF, CF without ABPA or *A. fumigatus* colonization; CF-AB, CF with ABPA; CF-AC, CF colonized by *A. fumigatus*; F, female; FEV1 (%), functional expiratory volume in 1 second expressed in % predicted; HO= F508Del homozygous; HZ= heterozygous (comprising one F508Del mutation, and a second mutation); M, male; ND, not determined; OT, two mutations other than F508Del; UNK: unknown.

Patient	Disease Category	Gender	Age (Yr)	CTFR Mutation 1	CTFR Mutation 2	Zygosity	FEV1(%)
1	CF-AB	F	45	dF508	dF508	HO	90
2	CF-AB	M	28	dF508	dF508	HO	55
3	CF-AC	F	22	dF508	dF508	HO	98
4	CF-AC	F	46	w1282x	w1282x	OT	93
5	CF-AC	M	51	dF508	dF508	HO	94
6	CF-AC	M	14	dF508	dF508	HO	67
7	CF-AB	M	9	dF508	dF508	HO	102
8	CF-AB	M	38	dF508	711+1G>T	HZ	40
9	CF-AC	M	13	dF508	dF508	HO	95
10	CF-AB	F	11	3849+10kbC>T	UNK	OT	97
11	CF-AB	M	19	dF508	dF508	HO	56
12	CF-AC	M	18	dF508	dF508	HO	36
13	CF-AC	F	15	dF508	dF508	HO	97
14	CF-AC	F	19	dF508	dF508	HO	99
15	CF	F	17	dF508	dF508	HO	90
16	CF-AB	F	11	G542X/C1811+1643G>T	7T/9T poly T	OT	42
17	CF-AB	F	51	dF508	dF508	HO	39
18	CF-AC	F	18	dF508	W1282X	HZ	93
19	CF-AC	M	17	dF508	dF508	HO	85
20	CF-AB	F	17	dF508	dF508	HO	95
21	CF-AC	M	20	dF508	1717-1	HZ	92
22	CF	M	14	dF508	dF508	HO	119
23	CF-AC	F	30	dF508	dF508	HO	92
24	CF	M	10	G178R	LA67P	OT	93
25	CF	F	14	dF508	dF508	HO	103
26	CF	F	14	dF508	dF508	HO	103
27	CF	M	7	dF508	dF508	HO	90
28	CF-AB	F	16	dF508	R334W	HZ	50
29	CF-AC	F	14	dF508	UNK	HZ	90
30	CF	F	20	dF508	3849+10KBC>T	HZ	51
31	CF	M	14	dF508	1898+7G>A	HZ	76
32	CF	M	15	dF508	dF508	HO	82
33	CF	M	18	dF508	711+1 G	HZ	87
34	CF-AC	M	26	dF508	dF508	HO	81
35	CF	F	14	dF508	E1371	HZ	88
36	CF-AB	M	69	6194V	7T/9T	OT	43
37	CF-AB	F	20	dF508	G542X	HZ	63
38	CF-AB	F	ND	dF508	dF508	HO	71
39	CF-AB	M	25	dF508	dF508	HO	90
40	CF-AC	M	35	dF508	G551D	HZ	77
41	CF-AB	M	45	dF508	dF508	HO	89
42	CF-AC	F	22	dF508	G511D	HZ	65
43	CF-AB	M	35	I507del	R117H	OT	59
44	CF-AB	M	35	I507del	R117H	OT	59
45	CF-AB	F	14	dF508	R1162x	HZ	97
46	CF-AB	M	ND	G542X	UNK	OT	94
47	CF-AB	M	ND	dF508	dF508	HO	68
48	CF-AB	M	9	L206W	D1152H	HO	113
N=48	CF=11 CF_AB=21 CF_AC=16	M=27 F=21	Age=22±13.6			HO= 27 HZ=13 OT=8	FEV1%=80±21

Table 4.6 Multivariate logistical model showing the effect of resistin on FEV1 in Cohort 3. Abbreviations: CF, CF without ABPA or *A. fumigatus* colonization; CF-ABPA, CF with ABPA; CF-AC, CF colonized by *A. fumigatus* ; HO= F508Del homozygous; HZ= heterozygous (comprising one F508Del mutation, and a second mutation); PA, *P. aeruginosa*;

Obs	Effect	ABA status	Visit	Genotype	PA	Estimate	StdErr	DF	tValue	Probt
1	Intercept					96.2097	11.8327	35	8.13	<.0001
2	Age					-0.3308	0.2245	42	-1.47	0.148
3	Visit		6 monhts			-0.6152	1.7294	42	-0.36	0.7238
4	Visit		12 months			-0.6591	2.2442	42	-0.29	0.7705
5	Visit		18 months			1.604	3.5157	42	0.46	0.6506
6	Visit		Baseline			0				
7	Sputum resistin log10					-4.4199	1.8488	42	-2.39	**0.0214**
8	ABPA status	CF				0.2051	7.4878	35	0.03	0.9783
9	ABPA status	CF-ABPA				-9.703	6.7562	35	-1.44	0.1598
10	ABPA status	CF-AC				0				
11	Genotype			HO		9.6114	8.0922	35	1.19	0.2429
12	Genotype			HZ		-6.046	8.8582	35	-0.68	0.4994
13	Genotype			OT		0				
14	PA				N	5.6111	2.5123	9	2.23	0.0524
15	PA				Y	0				

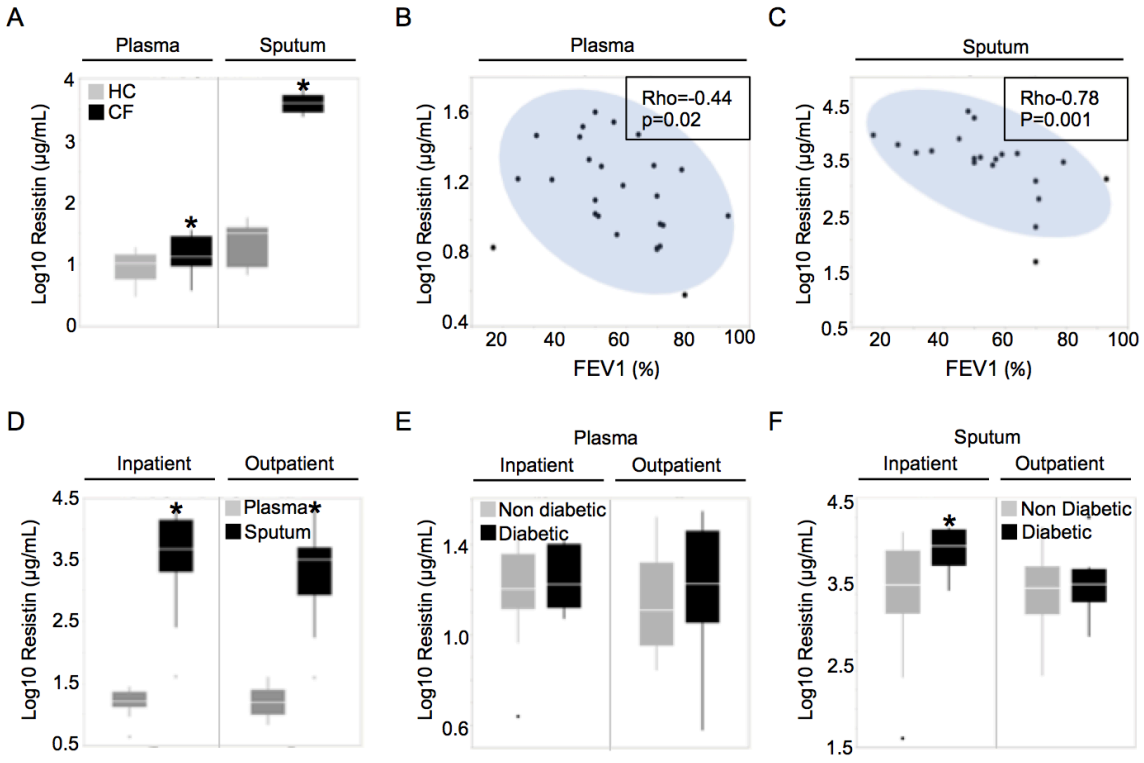

Figure 4.1. Plasma and sputum resistin levels are elevated in CF patients and correlate negatively with lung function. (A) Resistin levels were measured at baseline in plasma and sputum samples of CF (N=31), and HC (N=9) subjects. * indicates p<.05. **(B-C)** Correlations between CF lung function (FEV1, expressed in % predicted), and CF plasma and sputum resistin levels, respectively, were tested using the Spearman test. **(D)** Resistin was measured in the plasma and sputum of patients in cohort 1 during an active exacerbation with IV antibiotic treatment (inpatient) or 3 or 12 months later during a follow up stable visit (outpatient). **(E-F)** Plasma and sputum resistin levels, respectively, were compared between CF patients with and without diabetes at inpatient and outpatient visits using the Wilcoxon rank sum test, with * indicating p<.05. (N=31).

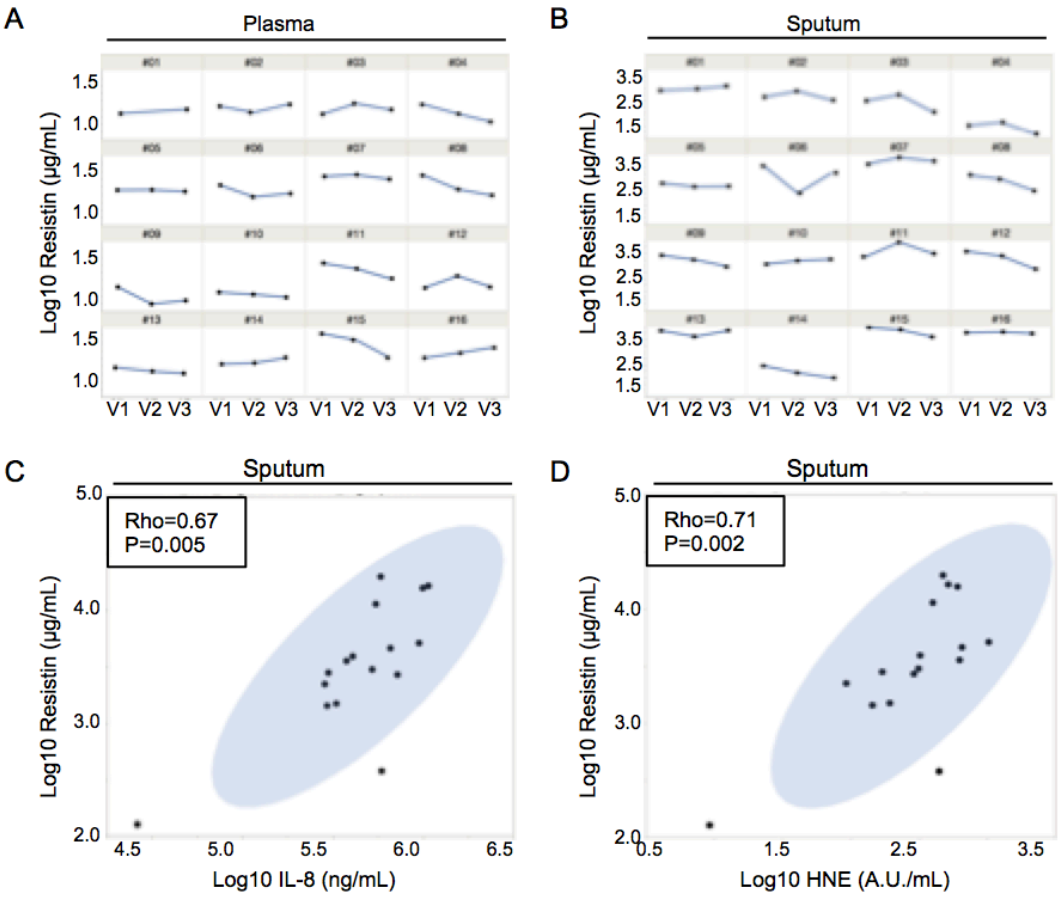

Figure 4.2. Resistin levels are stable in the short term and correlate with established biomarkers of CF airway inflammation. **(A-B)** Plasma and sputum resistin levels, respectively, were measured longitudinally over 3 visits separated by 4 week intervals to assess short-term stability. **(C-D)** Sputum resistin levels at visit 1 were correlated with sputum IL-8 and human neutrophil elastase (HNE) activity, respectively, using the Spearman test (N=16).

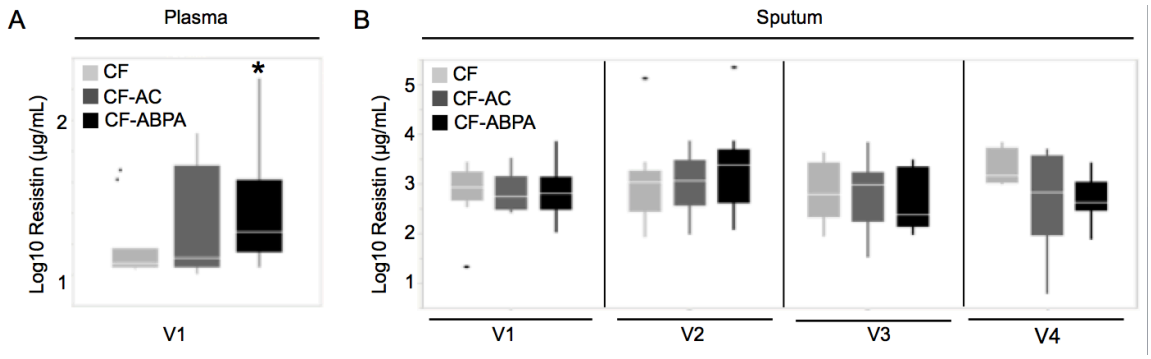

Figure 4.3. Plasma resistin is elevated in CF patients with ABPA. (A) Plasma resistin was measured at baseline in patients with ABPA (CF-ABPA), patients colonized by *A. fumigatus* but without ABPA (CF-AC), and control patients (CF). **(B)** Sputum resistin was measured in the same sets of patients at 4 visits with 6-month intervals between visits. Plasma and sputum resistin levels were then compared between groups using the Wilcoxon rank sum test (N=46, * indicates $p<.05$).

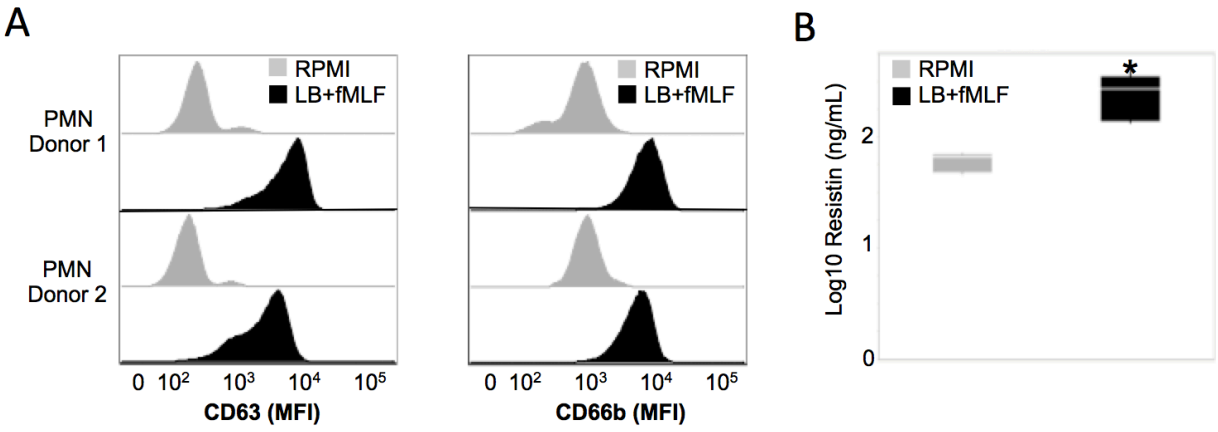

Figure 4.4. PMNs release resistin upon granule exocytosis *in vitro*. **(A)** PMNs were purified from the blood of HC donors, and stimulated with latrunculin B (LB, 5 μM) and fMLF (5 μM), after which the cells were analyzed for surface expression of CD63 and CD66b as markers of primary and secondary granule exocytosis, respectively. Median fluorescence intensities (MFI) for these markers are displayed in representative histograms showing PMNs treated with medium control (RPMI, grey) and LB+fMLF (black). **(B)** Resistin was measured in the supernatants from PMNs treated with medium control (RPMI, grey) and LB+fMLF (black), and compared using the Wilcoxon signed-rank test (N=5 independent experiments, * indicates $p<.05$).

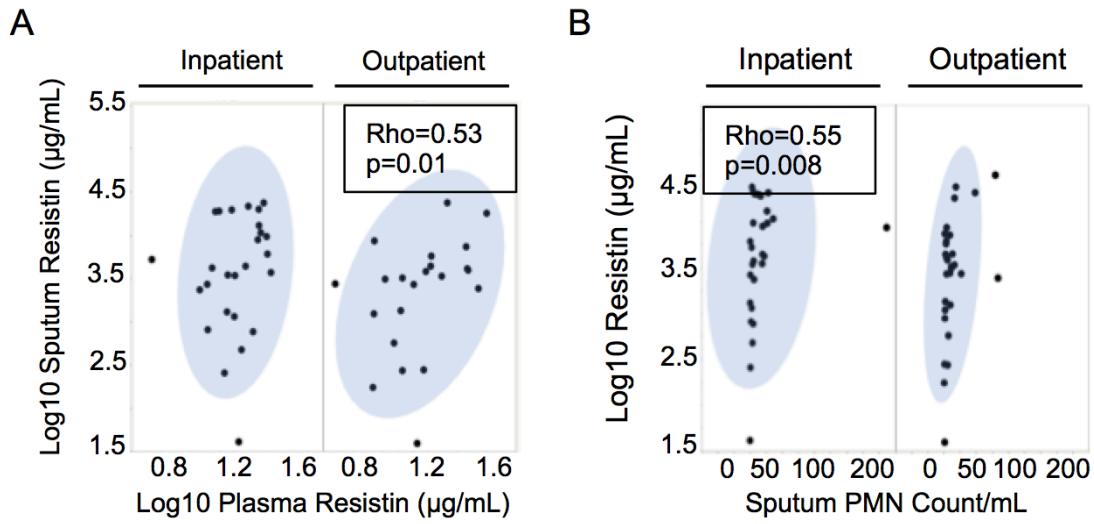

Figure 4.5. Sputum resistin correlates with plasma resistin and sputum neutrophil count. (A) Levels of sputum and plasma resistin in cohort 1 were measured using ELISA and correlated with each other using the Spearman test in both inpatient (N=??) and outpatient (N=??) visits, with * indicating $p<0.05$. (**B)** Sputum resistin levels were measured using ELISA in cohort 1, and correlated with the sputum PMN live count using the Spearman test (N=31, indicating $p<0.05$)

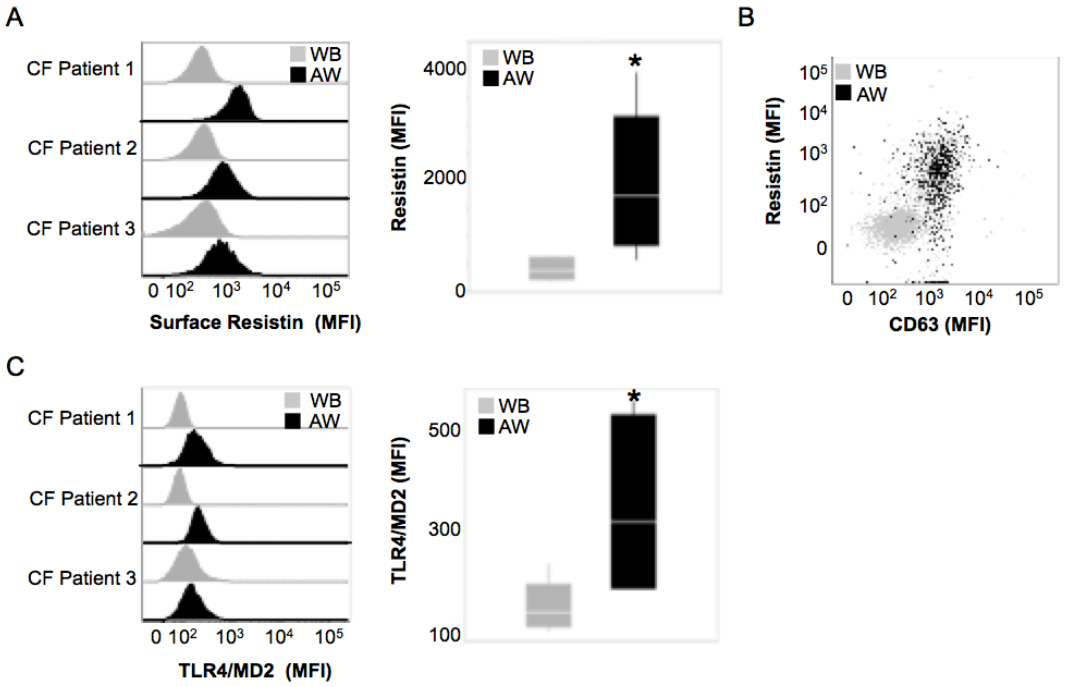

Figure 4.6. CF airway PMNs have increased surface resistin and TLR4/MD2 complexes. (A) Surface resistin was measured on whole blood (WB, grey) and airway (AW, black) PMNs from CF patients, as shown here in representative histograms and boxplots of median fluorescent intensities (MFI). **(B)** Levels of surface resistin and CD63 (reflecting primary granule exocytosis) are shown in a scatter plot with an overlay of whole blood (WB, grey) and airway (AW, black) PMNs from a representative CF patient. **(C)** Levels of surface TLR4/MD2 complexes were measured on (WB, grey) and airway (AW, black) PMNs from CF patients, as shown here in representative histograms and boxplots of MFI. In **(A)** and **(C)**, WB and AW expression levels were compared using the Wilcoxon signed-rank test (N=5, * indication $p<0.05$).

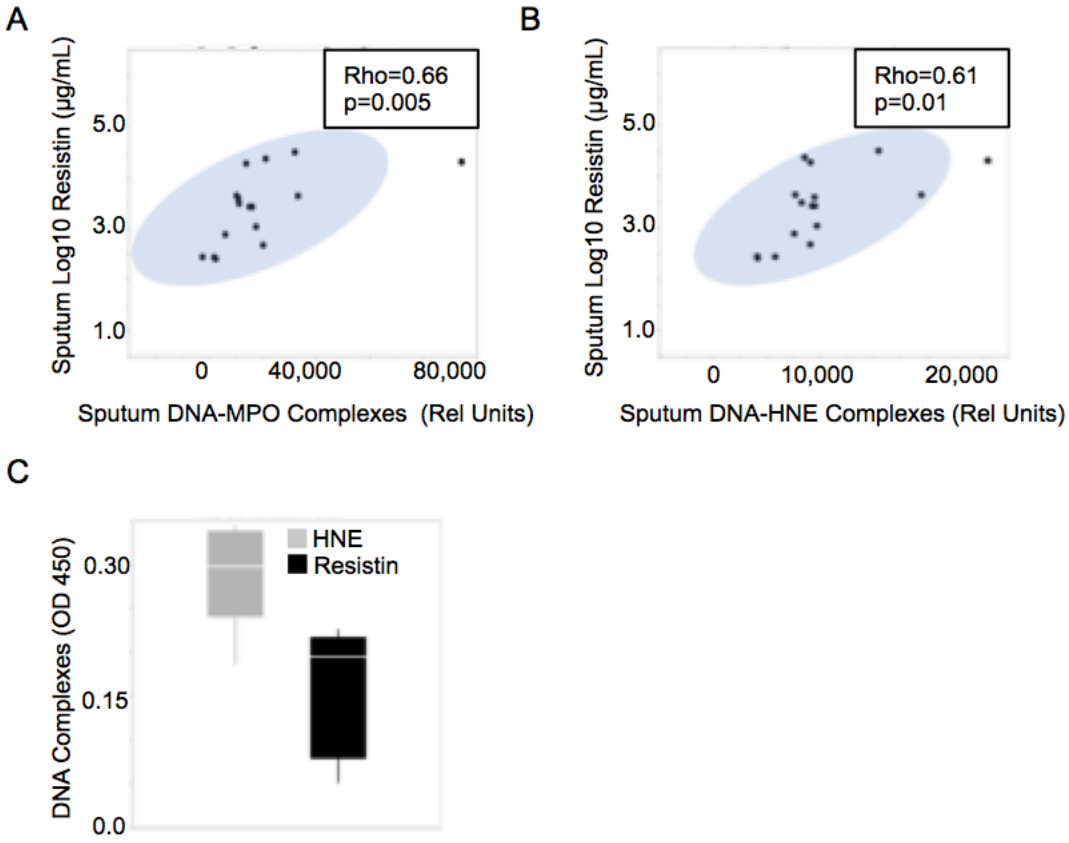

Figure 4.7. Resistin correlates with, and is compartmentalized on neutrophil extracellular trap (NET) complexes found in CF sputum. (A-B) Levels in CF sputum of resistin, and those of DNA-MPO and DNA-HNE complexes, respectively, were correlated using the Spearman test (N=12, * indicating $p<0.05$). **(C)** PMNs were stimulated with PMA to induce NET release *in vitro*, after which the amount of DNA complexes with HNE and resistin were quantified by ELISA (N=5).

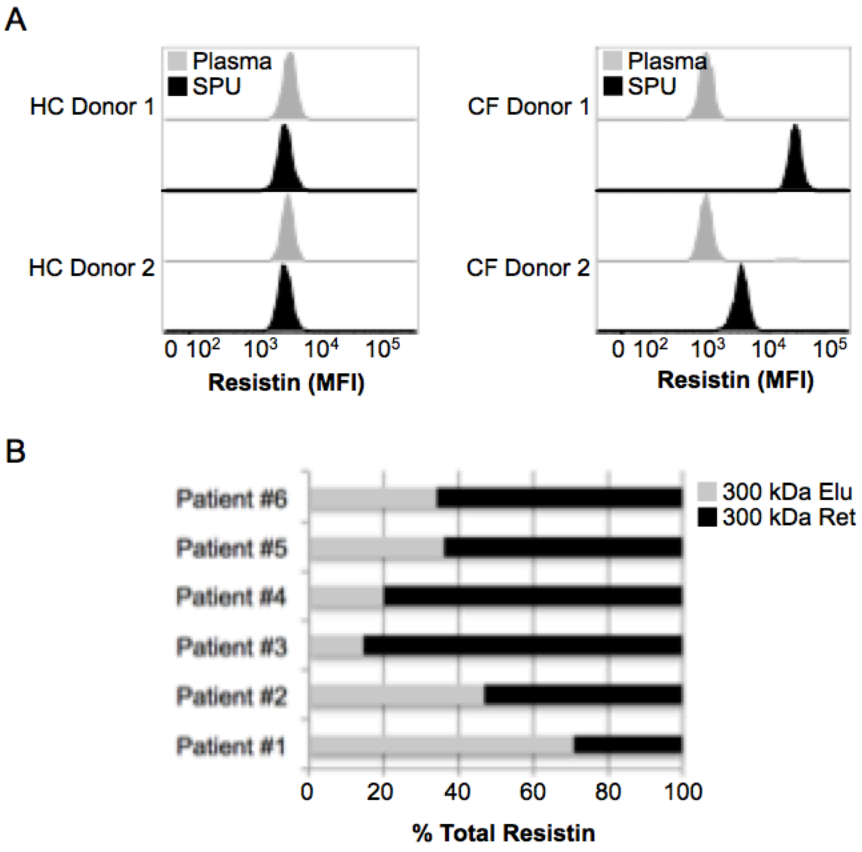

Figure 4.8. Resistin is expressed on extracellular vesicles isolated from CF sputum. **(A)** EVs were isolated from the plasma and sputum of HC subjects and CF patients, and characterized for surface expression of resistin using flow cytometry, shown here in representative histograms of median fluorescent intensities (MFI). **(B)** CF sputum was fractionated using a size exclusion column to assess the compartmentalization of resistin, and assessed by ELISA for fractions lower **(grey)** and higher **(black)** than 300 kDa, represented as percent of total resistin levels in the sample (sum equal to 100).

Parts of this work have been prepared for submission as a Brief Communication to Thorax

PART 2 : RESISTIN IS AN EARLY MARKER OF AIRWAY DISEASE IN INFANTS WITH CYSTIC FIBROSIS

Osric A. Forrest[1,2], Hamed Horati[3], Luke W. Garratt[4], Camilla Margaroli,[1,2], Milton R. Brown[1,2,], Bob J. Scholte[4], Lokesh Guglani[1,2], Stephen M. Stick[3], Limin Peng[5], Hettie M. Janssens[4], and Rabindra Tirouvanziam[1,2], on behalf of AREST-CF, and IMPEDE-CF

[1]Department of Pediatrics, Emory University School of Medicine, Atlanta, GA, USA; [2]Center for CF & Airways Disease Research, Children's Healthcare of Atlanta, Atlanta, GA, USA; [3]Department of Pediatric Pulmonology, Erasmus University Medical Center / Sophia Children's Hospital, Rotterdam, The Netherlands; [4]Telethon Kids Institute, Perth, Australia; [5]Department of Biostatistics and Bioinformatics, Emory University, Atlanta, GA, USA.

INTRODUCTION

Cystic Fibrosis (CF) is a fatal autosomal disease caused by mutations in the CFTR gene. Lung disease in CF starts early in infancy and features low-grade inflammation and progressive structural damage (233-235). CF lung disease eventually becomes dominated by inflammation featuring polymorphonuclear neutrophils (PMNs). Consistently, neutrophil elastase (NE) originating from the primary granules of PMNs serves as one of the best markers of CF disease severity and lung function decline into adulthood (214, 236). Chronic lung disease in older children and adults with CF is widely studied and relatively well understood, while the description of disease manifestations and mechanisms in children with CF remains incomplete (233). Recent studies focusing on CF infants in the first year of life have improved our understanding of early disease processes (237), notably by uncovering signs of inflammation prior to bacterial colonization, with detectable NE in the airway fluid of infants as young as 3 months of age (214). This pioneering work has emphasized the need to reach a better understanding of the early signs of lung disease in children that may coincide with structural lung function damage, and precede both chronic bacterial infection and full-blown inflammation.

One potential early sign of inflammation in CF is the extracellular presence and potential accumulation of resistin. Resistin is an adipokine and member of the resistin-like molecule (RELM) family of proteins that are often elevated in inflammatory diseases (204, 238). Resistin was originally identified as a mediator of insulin resistance in mice, but in humans it is primarily secreted by PMNs and other myeloid cells. and modulates inflammatory signaling in part through binding to toll-like receptor 4 (TLR4) the lipopolysaccharide (LPS) receptor (206, 222, 224). In adults with CF, resistin is elevated in

both the plasma and sputum and correlates negatively with lung function and positively with IL-8, NE, and PMN count (Forrest et al., J Cyst Fibros, 2018, accepted).

In this study, we explore the role of resistin in early disease by tracking resistin levels in broncheoalveolar lavage fluid (BALF) and plasma of CF children, while structural lung damage was measured in parallel using chest computed tomography (CT) scans combined with the sensitive PRAGMA-CF scoring method (237). Our study includes two distinct cohorts of CF children, ranging in age from 3-24 months, and 12 -88 months, respectively. We found that resistin was detectable in plasma and sputum of all CF children, even in those in whom NE was not detectable using conventional methods. BALF resistin levels correlated negatively with early structural damage, and positively with the percentage of PMNs in BALF. These data establish resistin as a marker of early lung disease, with the potential to improve our ability to monitor lung disease progression in children with CF.

MATERIALS AND METHODS

Human subjects. For this study, we utilized plasma and BALF samples from two CF cohorts and 1 disease control cohort enrolled at three institutions. All patients were included after informed parental consent under clinical protocols approved by our respective institutional IRBs. Demographic information on all three cohorts are described in detail in **(Table 4.8).** CF cohort 1 included CF patients from the Sophia Children's Hospital (Rotterdam, The Netherlands) ranging from 12-88 months in age. Cohort 2 included CF patients from the AREST CF program at the Princess Margaret Hospital for Children (Perth, Australia) and consists of patients ranging from 3-24 months in age. Cohort 3 includes disease control subjects from the Aerodigestive Clinic at Children's Healthcare of Atlanta (Atlanta, USA), from whom BALF and blood samples were collected during bronchoscopies conducted according to clinical indications for upper airway disorders. Cell counts and microbial cultures were performed by clinical laboratories at the respective clinical research sites.

PRAGMA-CF Scoring. Perth-Rotterdam Annotated Grid Morphometric Analysis for Cystic Fibrosis (PRAGMA-CF) scores were calculated on free-breathing chest CF scans (CF cohort 1) or volumetric chest CT scans conducted under general anesthesia (CF cohort 2), including total disease (Dis%), bronchiectasis (Bx%) and air trapping (TA%), as described previously (237).

Sample collection and processing. Blood was collected by venipuncture in EDTA tubes, and the cells and plasma isolated as previously described (139). Bronchoscopies with BALs were performed in the right middle lobe where three 1 mL/kg volumes of sterile saline were

instilled and recovered. The first fraction was used for microbial culture analysis, and the second and third fractions were combined and used for leukocyte counts by cytospin. The remainder of the combined 2 and 3 fractions was further processed with the addition of EDTA (2.5 mM), after which the cells where dissociated by passing through a 18-gauge needle, followed by sequential centrifugation at 800 g and 3,000 g for 10 min at 4 ºC. Resulting BALF supernatant was stored at -80 °C for resistin ELISA and NE activity assay.

Resistin quantification. Resistin levels were measured in BALF and plasma using a commercial ELISA kit (R&D Systems), according to the manufacturer's protocol.

IL-8 and NE activity assays. IL-8 levels were measured in BALF using an enzyme-linked immunosorbent assay (BD Opt EIA, BD Biosciences). NE activity was measured using a conventional chromogenic substrate assays previously described here (11).

Statistical Analyses. Data were analyzed using JMP13 (SAS Institute) using non-parametric statistics including the Wilcoxon rank sum (for between-group analysis) and signed-rank (for within-group analysis) tests, or the Spearman test (for correlations), as indicated.

RESULTS

Resistin is detectable in early CF disease and tracks with structural damage. In CF cohort 1 (ranging from 12-88 months of age), resistin was detectable in plasma and BALF of all patients **(Fig. 4.9A)**. When we binned patients into three categories based on age (averages of 12, 36 and 60 months, respectively), we observed that BALF resistin was increasingly elevated compared to plasma resistin as age increased **(Fig. 4.9A**). We next explored the relationship between resistin levels in the BALF with measures of structural lung damage using the PRAGMA-CF scoring system, and observed positive correlations between BALF resistin and total disease, trapped air, and bronchiectasis scores in CF cohort 1 **(Fig. 4.9B-D).**

Resistin correlates with PMN burden and extracellular NE activity in CF airways. We next sought to assess how resistin tracked with established markers of lung disease in CF cohort 1. We observed that resistin levels correlated positively with NE activity and the percentage of PMNs in the BALF **(Fig. 4.10A-B).** Conversely, we observed that resistin levels correlated negatively with the percentage of macrophages in BALF **(Fig. 4.10C).**

Resistin is detectable before NE activity in early CF airway disease. Next, we analyzed samples from a younger cohort of CF children (CF cohort 2, ranging from 3-24 months of age) to investigate the relationship between resistin and structural lung damage at an even earlier stage. We observed that BALF resistin levels were measurable in all patients within this younger CF cohort, although it was not significantly different from those measured in an age-matched disease control cohort with respiratory disorders other than CF **(Fig. 4.11A)**. Structural lung damage measured by PRAGMA-CF scoring was absent to minimal in

CF cohort 2, and did not correlate with BALF resistin levels. Consistent with the early stage of disease in CF cohort 2, NE activity was measurable in BALF of only some patients, while others had non-detectable levels. In those patients with measurable NE activity, BALF resistin levels and NE activity correlated positively **(Fig. 4.11B)**. Additionally, BALF resistin levels were higher in patients with measurable NE activity compared to those in whom it was not measurable **(Fig. 11C).** Finally, when we assessed how BALF resistin levels varied based on infection status, we observed a non-significant trend for elevated levels in those patients with detectable lung infections **(Fig. 4.11D).**

DISCUSSION

This study is the first to explore the relationship between resistin, an otherwise well-established immunometabolic mediator, and early CF airway disease. Our findings establish resistin as an early marker of CF early disease in two cohorts of infants and young children with CF. In CF cohort 1 (12-88 months of age) resistin was detectable in all patients, in both plasma and BALF. BALF resistin levels correlated negatively with BALF macrophage burden, and positively with BALF PMN burden, NE activity, and most importantly, structural lung damage. In CF cohort 2 (3-24 months of age), we were again able to detect resistin in all patients. Although BALF resistin levels did not correlatee with structural lung damage, which was minimal in this cohort, they were again positively correlated with NE activity when detectable, and trended towards elevated levels in patients with detectable lung infection.

Previous studies by our group (Forrest et al., J Cyst Fibros, 2018, accepted) and others have established resistin as a marker of disease severity in adult cohorts of CF and asthma (6, 39), and also in various chronic inflammatory diseases affecting organs other than the lungs (4). Like NE, resistin is compartmentalized in the primary granules of PMNs. Our findings that BALF resistin levels are elevated in CF infants as early as 3 months of age are consistent with previously published work showing that in CF disease the presence of PMN-driven inflammation occurs early, and in some cases in the absence of concomitant infection (11). Our further findings that BALF resistin levels in CF children increase as patients age, and display more pronounced inflammation and structural lung damage based on the sensitive PRAGMA-CF scoring system further establish resistin as a relevant marker of early CF airway disease. The fact that resistin is readily measurable in the BALF of young CF children for whom NE activity remains undetectable emphasizes its potential as a biomarker

for early disease monitoring. Further studies are needed to establish the relevance of BALF resistin in the context of therapeutic interventions targeted at CF airway disease in infants and children.

Resistin is known to signal primarily through its binding to TLR4 (receptor for the gram-negative surface molecule LPS), which makes it all the more interesting that we are able to detect it in BALF before we can measure detectable lung infection with gram-negative (or gram-positive) bacteria. Based on this observation, we could speculate that resistin may act as a host-derived damage signal to induce the TLR4 pathway in epithelial cells or recruited PMNs and initiate a cascade of pro-inflammatory signaling in the absence of infection, consistent with the recently proposed "sterile inflammation" paradigm of early CF airway disease. Of note, recent data gathered in the context of sepsis suggest that resistin may compete with LPS to block its ability to signal through TLR4 (24, 26). Therefore, resistin in the context of infection by gram-negative bacteria may hamper normal host immunity, leading to a maladaptive response that is believed by some to underlie chronic infection in CF (40). Further studies are needed to determine the precise onset of resistin accumulation in CF airways (prior to 3 months of age), and whether it plays a pro- or anti-inflammatory role therein, depending on the absence or presence of concomitant infection. Studies looking at BALF resistin levels in young CF children treated with anti-infective or anti-inflammatory agents, as well as CFTR modulators, are now warranted.

ACKNOWLEDGMENTS

We thank all children and parents willing to enroll in the study cohorts in Perth, Rotterdam, and Atlanta. We also thank the Emory Children's Center for 5 Pediatrics Research flow cytometry core for their cooperation. We also thank L. Peng for access to instrumentation and helpful discussions, as well as A. Portelli, A. Taurone, L. Silva, L. Berry, C. Mok, and Drs. A. Mohandas and T. Rosenow for help with data collection.

FIGURES

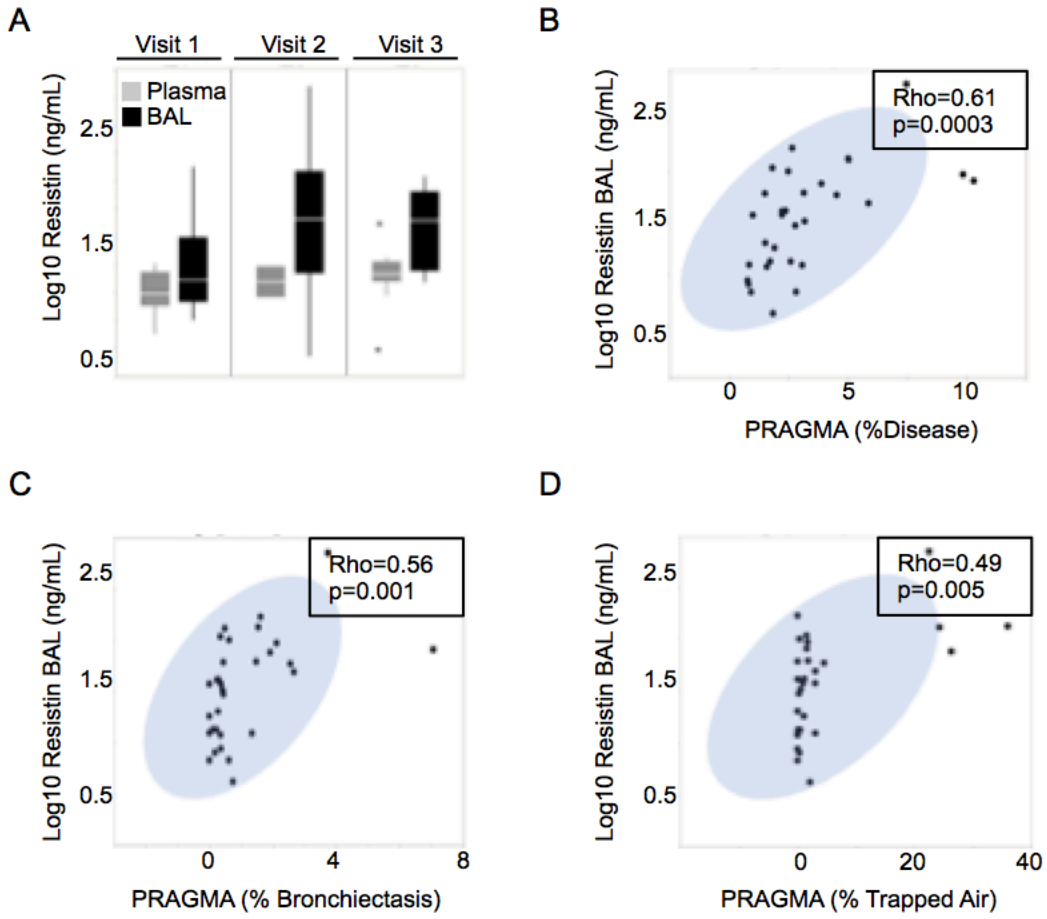

Figure 4.9. Resistin is detectable in early CF disease and correlates with structural lung damage. Resistin levels were measured in plasma **(grey)** and BALF **(black)** of CF children in cohort 1 presented here as three distinct categories stratified by age **(A)**. BALF resistin levels were correlated with structural lung damage measured by PRAGMA-CF scoring, represented here as percent total disease **(B)**, bronchiectasis **(C)**, and trapped air **(D)**, using the Spearman tests (N=40, * indicates $p<0.05$).

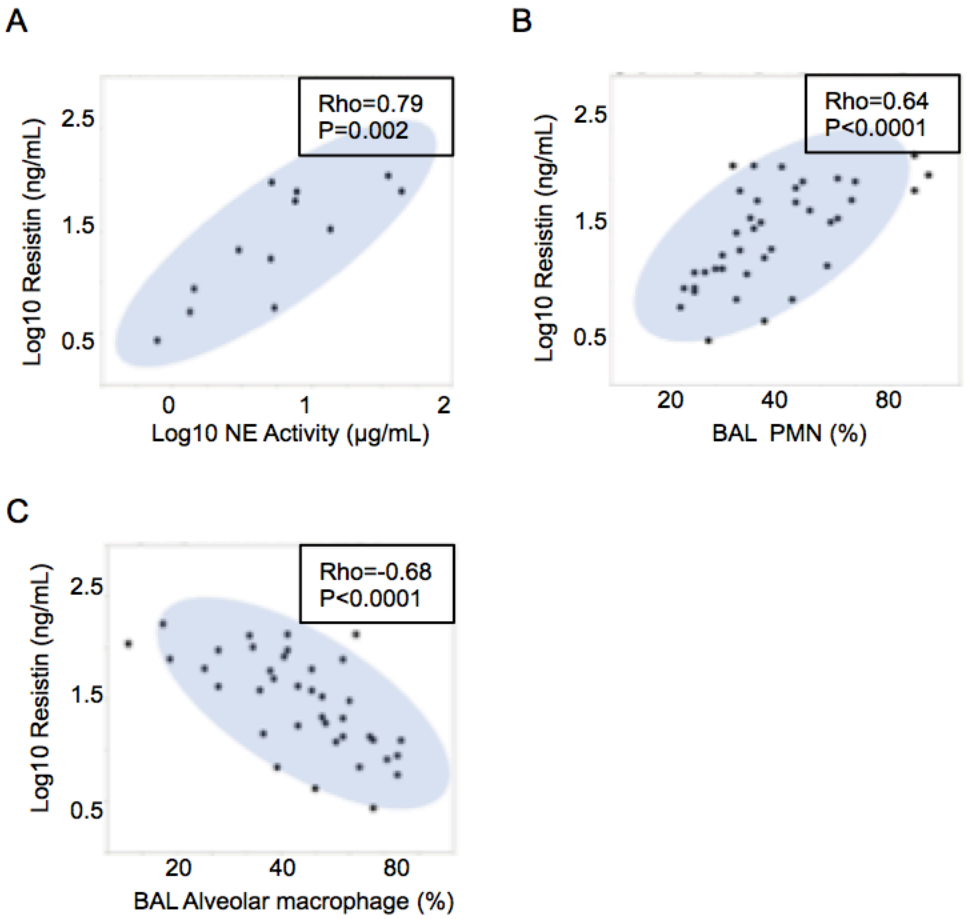

Figure 4.10. BALF resistin levels correlate positively with NE activity and PMN burden, and negatively with macrophage burden. BAL resistin levels for cohort 1 were correlated with NE activity **(A)**, percent PMN **(B)**, and percent macrophage **(C)** using the Spearman test (N=12 for **A**; N=40 for **B** and **C**, * indicates $p<0.05$).

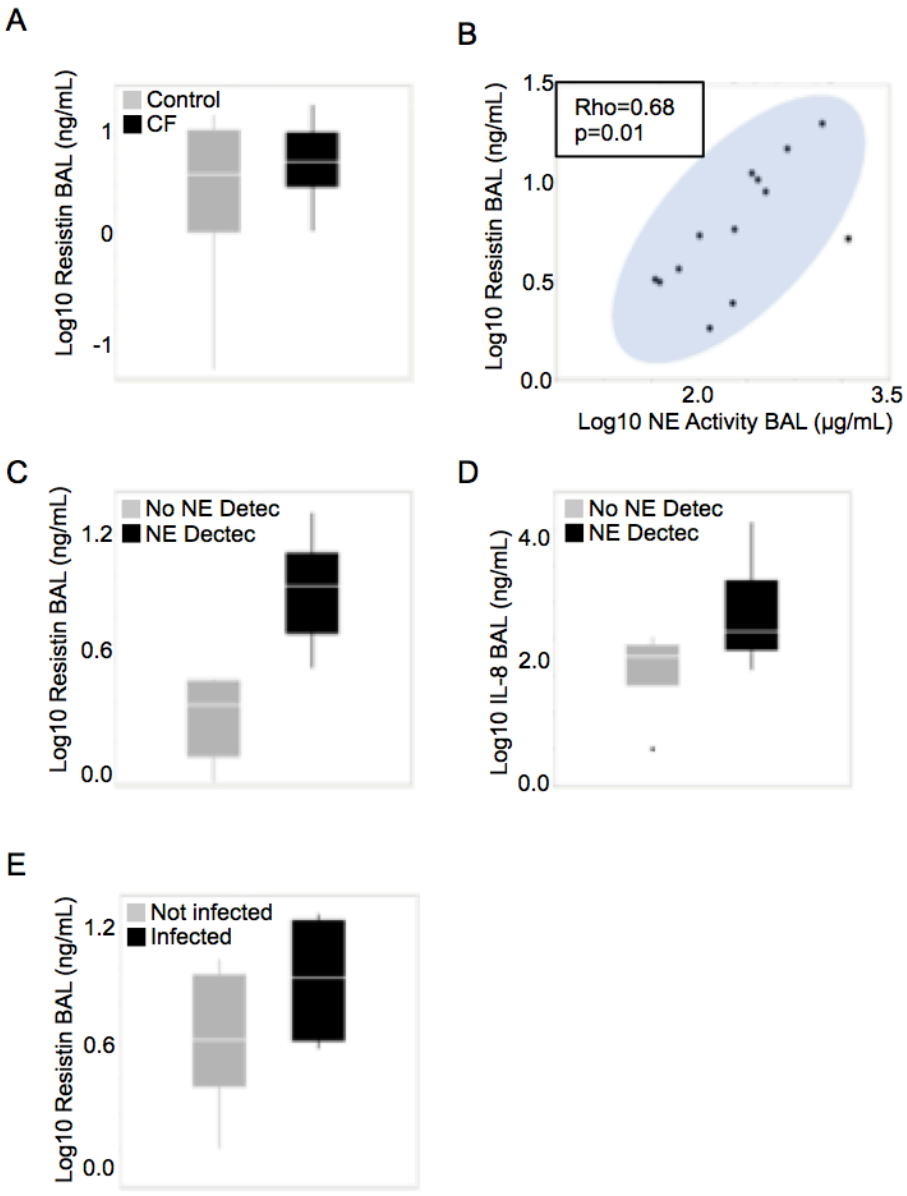

Figure 4.11. Resistin is detectable in BALF of CF children before NE. Resistin levels were measured in the BALF of CF cohort 2, and in an age-matched non-CF disease control cohort **(A)**. BALF resistin levels and NE activity in CF cohort 2 were correlated using the Spearman test **(B)**. Patients in CF cohort 1 with (N=13, black) and without (N=6, grey) detectable NE activity were compared for BALF resistin **(C)** and IL-8 **(D)** levels. BALF resistin levels were compared between patients in cohort 1 with (N=7, black) and without (N=12, grey) detectable lung infections **(E)**.

REFERENCES

1. Steppan CM, Bailey ST, Bhat S, Brown EJ, Banerjee RR, Wright CM, Patel HR, Ahima RS, Lazar MA. The hormone resistin links obesity to diabetes. *Nature* 2001; 409: 307-312.

2. Fehmann HC, Heyn J. Plasma resistin levels in patients with type 1 and type 2 diabetes mellitus and in healthy controls. *Horm Metab Res* 2002; 34: 671-673.

3. Adeghate E. An update on the biology and physiology of resistin. *Cell Mol Life Sci* 2004; 61: 2485-2496.

4. Filkova M, Senolt L, Vencovsky J. The role of resistin in inflammatory myopathies. *Curr Rheumatol Rep* 2013; 15: 336.

5. Sunden-Cullberg J, Nystrom T, Lee ML, Mullins GE, Tokics L, Andersson J, Norrby-Teglund A, Treutiger CJ. Pronounced elevation of resistin correlates with severity of disease in severe sepsis and septic shock. *Crit Care Med* 2007; 35: 1536-1542.

6. Ballantyne D, Scott H, MacDonald-Wicks L, Gibson PG, Wood LG. Resistin is a predictor of asthma risk and resistin:adiponectin ratio is a negative predictor of lung function in asthma. *Clin Exp Allergy* 2016; 46: 1056-1065.

7. Benomar Y, Amine H, Crepin D, Al Rifai S, Riffault L, Gertler A, Taouis M. Central Resistin/TLR4 Impairs Adiponectin Signaling, Contributing to Insulin and FGF21 Resistance. *Diabetes* 2016; 65: 913-926.

8. Bokarewa M, Nagaev I, Dahlberg L, Smith U, Tarkowski A. Resistin, an adipokine with potent proinflammatory properties. *J Immunol* 2005; 174: 5789-5795.

9. Lee S, Lee HC, Kwon YW, Lee SE, Cho Y, Kim J, Lee S, Kim JY, Lee J, Yang HM, Mook-Jung I, Nam KY, Chung J, Lazar MA, Kim HS. Adenylyl cyclase-associated

protein 1 is a receptor for human resistin and mediates inflammatory actions of human monocytes. *Cell Metab* 2014; 19: 484-497.

10. Daquinag AC, Zhang Y, Amaya-Manzanares F, Simmons PJ, Kolonin MG. An isoform of decorin is a resistin receptor on the surface of adipose progenitor cells. *Cell Stem Cell* 2011; 9: 74-86.
11. Sly PD, Gangell CL, Chen L, Ware RS, Ranganathan S, Mott LS, Murray CP, Stick SM, Investigators AC. Risk factors for bronchiectasis in children with cystic fibrosis. *N Engl J Med* 2013; 368: 1963-1970.
12. Cantin AM, Hartl D, Konstan MW, Chmiel JF. Inflammation in cystic fibrosis lung disease: Pathogenesis and therapy. *J Cyst Fibros* 2015; 14: 419-430.
13. Sly PD, Wainwright CE. Diagnosis and early life risk factors for bronchiectasis in cystic fibrosis: a review. *Expert Rev Respir Med* 2016; 10: 1003-1010.
14. Eickmeier O, Huebner M, Herrmann E, Zissler U, Rosewich M, Baer PC, Buhl R, Schmitt-Grohe S, Zielen S, Schubert R. Sputum biomarker profiles in cystic fibrosis (CF) and chronic obstructive pulmonary disease (COPD) and association between pulmonary function. *Cytokine* 2010; 50: 152-157.
15. Muhlebach MS, Clancy JP, Heltshe SL, Ziady A, Kelley T, Accurso F, Pilewski J, Mayer-Hamblett N, Joseloff E, Sagel SD. Biomarkers for cystic fibrosis drug development. *J Cyst Fibros* 2016; 15: 714-723.
16. Laval J, Touhami J, Herzenberg LA, Conrad C, Taylor N, Battini JL, Sitbon M, Tirouvanziam R. Metabolic adaptation of neutrophils in cystic fibrosis airways involves distinct shifts in nutrient transporter expression. *J Immunol* 2013; 190: 6043-6050.

17. Makam M, Diaz D, Laval J, Gernez Y, Conrad CK, Dunn CE, Davies ZA, Moss RB, Herzenberg LA, Herzenberg LA, Tirouvanziam R. Activation of critical, host-induced, metabolic and stress pathways marks neutrophil entry into cystic fibrosis lungs. *Proc Natl Acad Sci U S A* 2009; 106: 5779-5783.

18. Mackarel AJ, Russell KJ, Ryan CM, Hislip SJ, Rendall JC, FitzGerald MX, O'Connor CM. CD18 dependency of transendothelial neutrophil migration differs during acute pulmonary inflammation. *J Immunol* 2001; 167: 2839-2846.

19. Sil P, Yoo DG, Floyd M, Gingerich A, Rada B. High Throughput Measurement of Extracellular DNA Release and Quantitative NET Formation in Human Neutrophils In Vitro. *J Vis Exp* 2016.

20. Al Mutairi SS, Mojiminiyi OA, Shihab-Eldeen A, Al Rammah T, Abdella N. Putative roles of circulating resistin in patients with asthma, COPD and cigarette smokers. *Dis Markers* 2011; 31: 1-7.

21. Bostrom EA, Tarkowski A, Bokarewa M. Resistin is stored in neutrophil granules being released upon challenge with inflammatory stimuli. *Biochim Biophys Acta* 2009; 1793: 1894-1900.

22. Kunnari AM, Savolainen ER, Ukkola OH, Kesaniemi YA, Jokela MA. The expression of human resistin in different leucocyte lineages is modulated by LPS and TNFalpha. *Regul Pept* 2009; 157: 57-63.

23. Jiang S, Park DW, Tadie JM, Gregoire M, Deshane J, Pittet JF, Abraham E, Zmijewski JW. Human resistin promotes neutrophil proinflammatory activation and neutrophil extracellular trap formation and increases severity of acute lung injury. *J Immunol* 2014; 192: 4795-4803.

24. Cohen G, Ilic D, Raupachova J, Horl WH. Resistin inhibits essential functions of polymorphonuclear leukocytes. *J Immunol* 2008; 181: 3761-3768.

25. Chao WC, Yen CL, Wu YH, Chen SY, Hsieh CY, Chang TC, Ou HY, Shieh CC. Increased resistin may suppress reactive oxygen species production and inflammasome activation in type 2 diabetic patients with pulmonary tuberculosis infection. *Microbes Infect* 2015; 17: 195-204.

26. Jang JC, Li J, Gambini L, Batugedara HM, Sati S, Lazar MA, Fan L, Pellecchia M, Nair MG. Human resistin protects against endotoxic shock by blocking LPS-TLR4 interaction. *Proc Natl Acad Sci U S A* 2017; 114: E10399-E10408.

27. Lewis C, Blackman SM, Nelson A, Oberdorfer E, Wells D, Dunitz J, Thomas W, Moran A. Diabetes-related mortality in adults with cystic fibrosis. Role of genotype and sex. *Am J Respir Crit Care Med* 2015; 191: 194-200.

28. Kelly A, Moran A. Update on cystic fibrosis-related diabetes. *J Cyst Fibros* 2013; 12: 318-331.

29. Onuma H, Tabara Y, Kawamura R, Ohashi J, Nishida W, Takata Y, Ochi M, Nishimiya T, Kawamoto R, Kohara K, Miki T, Osawa H. Plasma resistin is associated with single nucleotide polymorphisms of a possible resistin receptor, the decorin gene, in the general Japanese population. *Diabetes* 2013; 62: 649-652.

30. Stevens DA, Moss RB, Kurup VP, Knutsen AP, Greenberger P, Judson MA, Denning DW, Crameri R, Brody AS, Light M, Skov M, Maish W, Mastella G, Participants in the Cystic Fibrosis Foundation Consensus C. Allergic bronchopulmonary aspergillosis in cystic fibrosis--state of the art: Cystic Fibrosis Foundation Consensus Conference. *Clin Infect Dis* 2003; 37 Suppl 3: S225-264.

31. Kraemer R, Delosea N, Ballinari P, Gallati S, Crameri R. Effect of allergic bronchopulmonary aspergillosis on lung function in children with cystic fibrosis. *Am J Respir Crit Care Med* 2006; 174: 1211-1220.

32. Grasemann H, Ratjen F. Early lung disease in cystic fibrosis. *Lancet Respir Med* 2013; 1: 148-157.

33. Belessis Y, Dixon B, Hawkins G, Pereira J, Peat J, MacDonald R, Field P, Numa A, Morton J, Lui K, Jaffe A. Early cystic fibrosis lung disease detected by bronchoalveolar lavage and lung clearance index. *Am J Respir Crit Care Med* 2012; 185: 862-873.

34. VanDevanter DR, Kahle JS, O'Sullivan AK, Sikirica S, Hodgkins PS. Cystic fibrosis in young children: A review of disease manifestation, progression, and response to early treatment. *J Cyst Fibros* 2016; 15: 147-157.

35. Birrer P, McElvaney NG, Rudeberg A, Sommer CW, Liechti-Gallati S, Kraemer R, Hubbard R, Crystal RG. Protease-antiprotease imbalance in the lungs of children with cystic fibrosis. *Am J Respir Crit Care Med* 1994; 150: 207-213.

36. Rosenow T, Oudraad MC, Murray CP, Turkovic L, Kuo W, de Bruijne M, Ranganathan SC, Tiddens HA, Stick SM, Australian Respiratory Early Surveillance Team for Cystic F. PRAGMA-CF. A Quantitative Structural Lung Disease Computed Tomography Outcome in Young Children with Cystic Fibrosis. *Am J Respir Crit Care Med* 2015; 191: 1158-1165.

37. Al Hannan F, Culligan KG. Human resistin and the RELM of Inflammation in diabesity. *Diabetol Metab Syndr* 2015; 7: 54.

38. Tirouvanziam R, Gernez Y, Conrad CK, Moss RB, Schrijver I, Dunn CE, Davies ZA, Herzenberg LA, Herzenberg LA. Profound functional and signaling changes in

viable inflammatory neutrophils homing to cystic fibrosis airways. *Proc Natl Acad Sci U S A* 2008; 105: 4335-4339.

39. Leivo-Korpela S, Lehtimaki L, Vuolteenaho K, Nieminen R, Kankaanranta H, Saarelainen S, Moilanen E. Adipokine resistin predicts anti-inflammatory effect of glucocorticoids in asthma. *J Inflamm (Lond)* 2011; 8: 12.

40. Cohen TS, Prince A. Cystic fibrosis: a mucosal immunodeficiency syndrome. *Nat Med* 2012; 18: 509-519.

Chapter 5

Summary and Future Directions

PMN adaptation and conditioning in the CF airways. Cystic fibrosis (CF) is a fatal airway disease characterized by abnormal bacterial clearance and inflammation by polymorphonuclear neutrophils (PMNs) from blood. There have been several accounts of intrinsic PMN defects in CF airway disease. CF PMNs have been shown to spontaneously produce higher levels of ROS (1), which function to not only to mediate lung damage, but further enhance recruitment of blood PMNs. Not only do CF PMNs have increased activation and degranulation, they also migrate at an increased rate to IL-8 (2). The extreme bacterial load in CF airways coupled with excessive release of proteases by PMNs has been shown to diminish the efficiency of PMN phagocytosis (3, 4). Prior work by our group has led to a change in paradigm, based on the observation that a large subset of live PMNs exist in the CF airway lumen *in vivo* that display high surface CD63 reflecting hyperactive exocytosis of NE-containing primary granules (5, 6). These findings established that not all PMNs die rapidly upon recruitment to the CF airway lumen as commonly thought. Instead, a large fraction of these cells undergoes a pathological conditioning process leading to high metabolic activity, loss of phagocytic receptors along with their hyperexocytic phenotype. Highlighting the clinical importance of this conditioning process of PMN in CF airways is the fact that NE activity in CF airway fluid is a strong predictor of lung function.

In CF airways, live PMNs display robust pro-survival signaling with activation of the mechanistic target of rapamycin (mTOR) pathway, a key anabolic signaling cascade (7) We also demonstrated previously that CF airway PMNs adapt to the metabolite-rich conditions in the fluid by increasing metabolite transporter expression and glucose uptake (8). These prior findings support the hypothesis that CF airway fluid induces PMN migration into the airway lumen and their dysfunction therein, and that specific drugs may be used to modulate these processes.

As a potential cause of PMN dysfunction in CF, previous studies have shown that CFTR is localized to secretory vesicles in non-CF subjects and participates to phagosome acidification and microbicidal activities, and that in CF patients, CFTR dysfunction results in impaired intracellular killing (9). However, such a pervasive intrinsic defect in PMN killing should cause recurrent and systemic infection in CF, as observed in other primary immunodeficiencies, which is not the case. In CF, the bactericidal dysfunction is localized to, and apparently caused by conditions inherent to the lung micro-environment (10). Abnormal PMN function in CF airways can account for many of the anomalies observed in the disease. For example, excessive HNE release can increase epithelial synthesis and secretion of IL-8 (perpetuating inflammation), reduced ciliary beat frequency (causing mucus stasis), and physical damage (11).

In a recent breakthrough described in this thesis **(Chapter 2)**, our group was able to mimic the pathological conditioning process as it impacts PMNs recruited to CF airways *in vivo*, using a novel airway epithelium /PMN transmigration model. In this model, airway supernatant (ASN) from CF patients added on top of the epithelium induces PMN migration and subsequent pathological conditioning. Remarkably, we found that exposure to CF ASN in our model triggers migration and conditioning of naive PMNs not only from humans (either CF or healthy), but also from mice. This model is poised to become a useful tool to study mechanisms of CF airway inflammation and infection, and also to develop new, targeted immunomodulatory drugs.

PMN antimicrobial function in CF airways. One of the vexing paradoxes of CF airway disease is that chronic bacterial infection is concomitant with the continued influx of PMNs.

Airway PMNs and bacteria may co-exist in CF airways in part due to potential *innate* defects of PMNs in CF, but work from our group and others has uncovered defects that are *acquired* upon recruitment to the airways. Proteolytic activity in the airways has been linked to cleavage and disabling of important phagocytic and opsonic receptors such as CXCR1 and C5aR (12, 13). In **Chapter 2**, we confirmed using our *in vitro* model system that PMNs recruited to CF ASN are less effective at killing *P. aeruginosa* compared to PMNs recruited to LTB4. We posit that this dysfunction is in large part due to conditioning by the CF airway milieu, because it affects PMNs from healthy control subjects and wild-type mice used in the system. We also went on to show that metformin treatment was unable to restore normal bactericidal capacity of PMNs recruited to CF ASN. There are many outstanding questions surrounding the mechanism driving this defective killing. For example, we do not know whether or not both intracellular and extracellular pathways of microbial killing are impaired in CF airway PMNs, and whether or not this killing defect is specific to certain gram-negative microbes such as *P. aeruginosa*. Moreover, it will be interesting to explore the relationship between excessive granule exocytosis in PMNs as observed in CF airways *in vivo* and in our *in vitro* model, and the ability of such PMNs to fuse granules with the phagolysosome in order to maintain optimal intracellular killing capacity. This is especially important considering the well-documented ability of *P. aeruginosa* and other microbes to evade extracellular mechanisms of bacterial killing by ROS and antimicrobial peptides in CF and other diseases (14-17).

Inflammasome activation driving airway inflammation in CF. The inflammasome is a key component of the innate immune response to pathogens. It is a group of multimeric protein complexes triggered by infection and tissue damage (18). Activation of the

inflammasome results in the release of inflammatory cytokines that allow for increased recruitment of immune cells. However, if dysregulated it also serves as a key component of chronic inflammation. In CF, levels of various cytokines and chemokines are increased as disease progresses. Unsurprisingly, extracellular IL-1β, which is dependent upon inflammasome activation, is increased in airway fluid from CF patients with ongoing infection (19, 20). Although macrophages are often thought as the major source of inflammasome-derived mediators, PMNs vastly outnumber them in CF airways. Here, we explored the contribution of the inflammasome in PMNs to CF airway inflammation **(Chapter 3)**.

To begin with, we demonstrated that IL-1β is significantly increased in CF compared to non-CF airways. However, the cellular source of this product of the inflammasome has been somewhat elusive, as the loss of CFTR in the epithelium was not shown to modulate IL-1β production (21). That study also showed that PBMCs derived from CF subjects secrete IL-1β in response to infection by *P. aeruginosa*. *P. aeruginosa* can also activate caspase-1 and induce IL-1β secretion in infected macrophages. On the other hand, PMNs are the dominant leukocyte subset in CF airways, and express key components of the inflammasome, namely ASC, AIM2, and caspase-1 (localized in the cytoplasm and in secretory vesicle and tertiary granule compartments), and they secrete IL-1β when stimulated (22). Here we showed for the first time that in CF airway PMNs intracellular caspase-1 activity is increased, as measured using FLICA, a membrane-permeable fluorescent probe that binds active caspase-1. CF airway PMNs also increase intracellular levels of IL-1β. Similarly, other IL-1 family members IL-1α and IL-18 are also elevated in CF sputum**.**

It has been recently proposed that epithelium-derived IL-1α may act as a early sterile inflammatory signal recruiting PMNs to the airways before infection, potentially promoting

continued recruitment and eventual activation of the inflammasome in PMNs themselves, which in turn would perpetuate further PMN recruitment via IL-1β signaling (23). Of note, both IL-1β and IL-1α bind to and signal through IL-1R1, which we have shown to be elevated on CF airway compared to blood PMNs. From the results presented in **Chapter 3,** it is clear that inflammasome activation both in epithelial cells and PMNs is likely to play a role in the pathogenesis of CF airway inflammation, and may provide an interesting target to delay early PMN recruitment. To this effect, recent work studying the efficacy of recombinant IL-1RA (Anakinra) in CF found that it was able to reduce inflammasome activation (24), which warrants further validation.

Pinocytosis as a potential route of pathological conditioning for CF airway PMNs.

PMNs are recruited to CF airways by various pro-inflammatory stimuli, which are described in details in **Chapter 1**. Having crossed into the airways, PMNs continue to be conditioned by signals present in the airway milieu. As phagocytes, PMNs are adept at sampling and surveying the extracellular space for debris and microorganisms. *Phagocytosis* itself is one particular mechanism by which PMNs and macrophages endocytose such extracellular material. Phagocytosis generally follows the binding of specific receptors on the PMN surface by adaptor molecules (antibodies, complement), leading to the formation of a phagocytic cup, which is a specialized membrane microdomain dedicated to receptor-mediated uptake (25). Another mechanism by which cells take up material is *pinocytosis*, which is particularly efficient for the internalization of soluble material and small particles present in the fluid phase to support cell growth and survival. Pinocytosis is an actin-dependent process that depends on the reorganization and invagination of the plasma membrane to allow for the creation of pinocytic cups, but unlike phagocytosis, it is not receptor mediated

(26). In immune cells such as PMNs, pinocytosis is an important regulator of antigen uptake and processing, but it can also mediate the uptake of bacteria, and in some cases, of viruses (27, 28). Extracellular nutrients that are taken up by pinocytosis can also modulate immune cell function and anabolic metabolism.

In **Chapter 2**, we show for the first time that PMNs recruited to the CF airways increase their pinocytic activity, a process that interestingly is positively correlated with primary granule exocytic activity **(Fig. 2.4)**. Such a functional link between PMN pinocytosis and primary granule exocytosis was suggested in prior work (29), which highlighted the importance of GlyRα2 / transient receptor potential melastatin 2/ p38 MAPK signaling in coordinating these two membrane movements (inward and outward, respectively). Therefore, it is interesting that in CF, which is dominated by excessive elastase release via primary granule exocytosis, PMNs also increase pinocytosis. This process may be important not only to counterbalance exocytosis (by reducing the plasma membrane surface area that is increased by exocytosis), but also as a critical nutrient uptake mechanism to support increased metabolism and lifespan of airway PMNs. As such, pinocytosis may be an interesting pathway to target to decrease PMN exocytosis and their survival in CF airways.

Metabolic adaptation of CF airway PMNs. The observation that CF airway PMNs are alive and actively exocytosing their primary granules has expanded our understanding of the contribution of PMNs to CF airway inflammation. Yet, it is still not understood how these cells are able to meet the robust metabolic demands that go with such a pronounced phenotypic change. To address this question, we explored whether PMN metabolism was altered after their migration and pathological conditioning in CF airways. In PMNs, the main energy-producing pathway is glycolysis. Because very few mitochondria are found in mature

PMNs, mitochondrial respiration accounts for only 5 percent of the glucose consumed by the PMNs, but because of its efficiency it provides nearly half of the ATP generated by these cells. Previous studies from our group sought to investigate the metabolic demands of PMNs in the airways. By direct flow cytometric analysis of CF airway samples, we found that a sizeable fraction of viable PMNs exhibited significant metabolic activity (8), and strong induction of mitogen activated protein kinase, cAMP response element binding (CREB) protein and mTOR signaling pathways (7). Activation of mTOR is of particular interest because it is highly conserved and has been shown to integrate signals from nutrients, energy demands, and inflammatory signals that are abundantly found in CF airways (30). In PMNs, mTOR signaling was previously shown to contribute to NET-mediated bacterial killing, which was reduced in the presence of the mTOR inhibitor rapamycin (31). Additionally, our group showed that PMNs in CF airways had increased expression of the glucose transporter Glut1, and increased uptake of glucose (8).

In order to understand how these cells were altered *in vivo* and to determine which pathways were modulated, we analyzed mRNA from matched FACS-sorted airway and blood PMN fractions from CF patients by microarray. Surprisingly, changes over 2-fold were seen in 10% of the genes in PMNs, which are not traditionally thought to be transcriptionally active. A gene ontology analysis shows that up-regulated mRNAs in viable CF airway PMNs relate to translation elongation, ribosomal formation, and cellular component biogenesis, all processes regulated by metabolism. By contrast, mRNAs related to wound healing, programmed cell death and protein phosphatase activity were shown to be down-regulated (data not shown).

The metabolic activation of CF airway PMNs is linked to the build up of agonists of metabolic signaling in the CF airway fluid, such as amino acids and other nutrients. It is now

increasingly appreciated that in order for an immune cell to unfold new function upon activation, there are increased needs on metabolic pathways to be fulfilled in order to support these new functions (32). Results shown in **Chapter 2** further support the role of metabolism in regulating PMNs function in the context of CF airway disease. We showed that PMNs recruited to CF airway fluid *in vitro* recapitulate the increase in Glut1 expression seen *in vivo*, and that their oxygen consumption and glycolytic rates were also elevated. Metformin, an agonist of the AMPK pathway (which antagonizes mTOR) was able to decrease granule exocytosis *in vitro*, concomitantly with decreased baseline PMN metabolism.

Modeling granulocytic inflammation in CF and other airway diseases. The strength of *the in vitro* transmigration model system highlighted in **Chapter 2** is that it allows for study of the dynamics of the pathological conditioning process affecting PMNs recruited to the CF airway lumen. Transmigration towards CF ASN robustly induced primary granule exocytosis and loss of the phagocytic receptor CD16, just as observed *in vivo* **(Fig. 2.1C-D).** Similarly, the model recapitulated the activation of the inflammasome with a time-dependent increase in intracellular caspase-1 activity and inflammasome signaling, as detailed in **Chapter 3**. These results illustrate the ability of our model to effectively recapitulate known changes seen *in vivo*, and also identify novel pathways that may be at play, which can then be validated by directed analyses of *in vivo* samples (i.e., bedside to bench, and back). Importantly, we observed that pathological conditioning did not occur upon simple incubation of PMNs with CF ASN, or when CF blood PMNs were transmigrated to HC ASN. These results emphasize the critical role of transmigration in the process of PMN pathological conditioning, and identify the CF airway micro-environment as the primary inducer of this process.

In addition to the effects of metformin treatment discussed above, we found that treatment with the NLRP3 inflammasome inhibitor MCC950 was able to reduce caspase-1 activity induced upon PMN transmigration to CF ASN *in vitro***.** Together, these observations show that our model can be used effectively to test drug candidates. Next, we will move to leverage this unique *in vitro* model for the testing of drug candidates able to target the pathological PMN phenotypes observed in a broader way. Another novel aspect of the model is the ability to utilize PMNs from different sources. To allow for more mechanistic studies, we tested whether PMNs from mice would act similar to the human PMNs used routinely. Indeed, we observed that murine PMNs recapitulated the phenotype seen both *in vivo* and in our *in vitro* system using human PMNs. This lays the foundation for studies using transgenic and knockout (KO) mice to study the mechanisms that control PMN pathological conditioning, as illustrated by our use of PMNs from caspase-1 KO mice in **Chapter 3**.

Moving forward, we are actively working to develop and microfabricate a medium-throughput version of our *in vitro* model system that will allow us to scale up and test a larger set of candidate drugs for their ability to modulate PMN dysfunction in CF. Another important extension of our approach stems from the observation detailed in **Chapter 2** that our *in vitro* system can be easily modified to accommodate ASN and cells relevant to other airway inflammatory diseases such as COPD and asthma. In those experiments, we showed that ASN from those patients was also able to recruit and condition PMNs *in vitro*. Recent unpublished work in our group utilized this model to study phenotypic changes occurring in eosinophils as well as PMNs, both of contribute to the development of asthma endotypes *in vivo* **(Fig. 5.1)**. Comparative analysis of results obtained in our *in vitro* system with those obtained in the direct analysis of eosinophils isolated from the airway fluid of asthmatics again showed the strong translational potential of this modeling approach **(Fig. 5.2)**.

Targeting pathological conditioning in CF airway PMNs. Our *in vitro* model has allowed us to make significant advances in identifying new pathways at play in PMN dysfunction *in vivo*. However, targeting PMNs *in vivo* is limited by our ability to effectively deliver drugs to these cells as they sit within the lungs of patients. To address this issue, we attempted to leverage a key functional change we observed in CF airway PMNs and described in **Chapter 2**, namely, the induction of a high pinocytic activity that makes them particularly apt at capturing small particles. In addition, we reasoned that CF airways being highly proteolytic, this property could be used to unpack drug payload.

In collaboration with the Roy group at Georgia Tech, we developed microgels that are kept intact by an outer structure of crosslinking NE-cleavable peptide, in which we encapsulated nanoparticles loaded with a drug payload ("nano-in-micro" delivery approach). We tested these nano-in microgels first in our *in vitro* model system, which uses the relevant biological milieu, i.e., CF ASN, as its site for PMN transmigration, and for drug testing. First, using fluorescent polystyrene nanoparticles encapsulated within NE-degradable microgels, we showed that PMNs transmigrated to CF ASN to which these nano-in microgels were added readily took up the nanoparticles and became fluorescent, after the NE-cleavable microgels were degraded, as expected **(Fig. 5.3A)**.

Next, we texted the efficacy of this method for *in vivo* delivery to PMNs in an acute LPS-induced lung injury model in mice. Similarly to our *in vitro* model, we found that PMNs were recruited to airways in this *in vivo* model exocytosed their primary granules, leading to an increase in extracellular NE levels in the BAL **(Fig. 5.3B-E)**. Importantly, we confirmed both degradation of the NE-cleavable microgels and uptake of nanoparticles by inflammatory PMNs in the BAL. Further studies are now needed to validate these proof-of-

concept data, and confirm whether this delivery platform has promise in providing precise targeting of exocytic/pinocytic PMNs in CF using protease-dependent triggers for delivery of drug payload.

Extracellular vesicles in CF airways regulate PMN conditioning. Our work has established a critical role for the airway milieu in conditioning recruited PMNs. However, it is still unclear which components of the fluid drive this altered phenotype of CF airway PMNs. Preliminary work in our group sought to address this question by fractioning the airway fluid, using filters with specific molecular weight restrictions. Using this method, we saw quite strikingly that the higher molecular weight fraction (>300 kDA), which contains EVs and other complexes, alone was able to induce the conditioning of PMNs we have documented in details in **Chapters 2 and 3**. These observation also build on data presented in Chapter 3 that illustrated the role of EVs in CF sputum in perpetuating inflammasome activation in PMNs and airway epithelial cells**.** We also went on to show that PMNs themselves are significant sources of inflammatory EVs *in vitro*.

EVs have been implicated as important pathophysiological mediators in other airway inflammatory diseases such as asthma. In some cases, EVs are anti-inflammatory in nature, as argued in a recent study in which PMNs were shown to produce and transfer EVs containing micro-RNAs to airway epithelial cells, dampening inflammatory signaling and lung injury (33). By contrast, exosomes (a type of EVs) enriched in the lungs of asthma and found to be mostly epithelial in origin were able to mediate the proliferation and migration of macrophages (34). Another study comparing airway exosomes between healthy and asthmatic subjects found that the latter promoted IL-8 release from airway epithelial cells (35). These and other data suggest that airway EVs may play a critical role in conditioning

recruited PMNs, and could serve as biomarkers and potential therapeutic vehicles, and targets, to modulate PMN-driven inflammatory in intractable airway diseases.

Conclusion. Studies presented here highlight the pivotal role that PMNs play in one shaping the lung microenvironment, and are themselves influenced by changes in that microenvironment that emerge in the context of chronic inflammatory airway diseases. Moreover, our studies emphasize the role that functional and metabolic pathways play in shaping adaptations characteristic of pathogenic PMNs. These findings suggest new ways by which we may leverage this new understanding to develop PMN-targeted therapies. Our studies also establish a potentially groundbreaking *in vitro* model system, which, as we showcased, allowed us to gain deeper insight into CF airway inflammation, but also to identify new targets that have the potential to be translated into the clinic. Ultimately, through these studies we have gained new insights into mechanisms by which PMN recruited to the airways orchestrate and dominate the immune response and overall pathogenesis in patients with CF and, potentially in other inflammatory airway diseases.

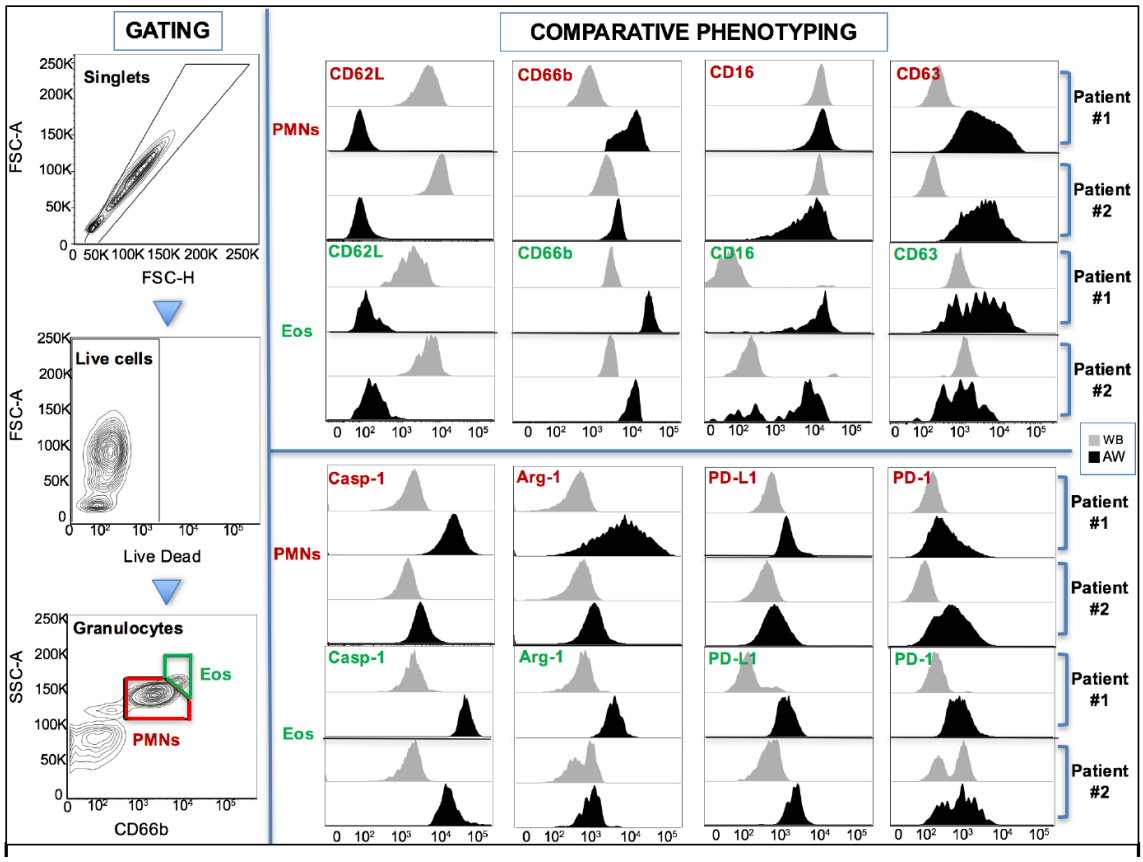

Figure 5.1 Phenotyping of sputum PMNs and Eos in asthma. Sequential gating of single, live, sputum PMNs and Eos is shown on the left (Eos are $SSc^{Hi,}$ $CD66b^{Hi}$, and $Siglec8^{+}$ -not shown). Comparative phenotyping of whole blood (WB, grey), and airway (AW, black) PMNs and Eos shows differential degranulation (e.g., CD62L, CD66b, CD63, CD16) and activation (e.g., intracellular caspase-1 activity, expression of T-cell inhibitory effectors arginase-1 and PD-L1, and of its binding partner, PD-1).

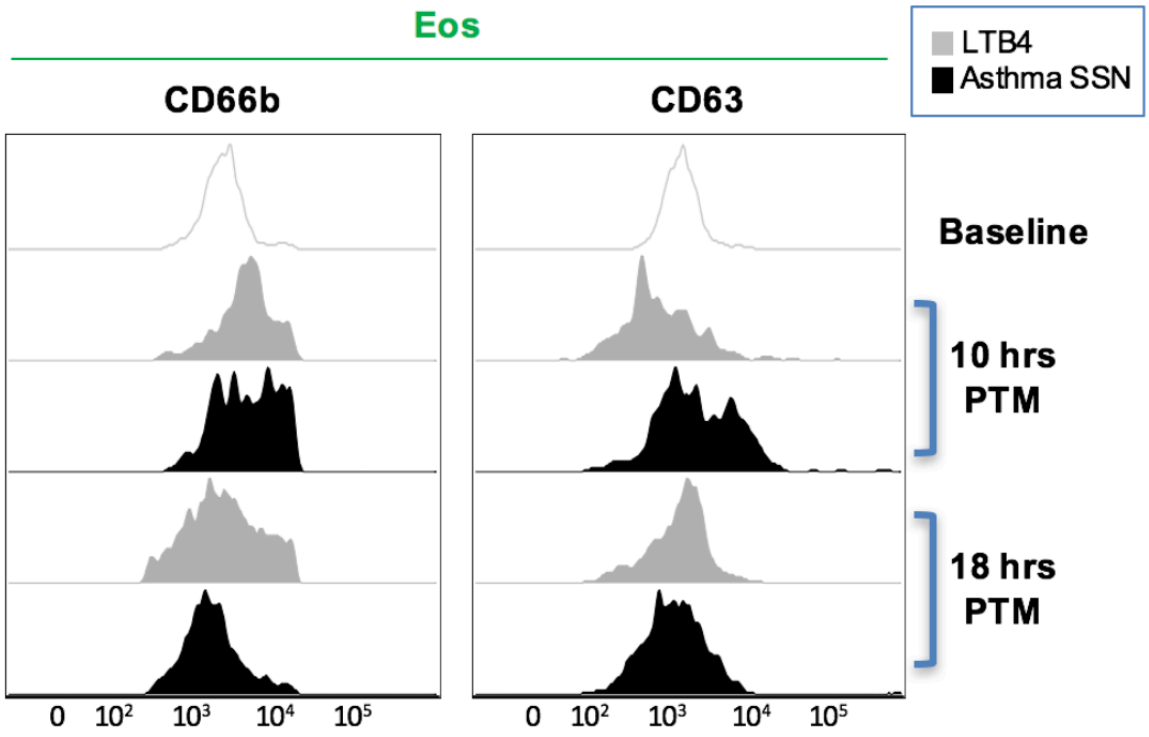

Figure 5.2 Recruitment of eosinophils to asthma SSN in our *in vitro* transmigration model system. Shown are levels of surface CD66b, and CD63, comparing baseline to asthma SSN and LTB4. Eos were harvested after 10 or 18h PTM.

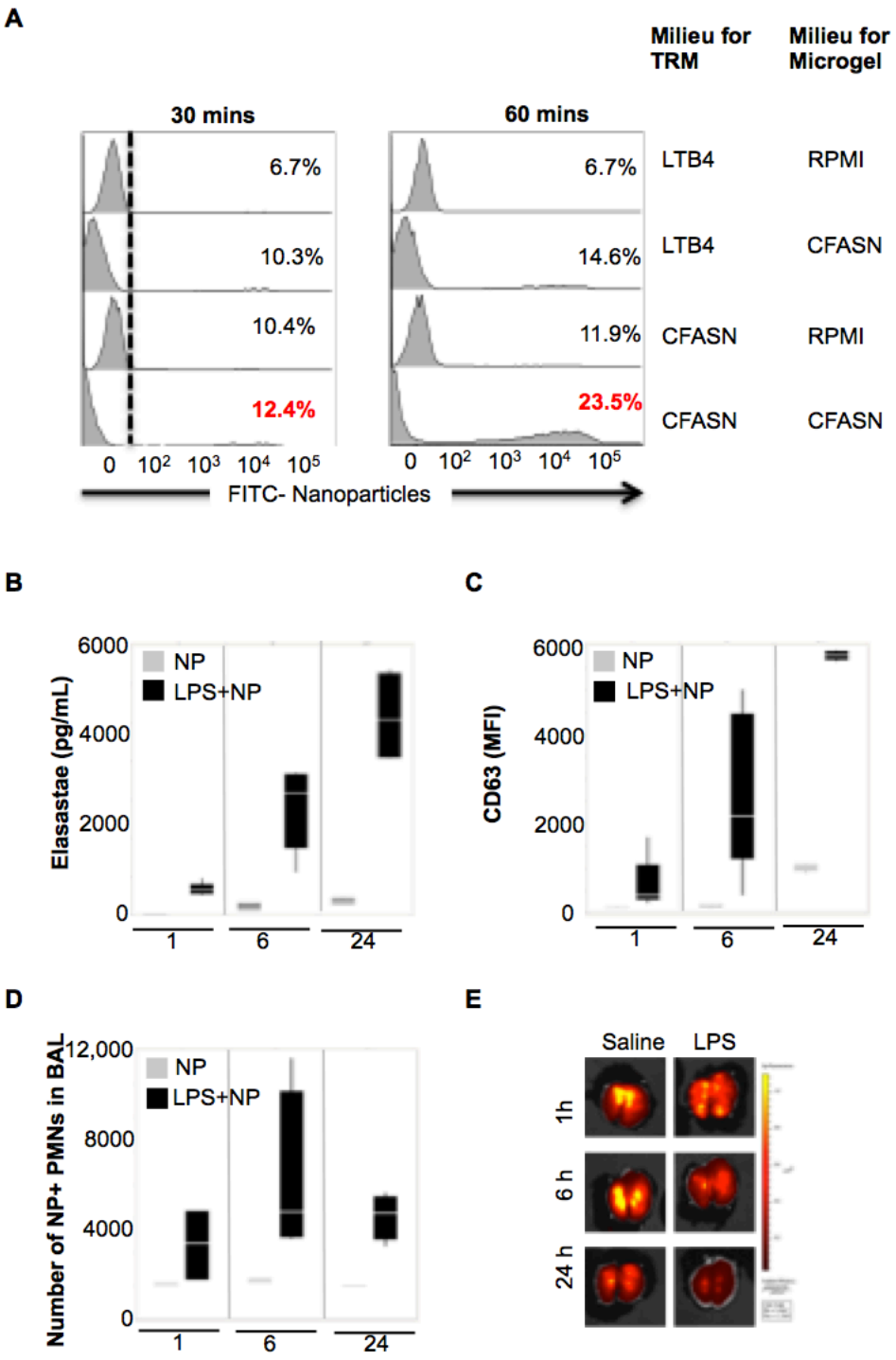

Figure 5.3. Degradation of NE-cleavable microgel, and nanoparticle uptake by PMNs recruited to lungs. A. Maximal uptake is seen with human PMNs transmigrated to

CF ASN (reprogrammed) and incubated with nano-inside-microgels in CF ASN for 60 minutes. **B-C.** The concentration of NE and surface CD63 expression were assessed on live BAL PMNs. **D.** Percent uptake of nanoparticles by mouse BAL PMNs after LPS treatment was assessed by flow cytometry. **E.** Degradation / clearance of microgels in LPS- and saline-treated mice showing a significant difference at 6, but not 1 or 22 hours *in vivo* (N = 5).

REFERENCES

1. Brockbank S, Downey D, Elborn JS, Ennis M. Effect of cystic fibrosis exacerbations on neutrophil function. *Int Immunopharmacol* 2005; 5: 601-608.

2. Brennan S, Cooper D, Sly PD. Directed neutrophil migration to IL-8 is increased in cystic fibrosis: a study of the effect of erythromycin. *Thorax* 2001; 56: 62-64.

3. Singh PK, Schaefer AL, Parsek MR, Moninger TO, Welsh MJ, Greenberg EP. Quorum-sensing signals indicate that cystic fibrosis lungs are infected with bacterial biofilms. *Nature* 2000; 407: 762-764.

4. Morris MR, Doull IJ, Dewitt S, Hallett MB. Reduced iC3b-mediated phagocytotic capacity of pulmonary neutrophils in cystic fibrosis. *Clin Exp Immunol* 2005; 142: 68-75.

5. Tirouvanziam R, Gernez Y, Conrad CK, Moss RB, Schrijver I, Dunn CE, Davies ZA, Herzenberg LA, Herzenberg LA. Profound functional and signaling changes in viable inflammatory neutrophils homing to cystic fibrosis airways. *Proc Natl Acad Sci U S A* 2008; 105: 4335-4339.

6. Margaroli C, Tirouvanziam R. Neutrophil plasticity enables the development of pathological microenvironments: implications for cystic fibrosis airway disease. *Mol Cell Pediatr* 2016; 3: 38.

7. Makam M, Diaz D, Laval J, Gernez Y, Conrad CK, Dunn CE, Davies ZA, Moss RB, Herzenberg LA, Herzenberg LA, Tirouvanziam R. Activation of critical, host-induced, metabolic and stress pathways marks neutrophil entry into cystic fibrosis lungs. *Proc Natl Acad Sci U S A* 2009; 106: 5779-5783.

8. Laval J, Touhami J, Herzenberg LA, Conrad C, Taylor N, Battini JL, Sitbon M, Tirouvanziam R. Metabolic adaptation of neutrophils in cystic fibrosis airways

involves distinct shifts in nutrient transporter expression. *J Immunol* 2013; 190: 6043-6050.

9. Painter RG, Valentine VG, Lanson NA, Jr., Leidal K, Zhang Q, Lombard G, Thompson C, Viswanathan A, Nauseef WM, Wang G, Wang G. CFTR Expression in human neutrophils and the phagolysosomal chlorination defect in cystic fibrosis. *Biochemistry* 2006; 45: 10260-10269.
10. Rieber N, Hector A, Carevic M, Hartl D. Current concepts of immune dysregulation in cystic fibrosis. *Int J Biochem Cell Biol* 2014; 52: 108-112.
11. Nakamura H, Yoshimura K, McElvaney NG, Crystal RG. Neutrophil elastase in respiratory epithelial lining fluid of individuals with cystic fibrosis induces interleukin-8 gene expression in a human bronchial epithelial cell line. *J Clin Invest* 1992; 89: 1478-1484.
12. Hartl D, Latzin P, Hordijk P, Marcos V, Rudolph C, Woischnik M, Krauss-Etschmann S, Koller B, Reinhardt D, Roscher AA, Roos D, Griese M. Cleavage of CXCR1 on neutrophils disables bacterial killing in cystic fibrosis lung disease. *Nat Med* 2007; 13: 1423-1430.
13. van den Berg CW, Tambourgi DV, Clark HW, Hoong SJ, Spiller OB, McGreal EP. Mechanism of neutrophil dysfunction: neutrophil serine proteases cleave and inactivate the C5a receptor. *J Immunol* 2014; 192: 1787-1795.
14. Usher LR, Lawson RA, Geary I, Taylor CJ, Bingle CD, Taylor GW, Whyte MK. Induction of neutrophil apoptosis by the Pseudomonas aeruginosa exotoxin pyocyanin: a potential mechanism of persistent infection. *J Immunol* 2002; 168: 1861-1868.

15. Allen L, Dockrell DH, Pattery T, Lee DG, Cornelis P, Hellewell PG, Whyte MK. Pyocyanin production by Pseudomonas aeruginosa induces neutrophil apoptosis and impairs neutrophil-mediated host defenses in vivo. *J Immunol* 2005; 174: 3643-3649.

16. Vareechon C, Zmina SE, Karmakar M, Pearlman E, Rietsch A. Pseudomonas aeruginosa Effector ExoS Inhibits ROS Production in Human Neutrophils. *Cell Host Microbe* 2017; 21: 611-618 e615.

17. Gellatly SL, Hancock RE. Pseudomonas aeruginosa: new insights into pathogenesis and host defenses. *Pathog Dis* 2013; 67: 159-173.

18. Schroder K, Tschopp J. The inflammasomes. *Cell* 2010; 140: 821-832.

19. Osika E, Cavaillon JM, Chadelat K, Boule M, Fitting C, Tournier G, Clement A. Distinct sputum cytokine profiles in cystic fibrosis and other chronic inflammatory airway disease. *Eur Respir J* 1999; 14: 339-346.

20. Bonfield TL, Panuska JR, Konstan MW, Hilliard KA, Hilliard JB, Ghnaim H, Berger M. Inflammatory cytokines in cystic fibrosis lungs. *Am J Respir Crit Care Med* 1995; 152: 2111-2118.

21. Tang A, Sharma A, Jen R, Hirschfeld AF, Chilvers MA, Lavoie PM, Turvey SE. Inflammasome-mediated IL-1beta production in humans with cystic fibrosis. *PLoS One* 2012; 7: e37689.

22. Bakele M, Joos M, Burdi S, Allgaier N, Poschel S, Fehrenbacher B, Schaller M, Marcos V, Kummerle-Deschner J, Rieber N, Borregaard N, Yazdi A, Hector A, Hartl D. Localization and functionality of the inflammasome in neutrophils. *J Biol Chem* 2014; 289: 5320-5329.

23. Fritzsching B, Zhou-Suckow Z, Trojanek JB, Schubert SC, Schatterny J, Hirtz S, Agrawal R, Muley T, Kahn N, Sticht C, Gunkel N, Welte T, Randell SH, Langer F, Schnabel

P, Herth FJ, Mall MA. Hypoxic epithelial necrosis triggers neutrophilic inflammation via IL-1 receptor signaling in cystic fibrosis lung disease. *Am J Respir Crit Care Med* 2015; 191: 902-913.

24. Iannitti RG, Napolioni V, Oikonomou V, De Luca A, Galosi C, Pariano M, Massi-Benedetti C, Borghi M, Puccetti M, Lucidi V, Colombo C, Fiscarelli E, Lass-Florl C, Majo F, Cariani L, Russo M, Porcaro L, Ricciotti G, Ellemunter H, Ratclif L, De Benedictis FM, Talesa VN, Dinarello CA, van de Veerdonk FL, Romani L. IL-1 receptor antagonist ameliorates inflammasome-dependent inflammation in murine and human cystic fibrosis. *Nat Commun* 2016; 7: 10791.
25. Gordon S. Phagocytosis: An Immunobiologic Process. *Immunity* 2016; 44: 463-475.
26. Miaczynska M, Stenmark H. Mechanisms and functions of endocytosis. *J Cell Biol* 2008; 180: 7-11.
27. Commisso C, Davidson SM, Soydaner-Azeloglu RG, Parker SJ, Kamphorst JJ, Hackett S, Grabocka E, Nofal M, Drebin JA, Thompson CB, Rabinowitz JD, Metallo CM, Vander Heiden MG, Bar-Sagi D. Macropinocytosis of protein is an amino acid supply route in Ras-transformed cells. *Nature* 2013; 497: 633-637.
28. Mercer J, Greber UF. Virus interactions with endocytic pathways in macrophages and dendritic cells. *Trends Microbiol* 2013; 21: 380-388.
29. Hong CW, Kim TK, Ham HY, Nam JS, Kim YH, Zheng H, Pang B, Min TK, Jung JS, Lee SN, Cho HJ, Kim EJ, Hong IH, Kang TC, Lee J, Oh SB, Jung SJ, Kim SJ, Song DK. Lysophosphatidylcholine increases neutrophil bactericidal activity by enhancement of azurophil granule-phagosome fusion via glycine.GlyR alpha 2/TRPM2/p38 MAPK signaling. *J Immunol* 2010; 184: 4401-4413.

30. McInturff AM, Cody MJ, Elliott EA, Glenn JW, Rowley JW, Rondina MT, Yost CC. Mammalian target of rapamycin regulates neutrophil extracellular trap formation via induction of hypoxia-inducible factor 1 alpha. *Blood* 2012; 120: 3118-3125.

31. Itakura A, McCarty OJ. Pivotal role for the mTOR pathway in the formation of neutrophil extracellular traps via regulation of autophagy. *Am J Physiol Cell Physiol* 2013; 305: C348-354.

32. Stienstra R, Netea-Maier RT, Riksen NP, Joosten LAB, Netea MG. Specific and Complex Reprogramming of Cellular Metabolism in Myeloid Cells during Innate Immune Responses. *Cell Metab* 2017; 26: 142-156.

33. Neudecker V, Brodsky KS, Clambey ET, Schmidt EP, Packard TA, Davenport B, Standiford TJ, Weng T, Fletcher AA, Barthel L, Masterson JC, Furuta GT, Cai C, Blackburn MR, Ginde AA, Graner MW, Janssen WJ, Zemans RL, Evans CM, Burnham EL, Homann D, Moss M, Kreth S, Zacharowski K, Henson PM, Eltzschig HK. Neutrophil transfer of miR-223 to lung epithelial cells dampens acute lung injury in mice. *Sci Transl Med* 2017; 9.

34. Kulshreshtha A, Ahmad T, Agrawal A, Ghosh B. Proinflammatory role of epithelial cell-derived exosomes in allergic airway inflammation. *J Allergy Clin Immunol* 2013; 131: 1194-1203, 1203 e1191-1114.

35. Torregrosa Paredes P, Esser J, Admyre C, Nord M, Rahman QK, Lukic A, Radmark O, Gronneberg R, Grunewald J, Eklund A, Scheynius A, Gabrielsson S. Bronchoalveolar lavage fluid exosomes contribute to cytokine and leukotriene production in allergic asthma. *Allergy* 2012; 67: 911-919.